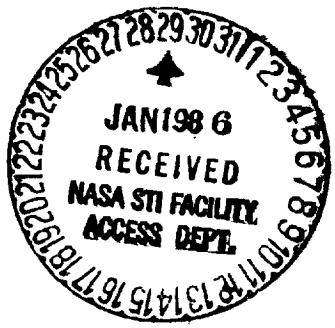

Final Report
Effect of Surface Texture by Ion Beam Sputtering on Implant Biocompatibility and Soft Tissue Attachment

by

DONALD F. GIBBONS

Prepared for

National Aeronautics and Space Asministration

May 1980

NASA Grant NSG - 3126

NASA Lewis Research Center
Cleveland, Ohio 44125
Space Propulsion and Power Division

Departments of Biomedical Engineering and Pathology
Case Western Reserve University
Cleveland, Ohio 44106

The research described in this report was carried out by Raymond A. Taylor in partial fulfillment of the requirements for the Master of Science Degree at Case Western Reserve University, under the supervision of the principal investigator Prof. D.F. Gibbons.

Abstract

This investigation examined the soft tissue response to a definable surface texture prepared by ion beam etching which was shown not to alter surface chemistry. Additional variables examined via the soft tissue response were: material composition and material compliance.

Two polymers were employed in this study - polytetrafluoroethylene (virgin) (γ_c = 20 dynes/cm.) and polyoxymethylene (Delrin) (γ_c = 38 dynes/cm.). PTFE develops a surface texture having conical projections with average dimensions: height - 12 μ, base width = 4 μ, tip radius = .1 μ. Delrin develops a surface texture with hairlike projection having average dimensions: height = 31 μ, fiber width = 1 μ, tip radius = .08 μ.

All implants were discs 1.0 cm. in diameter, with the thickness being either 50 μ, 125 μ, or 250 μ. Specimens were implanted under asceptic conditions in Sprague Dawley rats. Implants were inserted immediately adjacent to the fascia of the intercostal musculature.

Specimens were prepared for optical microscopy, SEM, and TEM. Histochemical staining was performed on frozen sections for succinic dehydrodenase, acid phosphatase, and alkaline phosphatase. Histological parameters that were quantified included: cell types, cell density, capsule thickness and cross-sectional area of blood vessels per field.

Smooth surfaces (as received, masked, ion polished) behaved identically by both histochemical and histological methods. Thus there was no effect of the ion beam environment on the tissue response to the material. Textured surfaces demonstrated increased cell adhesion, and increased SDH and acid phosphatase staining in the interfacial cells. The layer of cells adjacent to the texture consisted of foreign body giant cells and macrophages. These macrophages possessed an increased cytoplasmic to nuclear ratio, and increases in filopodia, interdigitation of filopodia, and vacuolization as demonstrated by TEM. Delrin surfaces developed increased cell density within the capsule and nonviable cells at the interface. This was attributed to leaching out of formaldehyde from the polymer.

The textured surfaces alter the kinetics of capsule development. Textured surfaces of both PTFE and Delrin show a significant reduction in capsule thickness at 8 weeks. A preliminary experiment indicates that there is no difference in capsule thickness between smooth and textured surfaces at 18 weeks. By increasing the compliance of textured PTFE samples (50 μ thick), the effect of capsule reduction is eliminated. Histological data reveals a sensitivity to the variables of texture, material composition, and compliance.

Table of Contents

List of Figures

List of Tables

CHAPTER I. INTRODUCTION

One important area of biomedical materials research is concerned with a quantitative determination of the response of tissue systems (soft tissue, hard tissue, blood, etc.) to a combination of the chemical, physiochemical, or morphological characteristics of a material's surface. Therefore, one of the goals of the biomedical materials researcher is to quantitatively determine the controlling interfacial parameter or parameters of the material which elicit the observed biological response and then understand the mechanisms involved. The cellular and humoral components of inflammation are in some way altered by the presence of an implant.

Many investigators have emphasized the importance of the material's chemical composition in determining the tissue response (4a,99,169,170,176), others the physiochemical factors (116), or the morphological features. Interest in tissue adhesion to surfaces and foreign body tumorigenesis has focused attention to the significance of morphological factors. However, data relating the biological response to variations in implant surface morphology has been predominately in the form of qualitative descriptive histology, with little quantification of parameters such as capsule thickness and cell types.

The NASA ion beam facility has recently been used to alter surface morphologies of a variety of materials in a controlled manner. Preliminary soft tissue attachment experiments on surfaces etched with the ion beam revealed intriguing results (71). By use of a

mask, a regular array of surface pits was developed on polytetrafluoroethylene (PTFE); the pit width, depth, and width to depth ratio were varied. After six weeks subcutaneous implantation in rats, histological sections revealed cells with a very large cytoplasmic to nuclear ratio within the pits. Either the morphological aspects of the surface or altered surface chemistry created by the ion beam etching process, or both were responsible for the altered cellular behavior.

The primary objectives of this investigation are (1) to characterize the altered surface morphology created by ion beam etching; (2) to characterize the soft tissue response to this altered surface morphology by using standard histology, enyzme histochemistry, and scanning electron microscopy; (3) to determine whether the surface morphology or changes in the surface chemistry (or physiochemistry) of the material accounts for the observed alteration in the biological response; (4) to observe and characterize the ultrastructural details of the "plump" cells adjacent to the textured surface; (5) to determine to what extent the material compliance influences the soft tissue response (135,158,263).

The effect of implant morphology on tissue adherence, foreign body tumorigenesis, and the soft tissue response to particulates, has received considerable attention in the past. Many of the morphologies used have characteristic features comparable to cellular dimensions, as is also the case with ion beam etching techniques, which may be the factor responsible for the observed behavior. The morphologies previously investigated have been achieved in a wide variety of ways -

it is therefore convenient to review the observations under four categories: (1) cloths, knits, and velours (2) porous materials (3) particulates (4) smooth surfaces that have been roughened.

Cloth, velours, and knits are all flexible fabrics in which relative movement between the individual strands occur. This adds additional complications to the interpretation of the results, unlike porous materials which represent fixed structures. Both of these structures differ from those under investigation in that they allow permeation of factors (ions, molecules, cells) through the material. Particulates, however, represent a distinct class primarily characterized by overall small dimensions and,because of this feature,may most closely approximate the characteristic surface dimensions of the ion beam etched surface. Particles are not, however,fixed in place, so again there is a disparity from the surface of interest. The final group considered involves materials whose surface has been roughened by some mechanical means and may most closely resemble the ion etched samples used in this study.

CHAPTER II. REVIEW OF THE LITERATURE

A. Biological Response to Materials

1. Knits, Velours, and Plain Weaves

Knits, velours and plain weaves all involve the use of yarns that can be constructed to give an infinite range of fabric tightness (see Table 1). Three immediately apparent parameters of these textiles which may affect the soft tissue response are: (1) material selection, (2) yarn denier, and (3) fabric tightness. With these cloths, the interface between the tissue and material is not smooth and uniform, but broken down to small morphological features (51).

Bonding between an implant and the surrounding tissue has been the focus of many investigations. Chemical bonding has been demonstrated in hard tissue (90), but never in soft tissue (51). The development of modern polymer chemistry and manufacturing techniques has enabled the production of fabrics that can provide acceptable mechanical interlocking between implant and host tissues. Fabrics have been used to anchor implants to soft tissue (31,54,80,81,82,83,138,197,216,217,224,258), hard tissue (45), the developing thrombus of arterial grafts (3,206,251), and to prevent exteriorization of transcutaneous implants (83,138,224,258).

Harrison implanted woven Dacron, Nylon, Orlon, and Teflon subcutaneously in dogs (86). The degree of fibrous enclosure and foreign body reaction to the materials investigated, listed in order of decreasing response were Nylon, Dacron, Orlon, and Teflon.

TABLE 1. TERMINOLOGY USED IN THE FABRIC INDUSTRY (24,238)

Fiber:	The basic individual filament of raw material from which threads, cordage, or fabrics are made.
Yarn:	The product of spinning loose fibers into a continous tight string; can vary in thickness, fiber content, and twist - all influencing the finished cloth.
Denier:	The size of the yarn; 1 denier rayon is 450 meters weighing 0.05 gm. (2 denier is 450 meters weighing 0.10 gm.)
Cloth or Fabric:	Made by weaving, knitting, or felting
Plain Weave:	A fabric made by the interlacing of two sets of yarns at right angles
Warp:	The threads that lie lengthwise in a woven fabric
Weft:	Threads combined with the warp that lie widthwise
Knit:	A fabric made by looping of yarn to form rows, one row of loops being caught into the previous row.
Felt:	A fabric formed by the mass interlocking of fibers by pressure
Velour:	A pile weave having a ground fabric plus an extra set of yarns woven into the ground projecting from it at 90° as loops
Fabric Tightness:	Term referring to the spacing between the woven or knitted yarns; a tight fabric has small interyarn spaces

The ranking of response was correlated to chemical stability and wettability; the greater the chemical stability and lower the wettability, the less the tissue response. It was suggested that the adsorption of protein on the surface of the plastic alters the molecular configuration in proportion to interfacial tension (86). This could then result in more foreign body reaction. No description of thread denier, or fabric tightness was given.

Usher, et al , examined the soft tissue response to Marlex mesh, porous-weave Teflon, and close weave Teflon by peritoneal implantation into dogs (216). Marlex, a high density polyethlene, was woven using .008 inch monofilament and a thread count of 42 x 40/inch. The Teflon weaves were not described. Very little fibrosis occurred through either the porous-weave or the close weave Teflon after 6 months, however, the Marlex mesh was found to be uniformly infiltrated with fibrous tissue to a thickness of 4.5 mm. A fibrous capsule of this thickness is quite unusual and may be specific to peritoneal implants.

Teflon (PTFE) felt, Orlon weave and Dacron weave were sutured to the abdominal wall of rats by Calnan (31). Sheet forms of Polyethylene, polyurethane, Teflon, and polyvinyl cloride were used as controls. "Round cells" were present around all materials several days post-implantation, Teflon having the least number. It is unclear whether "round cells" refers to lymphocytes or monocytes, although the two are indistinguishable at times under light microscopy. The fabrics were characterized by the presence of giant cells, increased cellularity, increased vascularity,

and decreased fibrous encapsulation in contrast to the sheet materials.

Dressler, et al, implanted Nylon 66 velour in the intestinal wall of rabbits, the urinary bladder of dogs and the skin of rats (54). These implants revealed a prompt emmeshing of the velour filaments with fibrin followed by an ingrowth of fibroblasts, capillaries, and an occasional foreign body giant cell (FBGC). Maturation of the wound resulted in a dense mature, collagen matrix around the implant. Although the velour morphology was not quantified, the critical factors affecting the tissue response were ascribed to the yarn denier, depth of the pile, and the number of pile loops per unit area (density).

Dacron weave and Dacron velour were compared by Tilney et al, using subcutaneous implantation into rats (209). The velour had a considerably tighter weave. The plain weave was initially filled with fibrin, serum, and inflammatory cells. Plasma cells were noted as well, suggesting the possibility of an immune response. Within 3 to 4 weeks, highly vascularized, mature collagen was noted throughout the mesh. Velour implants presented a markedly different response from that of the mesh. Portions of the velour grafts floated in abundant amorphous, friable, and caseous debris at time intervals up to 5 weeks. The pools of debris consisted of necrotic cells, fibrin and precipitated calcium (demonstrated by alizarin red S stain). An intense acute inflammatory response with many polymorphonuclear neutrophils (PMN) and foamy macrophages were also present. Resolution of the caseous areas was reported by 10 weeks, but mature collagen formation was absent at these sites. Although microbial contamination seems likely, no organisms were demonstrated by Gram stain or PAS, However, neither

of these methods detect fungi. In spite of this, it is uncertain whether the difference in response to the two fabrics is due to the difference in tightness of weave or to the loops of the velour pile. However, the tissue's sensitivity to changes in morphology was apparent.

Interest in the role of implant materials in foreign body tumorigenesis has helped us understand the sensitivity of the soft tissue response to morphologic variations in woven fabrics. The incidence of tumors using woven materials is considerably reduced when compared to their solid counterparts (25).

The extensive application of velours, weaves and knits as implants has identified several issues. A tightly woven fabric may allow fibrosis between the threads, but the thread spacing may be too small to allow for vascular infiltration resulting in ischemia, tissue necrosis, and eventual calcification (51). Although some investigators have ascribed the chemical nature of the material to be responsible for the tissue response (31), others feel that the fabric construction controls the histology (26). An increased yarn spacing in fabrics results in more rapid healing (26) and a decreased incidence of calcification (251). Additional trauma produced by the mechanical scissoring of the weft and warp yarns (26,51) has been suggested to be circumvented by a knitted fabric (251).

Correlation of results between different investigations involving the soft tissue response to fabrics is difficult if not impossible, due to lack of quantification of implant morphology. Many of these investigations were conducted at a time when the sensitivity of the tissue to slight variations in implant morphology had not been

recognized. Even if a uniformity in implants had been established, interpretation is further complicated by the use of a variety of animals and a variety of implantation sites. Some generalized statements about fabrics are possible, namely, that they elicit an increase in the number of foreign body giant cells, vascularity, and cellularity.

2. Porous Materials

Implant materials whose surfaces are interrupted with pores may also be considered as a material whose surface morphology possesses structural processes of cellular dimensions. Much of the interest in porous implants has, as with fabrics, focused on tissue adhesion and prosthesis stabilization in both hard (6,84,95) and soft tissue. Foreign body tumorigenesis studies have also stirred interest in porous materials because of the markedly decreased incidence of tumors associated with this morphology (25,153). Porous materials may be subdivided into (1) sponge-like structures with interconnecting or isolated pores in a material matrix such that communication between opposite sides is either impossible or via a tortuous path (2) filter membranes whose pores pass directly through the material. Both are of interest.

a. Sponge-like Materials

Porous sponge-like forms of polymers (15,36,55,134,188,198,231), metals (32,92), and ceramics (100,138), have been implanted in the soft tissue of a variety of animal species. Despite the wide differences between individual investigations, several morphological related effects on the soft tissue response may be gleaned.

Marzoni implanted silicone rubber sponges of three pore sizes (dimensions unspecified) subcutaneously into dogs (134). All implants became encapsulated, but the smallest pore size developed the thinnest fibrous capsule. Histiocytes and plasma cells were noted at the tissue material interface. Again, the presence of plasma cells may implicate an immune response, but they were only occasionally present in the smallest pore size. The differences in tissue reaction were attributed to the increased firmness of small-pored implants and subsequent tissue trauma (134), however, the morphologic effect of the pore size should not be ignored. Others have noted the effect of decreased capsule formation associated with a decreased pore size (36,198). This effect of pore size is apparently eliminated when highly compliant glycol methacrylate sponges are implanted (15).

The initial response to an implanted sponge is absorbtion of wound exudate. The extent to which the material absorbs or becomes coated with the wound fluids appears to affect the ensuing biological events. Polyurethane sponge with a very small pore size (90 pores/ inch) was filled by vascular connective tissue more rapidly and to a greater depth than the same material with a larger pore size (8 pores/ inch) (188). Proplast (a porous PTFE/carbon fiber composite) when pre-impregnated with blood, exhibited more rapid collaginization, vascularization, and organization than those which were not pre-impregnated (95). The elimination of the air/material interface might be responsible for this observation.

FBGC's are observed with many of the porous implants. No single parameter appears to correlate with their presence. They have been

reported with polyvinyl sponge (Ivalon)(55), polyurethane sponge (231), porous polyglycol methacrylate (198), and Proplast (84,95). However, no FBGC's were reported using porous titanium (92). Parameters that have been associated with increased FBGC formation include: increased porosity (198), decreased pore size (36), and increased motion of the implant (84,95). A connection between the presence of FBGC's and decreased collagenization has been suggested (84).

As with woven fabrics, sponges are also susceptible to calcification (55,231,256). The mechanism is probably similar to that described for fabrics, where the ingrown fibrous tissue outstrips the blood supply and becomes ischemic which leads to calcification.

b. Filter Membranes

The uniformity of the pores in filter membranes and the availability of a range of pore sizes has allowed a quantitative approach to the study of the soft tissue response.

Millipore filter membranes with pore sizes of 0.65, 0.8, 1.2, 3.0, and 5.0 microns were implanted intraperitonially in rats by Curran, et al, (47). Material composition was not specified, but cellulose acetate was most likely used. The smallest sizes - 0.65 and 0.8 μ - produced a weaker acute inflammatory response with fewer PMN's and a thinner fibrous capsule. If the larger pored membranes were filled with a cement to eliminate the pores, acute inflammation was reduced. Additionally, if the membranes were softened with a non-irrating solvent to reduce the compliance, inflammation was reduced. It is not clear, however, whether this effect is attributable to the reduced compliance or swelling of the material which would reduce pore size.

It was concluded that above a critical size, the pores created an irritating surface and acted as PMN traps. Large pore sizes favoring PMN accumulation has been reported by other investigators (145).

Tumorigenic studies using Millipore filters (assumed to be cellulose acetate) in mice demonstrated that pore sizes greater than or equal to 0.22 μ were nontumorigenic, while pore sizes less than or equal to 0.1 μ produced tumors with an incidence of 80% (110). Pore sizes in the range of 0.22 to 8.0 revealed invasion of the pores by macrophages or their processes. After one month implantation, a layer of mononuclear and FBGC's formed along the surface of the filter membrane which was separate from the capsule. This is quite similar to observations of other investigators (145). Interfacial cells of tumorigenic filters revealed an increased presence of phagolysosomes indicating increased phagocytic activity as compared to nontumorigenic filters (110). Pore sizes in the range of 0.22, 0.10, 0.05, and 0.025 μ produced fewer FBGC's, less cellularity and a thicker fibrous capsule than larger pore sizes. Calcification was observed, but at the imtermediate pore sizes of 0.22 and 0.45 μ (110).

Compilation of data from the investigations using millipore filters reveals a pore size range of 0.65 to 1.0 μ where the fibrous capsule is thin. Pores of greater and lesser size appear to generate thicker capsules. The ability of cells to respond to subtle changes in implant morphology is strongly implicated.

3. Particulates

The generation of particulates by the articulating surfaces of joint prostheses and the presence of solid pollutants in the air that

we breath has brought the tissue response to particulates under closer scrutiny. Many materials have been shown to be well tolerated in bulk form - PTFE, silica, polyethylene - yet when these materials are implanted in particulate form, they produce a very cellular inflammatory response (58). One obvious assumption for the discrepency is the altered morphology of the material (33a). However, several investigators support the idea that more than just the physical size and shape of the particles is involved (4a, 253, 254). Carbon is tolerated in both solid and particulate form (58).

The soft tissue response in dogs to particulate nylon, celluloid, polymethylmethacrylate, and PTFE was investigated by LeVeen and Barberio in 1948 (125). It was reasoned that the use of particulates would increase surface area and consequently accentuate the tissue reaction to the material. Adsorption of proteins was observed on all particles except PTFE and a proliferative foreign body reaction paralleled this adsorption. We now know that all materials adsorb proteins. The minimal reaction to PTFE particles is in disagreement with more recent research showing a very reactive foreign body response with the formation of FBGC's (123, 128, 216). The particles used by LeVeen were not described and may have been above some critical size.

The appearance of FBGC's may be related to both the material and the size of the particles. FBGC's are rarely seen in association with metallic particles (257, 259), yet are observed frequently with polymers and ceramics (33, 58, 199, 216). Particles of polyethylene, polyethylene terephthalate, and polymethylmethacrylate less than 5 μ can be phagocytized while particles greater than 5 μ become

surrounded by FBGC's (253, 254). Polyethylene terephthalate evokes very few FBGC's in contrast to polyethylene in the same size range, implicating the importance of the chemical composition as well as size (253, 254).

Metallic particles 10 μ and less in diameter are phagocytized by macrophages (230). Scores of metallic particles may be within one cell occupying up to one third of the cytoplasmic volume (257, 259). As with polymers, not all metallic particles ellict the same response. A 5 μ Ni particle is phagocytized and well tolerated within the cell for several days, whereas a 5 μ Co particle causes immediate cell death (87). In vitro investigations reveal Ti, Mo, and Cr particles to be well tolerated upon phagocytosis, while Co, Ni, and Co-Cr alloy particulates damage the cell membranes as demonstrated by lactic dehydrogenase activity (163). Cells which have phagocytized 0.5 μ Cr-Ni-Mo alloy particles appear "sick" with numerous vacuoles and no recognizable organelles (259).

A marked increase in fibrosis has been associated with particulates of all materials (4a, 37, 87, 253, 254). If ingestion of the particles eventuates in macrophage death, phosholipids can be liberated which can stimulate a fibrotic reaction in the surrounding tissue (87). In the case of silica particles, silacic acid causes protein denaturation within the lysosomal body wall which make them suseptible to tryptic digestion (4a). Damage to the lysosomal wall leads to leakage of digestive enzymes into the cell which ends in autolysis. An increased fibrotic reaction was found when 0.05 -0.5 μ Co-Cr particles were implanted subcutaneously in rats as

opposed to 35 μ particles and was attributed to an increase in metallic hydroxides exposed to the tissue (37). Particles 35 μ in size are not phagocytizable and would therefore, be less likely to cause autolysis. Similarly, silica, which is extremely toxic to cells when in the micron to submicron range (4a), is practically inert when implanted in the 200 to 2000 μ range (37,38).

It has been suggested that PTFE particles kill the surrounding cells by the actual physical shape of the particle (33a). Others have ascribed differences in the soft tissue reaction between polyurethane and polyethylene particles to compositional differences and subsequent protein adsorption (169). Slow protein adsorption has been conjectured to cause slow PMN migration (169).

Experiments with well controlled particle sizes and shapes have not been performed. Such investigations will be necessary to elucidate the role of the physical and chemical factors in the cellular response to particulates.

4. Roughened Surfaces

The surface of morphology most resembling the ion beam etched surfaces used in this study is a solid material that has had its surface roughened by some mechanical means such as rasping, grit blasting, etc. These surfaces present to the surrounding tissue a non-porous, solid material with microscopic projections.

Curran and Ager noted that the tissue reaction of rats to agar gel was greatly influenced by the physical state of the surface (48). Agar was cast in a capsule form and implanted in the peritoneal cavity of rats. Agar surfaces that had been roughened by cutting

were associated with a phagocytic population of PMN's which was rapidly replaced by mononuclear cells. Smooth as-cast surfaces retained non-phagocytic PMN's for a longer time and were only slowly replaced by mononuclear cells. Additionally, a thicker and denser fibrous capsule was associated with roughened surfaces at 28 days. It was suggested that substances released from leukocytes at the interface caused an increase in local blood vessel permeability, migration of monocytes, and stimulation of fibroblastic activity (48).

In a similar experiment, egg white in addition to agar, was implanted intraperitoneally in rats (49). Several hours after implantation the surfaces of all implants were covered by a monolayer of macrophages. Roughened surfaces formed by slicing of egg white formed FBGC's, but the roughened surfaces of agar did not. Collagen formation was limited precisely to areas where phagocytosis had occurred. Fibroblastic activity was suggested to be secondary to the phagocytic activity (49). These differences in response may be ascribed to the ability of PMN's and mononuclear cells to detect the microscopic irregularities on the contacting surface (49).

Contrary to these findings, roughened Co-Cr-Mo alloy rods revealed no difference in tissue response when compared to the smooth control after subcutaneous implantation in rats (143). Macrophages were described as incapable of detecting roughened surfaces. Similar results have been reported in bone (39).

The decreased incidence of tumors in association with perforated discs and powders may not be due to their ability to allow diffusable substances to pass through as suggested by Oppenheimer (153).

The character of the implant surface is an equally tenable hypothesis (17). Roughened (rasped) polyethylene discs produced a decreased incidence of tumors in mice in contrast to the smooth controls (17). At 6 months, the smooth surfaced polyethylene possessed a "better" developed capsule that was less cellular, more compact, and contained thicker collagen fibers in contrast to roughened surfaces.

Salthouse abraded PTFE rods and implanted them into the muscle of rats (186). The surface morphology profoundly influenced the cellular response, lysosomal enzyme activity and kinetics of cells adjacent to the implant. An increase in cellularity and enzyme activity was noted at abraded surfaces. Macrophages and giant cells predominated with some fibroblastic activity at the periphery of the reaction area (186, 187). Semiabraded rods evoked a giant cell reaction only along the abraded surface. No quantitative differences in cell types, capsule thickness, or vascularity were given. Roughened surfaces demonstrated increases in acid phosphatase, succinic dehydrogenase, aminopeptidase, and glucose-6-phosphate dehydrogenase (indicative of pentose shunt activity and DNA synthesis). Thymidine incorporation studies revealed a proliferative self-sufficient macrophage population at roughened surfaces independent of bone marrow recruitment.

5. Concluding Remarks

A spectrum of surface morphologies has been presented. Few comparisons can be made between experiments even within a single class of implants due to lack of material characterization, differences in implantation site (36), and differences in host species (143,145,168). One unifying concept may be gleaned, however, the

cellular and humoral components of soft tissue are sensitive to variations on a microscopic scale to surface topology.

B. The Reparative Process

The surgical procedure used for implantation inevitably produces discontinuities in the structure and composition of the surrounding tissues. Blood vessels are severed causing hemorrhage together with cell destruction at the immediate site of injury (158). The subsequent response is that of imflammation, which tends to destroy or limit the spread of the injurious agent (252). An understanding of the inflammatory sequence is thus required in order to interpret the soft tissue response to an implanted foreign material.

The inflammatory response has been divided into short (acute) and long (chronic)phases. The acute response invariably takes place for the first few days, irrespective of the presence of an implant. Chronic inflammation occurs when the injurious agent persists (158,252). The foreign body response is typically associated with the duration of the chronic inflammatory response (42). Although inflammation has been described in terms of phases (57), it is important to remember that inflammation is actually a dynamic continuum of events.

1. Acute Inflammation

The early features of inflammation result from the reactions of the small blood vessels in the injured tissue. Immediately following injury, there is a transient vasoconstriction of the arterioles (252). This helps counter the tendency for hemorrhage (158). A progressive dilation involving all elements of the local vasculature follows within minutes (158,252). Erythrocytes adhere to each other

and to the endothelium within the local blood vessels and results in stasis by 2 to 6 hours (252). Platlet-fibrin thrombi do not form until later, so this occlusion can be reversed (158).

Two further events are important in the development of the acute inflammatory response. First, the exudation of plasma through blood vessel walls into the injured tissues. Second, the migration of polymorphonuclear leukocytes (PMN's) into the injured tissue (252).

Immediately adjacent to the site of injury, edema begins to develop in the first 10 to 15 minutes. The fluid in the inflamed tissue, known as exudate, is characterized by a high specific gravity, high protein content (1-6 gm/dl), and ready coagulability (contains fibrinogen). Some report that exudate has exactly the same composition as plasma (158). The loss of plasma (exudate) into the tissues increases the blood viscosity in the local vasculature. This results in increased hydrostatic pressure assisting loss of more plasma. A positive feedback loop is developed which eventually terminates in stasis (252). Concurrently, red blood cells clump and leukocytes are displaced to the periphery of the blood vessels. Leukocytes begin to adhere to the venular endothelial surface nearest the site of injury. As leukocytes adhere to the venular endothelium, erythrocytes and plalets adhere and form a temporary plug. Fibrin is eventually formed in the severed vasculature and in the surrounding traumatized tissue.

The theory of increased hydrostatic pressure does not adequately explain the high concentration of the large-molecular globulins and fibrinogen (252). It is generally accepted that biochemical mediators

are released or activated by tissue damage resulting in a permeability response of the vascular membrane.

Although the pattern of the permeability response is influenced by the type and intensity of injury and the species of the test animal, the increased permeability of the venules is basically a biphasic event. An immediate permeability response (peak in 5 min. subsided by 30 min.) appears to be due to the pharmacologically active amines - histamine and serotonin (5-hydroxytryptamine) (158,252). Both histamine and serotonin are widely distributed in the body tissues, being stored mainly in the mast cell and platelets (158,252). In the mouse and rat, serotonin is the dominant vascular amine (158,252).

A delayed permeability response peaks approximately 4 hours after injury and subsides by 10 hours, depending on the nature and extent of injury (252). Several mediators have been implicated for this response. Kinins, a group of biologically active peptides, are found in the areas of injured tissue and appear involved in the inflammatory process. Although kinins have been proposed as the natural mediator for the delayed permeability response (252), some have suggested that kinins are too short-lived (due to kininases) to produce the delayed permeability response (158). Other permeability factors that have been associated with the delayed response are the protaglandins E1 and E2 (158,252). PGE_1 and PGE2 affect the release of histamine and serotonin (158,252). Other permeability factors suggested in the delayed permeability response are C3 and C5 (also owing their effects to histamine release), certain bacterial toxins, globulin permeability factor, and a substance released by PMN's (252).

The effect of the permeability factors is to cause a contraction or rounding of the endothelial cells within the venules, so that gaps occur at cell junctions (158,252). The scene is now set for the migration of PMN's and mononuclear cells through the wall of the "leaky" blood vessels into the adjacent tissue. This represents the main cellular phase of acute inflammation (42,193,252,255).

Although PMN's and monocytes migrate from the microvasculature simultaneously, PMN's move through the connective tissue at a much faster rate (2,118,157,233), and subsequently arrive at the lesion first. After 24 to 48 hours, the ratio of neutrophils to monocytes entering the lesion falls (193), due to a decrease in migrating neutrophils. The plugging of lymphatics, vascular stasis, and resulting anoxia decreases the pH of the lesion and results in PMN lysis. Monocytes maintain viability in this environment and predominate by day 2 to 3. These events help explain the well documented cellular response that occurs in acute inflammation (42,158,193,233,252).

Just as increased hydrostatic pressure could not fully explain the high protein concentration in the exudate, the increased vascular permeability is insufficient to account for the accumulation of cells at lesion sites. The process of tissue injury sets into operation a series of interdependent proteolytic enzyme systems - the coagulation system, the kinin system, the fibrinolytic system, and the complement system - which give rise to a number of chemotactic and inflammatory mediators.

Local vasodilation, leakage of fluid in the extracellular space,

and stoppage of lymphatic drainage produce the classic signs of acute inflammation - redness, swelling, and heat. Pressure and chemical stimulation by kinins produce the fourth sign - pain.

2. Chronic Inflammation

In a noncontaminated wound, the acute inflammatory reaction subsides and recognizable repair begins in 3 to 5 days. However, in the situation that the wound becomes contaminated by an injurious agent such as talc (from the surgeon's glove), bacteria, or an insoluble implant material, inflammation may persist for months and is typically classified as chronic inflammation (42,59,252). The tissues are infiltrated by cells derived from three lines: the mononuclear phagocytes, the lymphoid cell, and fibroblasts. The mononuclear cell is represented by monocytes, macrophages, epitheloid cells, and multinucleated giant cells (MGC) with the macrophage usually considered to play a central role in chronic inflammation (59). The lymphoid cells are represented by lymphocytes, lymphoblasts, and plasma cells. Fibroblasts produce collagen, mucoproteins, elastin, and protein-polysaccharides of the ground substance (50,173,174,223).

The accumulation of these cells in the chronic lesion may be diffuse or focal. A locally confined, persistent response to the presence of a generally poorly soluble substance, mediated through the accumulation, proliferation, and differentiation of the mononuclear phagocyte system is definitive of granulomatous inflammation (59). Most, but not all granulomas are the end result of chronic inflammation associated with a foreign material (158).

The persistance of an inciting agent maintains a local population

of mononuclear cells through proliferation (193). The macrophage generally attempts to phagocytize the foreign material but frequently the material is non-degradable or too large to be internalized . In many instances the macrophages may then merge their cytoplasms to become FBGC's. The continuing presence of the foreign material in some way induces the fibroblasts to lay down a matrix of collagen encapsulating the object and attached macrophages/FBGC's in a dense membrane of connective tissue (42).

During normal tissue injury, acute inflammation is followed by the appearance of fibroblasts within 48 to 72 hours (173). Capillaries follow which continue to proliferate until approximately the 8th day. After the fibroblasts lay down collagen, the inflammatory cell numbers (PMN's macrophages) subside, and the number of fibroblasts and blood vessels decrease to a constant level by 2 weeks. The collagen eventually becomes remodelled to restore contuinity and full strength to the wound by 12 months. Why the presence of a foreign object induces fibrous capsule formation is a continuing dilemma to biomaterials investigators. Since the fibroblast and its products are focal in the healing response and the foreign body response, some attention is justifiable.

The fibroblast is derived from the mesoderm (223), however, its orgin in wound healing has created much controversy. Two major theories have evolved. Some feel that fibroblasts are derived from large monocytes or possibly from macrophages which enter the wound site from the blood (49,117). Others maintain a more strongly supported idea, that fibroblasts are derived from resting fibroblasts

in the loose connective tissue, the adventitia of small blood vessels and capillaries, or from cells in the fatty tissue (173). The issue is far from resolved (34,117,173,223).

The stimulus for collagen production has received much attention. Irritants that evoke a marked exudation of PMN's have been associated with a marked and rapid fibroplasia, likewise irritants that evoke minimal exudation have been shown to have delayed and minimal fibroplasia (173). Stimulating factors from mononuclear cells have been revealed as well (35,121,122,167). What has received less attention are the mechanisms involved in turning the fibroblast "off". Human mononuclear cells have been reported to release a factor in culture which produces selective inhibition of collagen synthesis when added to normal human skin fibroblasts in culture (104). It has been suggested that during the development of an inflammatory response, the participation of connective tissue cells occurs in two phases (104). Initially, there is a stimulation of fibroblast proliferation mediated possibly by factors released by platelets and/or mononuclear cells. Production of collagen and other substances would then occur. When the fibroblastic response is complete, and repair adequate, the inhibitory factors (previously described) would terminate the deposition of collagen. Normally, there is an adequate balance between stimulation and inhibition which is strictly maintained, but capable of being perturbed under certain conditions (104). This may result in either deficient or excessive accumulation of connective tissue substances. Fibroblasts may also be stimulated to produce collagenase by a substance released by macrophages (223).

One of the basic problems in the study of fibroblasts is their identification (223). It is polymorphic - some cells are elongated with elongated nuclei, others are oval or irregular in shape. Using light microscopy, shape can be a misleading criterion for deciding whether a given cell is a fibroblast. Transmission electron microscopy must be used for definitive analysis, but even then confusion may arise (117). Ultrastructurally, the typical fibroblast has abundant dilated rough endoplasmic reticulum, a prominent golgi zone with groups of saccules and vessicles randomly located throughout the cell, large mitochondria with irregular cisternae, a large nucleus with one or more prominent nucleoli, and small vacuoles in the peripheral cytoplasm (174,175,223).

Recently, a contractile fibroblast responsible for wound contracture and possibly contracture of the fibrous capsule around breast implants has been described (78,178,179). Combining the ultrastructural features of fibroblasts and smooth muscle cells, they have been named myofibroblasts. The "classical" myofibroblast contains 60-80 Å diameter microfilaments parallel to the cell membrane (sometimes extending through the membrane), rough endoplasmic reticulum, convoluted nuclei, desmosomes, and a basal lamina (78,178,179). Although their origin is unknown, they appear in normal wounds as early as 7 days (78), and disappear once the wound has become stable.

C. Humoral Mediators of Inflammation

It is now well established that the coagulation sequence in blood is coupled to specific components of the inflammatory response (271).

Activated Hageman Factor (FXII) has the ability to trigger four proteolytic enzyme systems in plasma - the coagulation, fibronolytic, complement, and kinin-forming pathways (43,131,164,271). Activation of these systems generates substances that induce the symptoms of acute inflammation - increased vascular dilation, increased vascular permeability, pain, and chemotaxis of inflammatory cells.

The common link between these effector pathways is Hageman Factor (HF), a plasma protein (M.W.90,000) that is converted to a proteolytic enzyme factor (FXIIA, HFA) by exposure to negatively charged surfaces (43,164). Many substances have been shown to activate Hageman Factor (See Table 2). In vivo, collagen is a likely activator due to negatively charged sites on the free carboxyl groups of glutamic and aspartic acid (43,164,165); in the situation of an implant, negatively charged sites on the surface or some other parameter may also be responsible. Hageman Factor activation has been reported to be dependent on material size, or possibly radius of curvature, as proven with colloidal silica particles (43). The amount of HF activation decreases as the diameter of silica particles falls below 150 Å, and below 20 Å, there is no activation.

One of the proteolytic enzyme systems initiated by HFA is the kinin-forming system (43,164). The kinins are a group of polypeptides capable of influencing smooth muscle contraction, inducing hypotension, increasing blood flow, increasing microvascular permeability, and inciting pain (43,77,112,164,271). The kinin-forming system is an essential link in the chain of events comprising the inflammatory

TABLE 2

SOME ACTIVATORS OF HAGEMAN FACTOR (FACTOR XII)

SOLID ACTIVATORS	SOLUBLE ACTIVATORS	ACTIVATORS BY ENZYME CLEAVAGE
Glass	Ellagic Acid	Kallikrien
Silicon Oxide	Cellulose Sulfate	Plasmin
Fused Alumina	Carrageenan	Activated Factor XI (PTA)
Feldspar	Chondroitin Sulfate	
Kaolin		
Diatomaceous Earth		
Talc		
Barium Carbonate		
Anodized Tantalum		
Stainless Steel		
Titanium		
Zinc		
Nylon		
Sebum		
Sodium Urate		
Collagen		
Skin		
Celite		
Spider Webs		
Asbestos		

response and has been shown to be capable of modifying the foreign body response (237). Other activators of the kinin system include plasmin (operating on kininogen and prekallikrein) and agents within granulocytes capable of liberating kinins from plasma in the presence of HF (43,164). Granulocytes also contain kininases, thus the accumulation of these cells at inflammatory sites has the potential to both liberate and deactivate kinins (112).

Kallikrein, an enzyme in the kinin system cascade, is a chemotactic agent (43). This enzyme can catalyze a positive feedback reaction that converts HF into a more effective activator of prekallikrein (43,271). Kallikrein may also play an important role in leukocyte migration inhibition in acute inflammatory exudates (204, 205).

The interaction of the fibinolytic and coagulation system generates several chemotactic factors. The fibrin split products produced by the action of plasmin on fibrin are chemotactic for eosinophils and PMN's (164). Plasminogen activator, present in plasma as well as endothelial cells, macrophages, and fibroblasts is chemotactic for PMN's and mononuclear cells (234,271). Plasmin can activate the kinin system at several points and can also initiate the complement system.

The consequences of complement activation include increased vascular permeability, chemotaxis of PMN's and monocytes, the adherence of complement-coated complexes to formed elements of the blood, enhanced phagocytosis, and cell membrane disruption (91,177,235). The complement system may be activated by two different sequences:

FIGURE 1. SOME HUMORAL MEDIATORS OF INFLAMMATION (131, 177, 204, 205, 208, 232, 233, 234, 271)

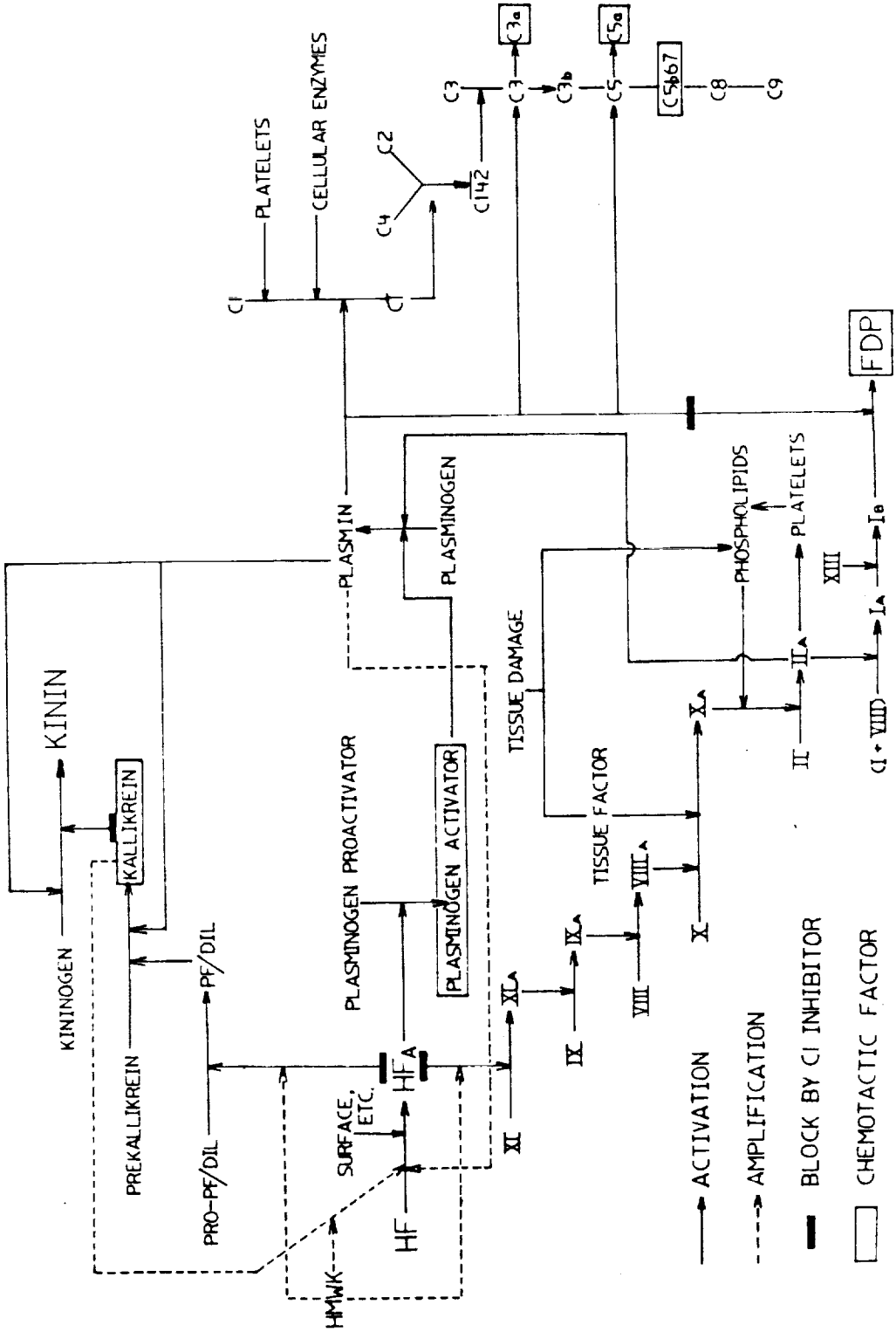

the "classic" pathway, initiated by immune complexes, and the "alternate" (properdin) pathway, activated by complex polysaccharides in yeast and bacteria cell walls (177). It has been suggested that the alternate (properdin) pathway is activated only if particulate materials are present (177). The composition of these particulates was not specified, however. The $\overline{C567}$ complex (part of the complement activation sequence) and fragments of C3 and C5 (formed during the proteolytic activation) which are released into the plasma, have been shown to be chemotactic for PMN's and mononuclear cells (91,164,233, 234,235,271). In addition to antigen-antibody complexes, aggregated or altered immunoglobulin proteins may also initiate the classical pathway (177). Protein denaturation at a material surface could therefore conceivably initiate complement activity directly without the need for plasmin.

The enzyme cascades involved during inflammation are organized into a complex web of events. Each pathway may be initiated by multiple factors so that a deficiency in one (or more) component may be compensated by alternate sequences. An understanding of these enzyme sequences and their interactions will not only help in understanding inflammation, but the tissue response to implant materials as well.

D. The Effect of Chemotactic Factors on Leukocytes

An important consequence of the humoral events activated by tissue trauma is the generation of substances which direct leukocyte migration to the site of injury. Chemotactic factors in some way, as yet poorly understood, interact with the leukocyte cell membrane

and elicit a series of changes which prepare the leukocyte for directed movement and phagocytosis. This interaction may occur via specific cell membrane receptors for these factors (151) or through membrane bonding to the hydrophobic groups common to all chemotactic factors (235).

When activated chemotacticly, the PMN assumes an oriented morphology with the nuclei at the back of the cell and pseudopodia toward the leading end (70). A microtubule system within the cell maintains cell orientation and provides the vector of locomotion during chemotaxis, while a microfilament system provides the locomotory apparatus (70). Chemotatic factors (CF) induce several changes in the neutrophil: 1) swelling (69,70,150,151,235), 2) aggregation (150,151), 3) surface membrane ruffling with an increased number on the side facing the chemotactic factor (150,151,235), 4) increased adhesiveness (150,151), 5) transmembrane ionic flux and membrane depolarization (69,70,150,151,235). Biochemical changes include increases in: oxygen uptake, glycolysis, hexosemonophosphate shunt, proesterase activation, lysosomal enzyme discharge, and microtubule assembly (234).

Several factors have been suggested to regulate leukocyte chemotaxis. Chemotactic Factor Inhibitor (CFI) exists in serum and inactivates the C3 and C5 fragments (234,235). Cell Directed Inhibitor (CDI) blocks the ability of monocytes and PMN's to respond to a variety of chemotactic factors as well as impair the phagocytic response of PMN's (234,235). Neutrophil Inhibitory Factor (NIF), contained in neutrophils, can block chemotaxis of PMN's and eossinophils

(235). A similar factor has been described which irreversibly depresses random and directed migration of PMN's and is released by PMN's and mononuclear cells in acidic medium or following phagocytosis (111).

E. The Mononuclear Phagocyte System

The mononuclear phagocyte system plays a central role in the complex cellular and humoral events that attend chronic inflammation (2,10,75,121,181,194,195,214,219,221). The cells of this system are actively involved in phagocytosis and are essential for the elimination of various kinds of micro-organisms, debris, dead cells and tissue during the debridement of wounds (121,122,214). This group of cells is widely distributed in the body and includes the following elements:

1. Promonocyte (bone marrow)
2. Monocyte (blood)
3. Macrophage (tissues)
   - Histiocyte (connective tissue)
   - Kupffer cell (liver)
   - Alveolar macrophage (lung)
   - Sinusoidal lining cell (spleen)
   - Free and fixed macrophage (lymph node)
   - Peritoneal macrophage (serous cavity)
   - Osteoclast (bone tissue)
   - Microglia (nervous tissue)
4. Epitheloid cells (connective tissue)
5. Foreign body giant cell (connective tissue)

1. Origin and Kinetics of Mononuclear Cells

The origin of monocytes has been established unequivocably to be the bone marrow (219,226,227). Within the bone marrow, a pluripotential cell has been suggested to form into a committed stem cell (221). This stem cell then further differentiates into a monoblast which divides to form two promonocytes. These cells in turn divide and mature to form monocytes (221). Newly formed monocytes leave the bone marrow and enter the peripheral blood (221,252). The disappearance of monocytes from the circulation is a random process (221). The average transit time to the tissues is about 32 hours (221,252). Once in the tissues, the mononuclear cell may become phagocytic and is then called a macrophage.

Macrophages are the predominant cell type within injured tissue 24 to 48 hours after injury (140,180). The persistance of macrophages during chronic inflammation or a foreign body response could be due to (a) mitosis, (b) recruitment from the bone marrow, or (c) longevity. Evidence has been presented supporting all three (190).

Investigations by Volkman and Gowans (226, 227) employed a thymidine label for monocytes along with bone marrow destruction via x-irradiation to determine the origin of inflammatory macrophages. It was concluded that the macrophages which accumulated at inflammatory sites in the rat are derived from cells which migrate from the blood. Furthermore, the precursor of these blood cells are dividing continuously and at a rapid rate in the bone marrow.

In the early stages of inflammation, the macrophage population is dependent upon fresh recruitment from bone marrow (181). A

monocytosis factor has been described which increases the production of monocytes in the bone marrow by decreasing the cell-cycle time of promonocytes (221). Immediately after leaving the circulation, monocytes undergo one burst of DNA synthesis (presumably premitotic) which is then followed by a period of quiescence. It is during this time that the cells migrate to the implant material. After a few days, the monocytes in the vicinity of the implant come under influence of additional factors leading to considerable DNA synthesis and mitotic activity (181). The intrinsic properties of mononuclear cells together with environmental conditions eventually reduce or in some circumstances eliminate a dependence upon recruitment from the bone marrow (181,195); mitosis and longevity are then responsible for maintaining the macrophage population. There is no set pattern, however, and the most important factor is that macrophages respond to their environment (10,75,181,194). Dependent upon the inciting agent, a granuloma may be either low-turnover or high-turnover (194). Environmental stimuli may induce mitosis (194) or differentiation with morphological, functional, and biochemical changes, many of which are reversible (10).

The fate of macrophages in wounds can take one of several courses. It can disappear quickly as a result of cell death, drain to lymph nodes, divide, become immobilized in the foreign body response for months without dying or dividing, form epithelioid cells (2,40,154, 195), form foreign body giant cells (2,59,133,155,195,205a,236), or possibly differentiate into fibroblasts (49,117).

2. The Macrophage

The conversion of monocytes into mature macrophages is accompanied by metabolic, biochemical, and structural changes.

a. Metabolic Features

The differentiation of monocytes into macrophages is attended by an increased dependence on the Krebs cycle. There are also increases in cytochrome oxidase activity, mitochondrial mass, phagocytic activity, glucose utilization, and lactate production (10). Phagocytic stimulation results in a marked increase in the hexosemonophosphate shunt (2).

b. Biochemical Features

As monocytes differentiate into macrophages, they develop the ability to secrete a number of materials into the extracellular environment (214), the specific products being dependent upon the environmental stimuli (40,41). The macrophage produces enzymes such as collagenase (249), elastase (250), lysosomal proteases, and plasminogen activators (214), that are capable of affecting extracellular proteins. An "activated" macrophage phagocytizing large, particularly insoluble materials releases continuously amounts of enzymes which could affect the structure of proetins in its extracellular environment (214).

Macrophages also produce factors which regulate the activities of surrounding cells (214). These include lymphostimulatory factors, a fibrogenesis factor (35,121,122,167), an angiogenesis factor (35,59), and inhibitors of cell growth (122,214). Elimination of macrophages from wounds delays the appearance of fibroblasts and reduces their subsequent rate of proliferation (121). Macrophages are not only

TABLE 3

MACROPHAGE SECRETION PRODUCTS (35,59,75,122,214)

Enzymes:	lysozyme
	neutral proteinases
	- plasminogen activator, collegenase, elastase, gelatinase
	esterases
	acid hydrolases
Proteins:	complement factors - C2, C3, C4, C5
	pyrogen
	interferon
	prostaglandins
	cyclic AMP
Factors:	colony stimulating factors
	lymphostimulatory molecules
	fibrogenesis factor
	angiogenesis factor
	inhibitors of cell growth

LYSOSOMAL ENZYMES PRODUCED BY MACROPHAGES

acid deoxyribonulease	cathepsin - D
acid phosphatase	lipase
acid ribonuclease	hyaluronidase
aryl sulfatase	aminopeptidase
BPN hydrolase	carboxylic esterase
α- galactosidase	
β- galactosidase	
β- glucuronidase	
β- N - acetylglucosaminidase	

crucial for wound debridement, but play a central role in the initiation of the healing process through the production and secretion of various stimulatory and inhibitory substances. The environment can change the functional state of the macrophage and vice versa (75).

c. Structural Features

The monoblast, promonocyte, and macrophage all share common physical features: ruffled surface membranes, lysosomes, pinocytic visicles, and a kidney-shaped nucleus. As mononuclear cells age at the site of a lesion, there is an increase in cytoplasm, a lessening of the intensity of staining of the nucleus, enlargement of the nucleus, and an increased vacuolization as seen with light microscopy (157). Ultrastructurally, margination of chromatin, evident in monocytes, decreases in the macrophage. The maturing macrophage shows a decrease in primary and secondary granules and an increase in microtubules (218). Other ultrastructural characteristics of the macrophage include: a sparse undilated rough endoplasmic reticulum (RER) with widely separated groups of attached ribosomes, numerous free ribosomes, an occasional nucleoli, and numerous microvilli at the cell periphery (121). As the monocyte matures into a macrophage, there is an increase in lipid droplets.

3. Epithelioid Cells

Many investigators have viewed epithelioid cells in vivo as mature macrophages (2). Some have suggested that epithelioid cells arise directly from undifferentiated circulating monocytes (59). Regardless of their origin, epithelioid cells have no known function (154,195).

Epithelioid cells synthesize acid prosphatase, yet are poorly

phagocytic (154). Although they have been said to be active in degradation and microbial destruction, the epithelioid cell seems to be more strongly implicated as a secretory cell (2,154,195).

The stimulus for epithelioid cell formation is not known. Some have suggested that epithelioid cells originate from magrophages whose capacity to initiate phagocytosis is "frustrated" (195). Others have postulated that macrophages modulate into epithelioid cells when they become immobolized at a site of inflammation without being called upon to undertake phagocytosis or when phagocytosis leads to complete elimination of the particle (154). The uptake of indigestible non-excretable material has been reported to prevent macrophages from becoming epithelioid cells (154).

Epithelioid cells have the appearance of a cloudy eosinophilic cytoplasm whose outline tends to merge with that of its neighbor. Their nucleus is elongated with dense banding of chromatin at its periphery, nucleoli are prominent, lysosomes are few and small, the Golgi apparatus is prominent, RER is abundant, and there are a large number of lipid droplets (59,154,195). A distinguishing feature of the epithelioid cell is a high degree of interdigitation of pseudopodia between neighboring cells (2,154, 205a). Although epithelioid cells have been reported to be capable of cell division (2), it has been suggested that they eventually fuse to form FBGC's (205a).

4. Multinucleated Giant Cells

Frequently during the course of granulomatous inflammation and foreign body reactions, giant cells are formed containing anywhere from 2 to 200 nuclei (133). Neither the function nor the reason

for formation of giant cells are fully understood, yet several theories have been suggested.

It is generally accepted that one mode of formation of multinucleated giant cells (MGC) is through the fusion of macrophages (2,59,133,195,236), however, fusion of epithelioid cells has also been reported (205a). Experiments utilizing labelled monocytes and millipore chambers have indicated that giant cells are formed as a result of fusion of new macrophages to old ones (133). Giant cells cut-off from resupply of new macrophages by whole body irradiation diasppear within 7 to 10 days (155,195).

Of all the cells in the mononuclear phagocyte system, giant cells contain lysosomes in the greatest number with maximal structural variation. These lysosomes decrease in number as the giant cell ages (205a). The Golgi apparatus increases to maximal size and complexity, and the mitochondria reach a maximum in the giant cell (205a).

Scanning electron nicroscopy reveals MGC's to have tortuous outlines and a rough cell surface (133). Intimate contact with mononuclear cells and other polykaryons is also seen (133).

Histochemical observations reveal acid phosphatase and succinic dehydrogenase activity in giant cells (133). They have the capacity to phagocytize, but do so inefficiently (59,133,195).

Several mechanisms have been proposed for the fusion of macrophages into giant cells. Some have suggested that the convoluted cell membrane, phagocytic potential, and capacity for adhesion makes the macrophage suseptible for fusion (133). Giant cell formation

may be due to "recognition" by wound macrophages of older ones that may have altered surface features, facilitating a fusion that is in effect a "cannibalistic phagocytosis" (195). Cell fusion almost always occurs in the neighborhood of discharging macrophage lysosomes, and it has been proposed that the activity of certain hydrolytic enzymes is required for the membrane changes (205a). On the other hand, phagocytosis by macrophages has been reported to have an inhibitory effect on cell fusion (59). The morphogenesis of giant cells may be regulated by surface antigens, since specific surface antigens of macrophages are reported to increase with cell age (2). At least in some circumstances, fusion appears to be mediated by a lymphokine, termed macrophage fusion factor (MFF) (67). The production of this factor occurs during in vitro sensitization of lymphocytes with BCG (Bacille Calmett-Guerin) (67). Regardless of the cell fusion mechanism, the ability of macrophages to form multinucleated giant cells varies for each individual animal (2).

Teleologically, polykaryons have been suggested to be a disposal mechanism for unwanted cells (59,133). They may remove rapidly dividing macrophages which may become neoplastic otherwise. Giant cells may engage in active transport in addition to sequestering foreign particles (205a).

CHAPTER III. EXPERIMENTAL METHODS AND MATERIALS

A. Ion Beam Sputtering

Technology developed from the NASA electric propulsion program has been extended to obtain controlled surface morphologies with definable dimensions (242). Propellant atoms are ionized in the discharge chamber by electron bombardment in a process that is similar to that in a mercury arc lamp (144). The ionized propellant atoms can then be accelerated by an electric field and focused into an "ion beam". A neutralizer cathode provides an electric current equal to the ion beam and provides for the space charge and current neutralization of the ion beam (242). When an energetic ion strikes the surface of a material, one or more atoms, molecules, or fragments of molecules may be removed; this process is called "ion-beam-sputtering", "ion-beam texturing", or "ion-beam-etching".

Argon was used as the working gas, however, any of the inert gases, nitrogen, freon, or mercury vapor can be used (144,242). The entire ion-beam-thruster operates with a vacuum of 1×10^{-5} to 3×10^{-7} torr. The beam intensity may be adjusted via the propellant flow or the discharge power.

The slightly divergent, neutralized beam can be used to suptter target materials. Materials vary in sputter yield when placed in the ion beam. Materials having high melting points (metals, ceramics) erode at much slower rates than lower melting solids (polymers) (242). Materials also vary in their ability to develop a surface texture from the ion erosion process. Some materials (pure metals) erode

uniformly, while others etch preferentially at certain sites resulting in a surface texture. Teflon (PTFE) and Delrin (polyoxymethylene) are two polymers which do develop a surface texture. This fact, in addition to the short times needed to produce textures on these materials (242,268,269), were the criterion used in selecting Teflon and Delrin for this investigation.

Sputtering targets were mounted on "shepherd's crook" supports that could be rotated or displaced parallel to the beam axis. The targets could be mounted with their surface at any angle with respect to the ion beam (97). This capability allowed for ion etching as well as for "ion polishing". The capabilities of the NASA ion engine may be summarized as follows:

(1) Ion beam etching - the target material is placed in the ion beam with the surface normal to the beam axis. The target is eroded by impinging ions and develops a "natural" texture characteristic of the material used.

(2) Ion polishing - the target material is placed in the ion beam with the surface at a 10 degree angle to the beam axis. The target is then rotated, so that the grazing ions "polish" the material surface.

(3) Sputter Deposition -the ion beam impinges on the target material to be deposited. The energetic ions striks the target surface

causing the ejection of target material, which is then deposited onto a substrate.

(4) Ion machining - a mask is placed between the source and the target, so that target material is selectively removed from the unshielded locations.

B. Sample Scheme for In Vivo Observations

In order to separate the biological effects of the surface texture from chemical alterations at the surface caused by the ion beam, the following sample scheme was utilized (specific beam parameters are given in Table 4):

(1) As received: surfaces are those "as received" from the manufacturer. This would test for the soft tissue response of the material with no additional physical or chemical alterations.

(2) Textured: surface of interest was placed normal to the ion beam and ion etched. This would test for the soft tissue response to the developed "natural" texture.

(3) Masked: these samples were as received samples placed in the ion beam chamber, but covered by a piece of material of the same composition as that being treated (Teflon mask on Teflon sample). This would test for any effect the ion beam

environment might have on the material surface.

(4) Ion polished: the surface of the material was placed at a 10 degree angle to the beam axis and rotated while in the ion beam. In this manner, the material surface is exposed to the ion beam, but a "natural" texture is not developed. This would assay for the tissue response to any chemical alterations produced by the ion beam.

(5) ½ masked/½ texture: a sample was produced which was textured on one side and smooth on the other, due to the presence of a mask (mask was of same material being treated). Any difference in biological response could then be immediately observable.

Sheets of Teflon and Delrin (approximately 10 cm.x 10 cm.x 250μ) were processed using the preceding sample format. 250 μ Delrin sheet was obtained by machining 1/8 in. sheet. 1 cm. discs were punched out, cleaned, sterilized and implanted subcutaneously into the dorsum of Sprague Dawley rats so that the soft tissue response could be observed (263). Methods of analysis included standard histology (using parafin sections), enzyme histochemistry (using frozen sections), scanning electron microscopy, and transmission electron microscopy.

An additional variable of interest was the effect of material

TABLE 4. ION BEAM EXPOSURE PARAMETERS

MATERIAL	SURFACE CONDITION	ION BEAM ENERGY	ION CURRENT DENSITY	SPUTTERING DURATION	GRID TO SAMPLE DISTANCE
PTFE	Ion Polished[a]	500eV	.07 $\frac{mA}{cm.^2}$	3 Hr.	50 cm.
	Sputtered [b]	500	.4	.5	50
DELRIN	Ion Polished[a]	500	.07	3	50
	Sputtered[b]	500	.4	.5	50

a. Samples at a 10° angle with respect to ion beam axis and rotated at 2 revolutions/minute.

b. Both whole samples and textured sides of $\frac{1}{2}/\frac{1}{2}$ samples.

compliance on the soft tissue response. Thin Teflon discs were implanted and analyzed by standard histology and enzyme histochemistry. Thin "as received" Teflon discs were 1 cm. diameter x 125 μ (5 mil) thick. Thin "natural" textured Teflon discs were 1 cm. diameter x 50 μ (2 mil.) thick. The 2 mil textured Teflon was produced by ion beam etching the 5 mil "as received" Teflon to a 2 mil thickness. In this manner, Teflon samples of different compliance could be compared in terms of soft tissue response.

In summary, the parameters to be investigated in vivo include: textured versus smooth surfaces, Teflon versus Delrin, low compliance Teflon (10 mil) versus higher compliance (5 and 2 mil), and the possible alterations in tissue response caused by exposure of the material to the ion beam environment in a non-texturing manner.

C. Material Characterization

Teflon's chemical inertness has made it attractive as an implant material (14). Its tissue response is typically described as "well tolerated" when implanted in sheet form (3,31,124,190,206,216). Virgin Teflon was used in this investigation.

Delrin[1] is the commercial name for the homopolymer of formaldehyde and was the particular poloxymethylene used in this study (225). Delrin contains polymerization catalyst residues, stabilizers, and an antioxidant in addition to a lubricant (56). This polymer is highly crystalline and soluble only in strongly hydrogen bonding

---

1. E.I. DuPont de Nemours and Co., Wilmington, Delaware

TABLE 5.

PHYSICAL CONSTANTS OF POLYTETRAFLUOROETHYLENE AND POLYOXYMETHYLENE (28,56,196)

PROPERTY	UNITS	PTFE	DELRIN
Monomer Unit		$\left(\begin{matrix}F & F\\ C-C\\ F & F\end{matrix}\right)$	$\left(\begin{matrix}H\\ C-O\\ H\end{matrix}\right)$
Crystallinity	(wt. %)	762.3-(1524.5/Density)	64-74
Density	($gm./cm^3$)	2.15 - 2.29	1.42
Ultimate Elognation	(%)	320-350	20-70
Compressive Strength	(N/mm^2)	11.7	35.9
Tensile Strength	(N/mm^2)	31.0 - 33.1	69.1
Tensile Modules	(N/mm^2)	400	2600-3400
Melting Point	°C	342	181
Tg	°C	-112	-82

liquids (fluoroalcohols, fluoroketone hydrates) (27). Many of the investigations concerning the tissue response to Delrin have not been completed (56). It has been reported to develop a thicker fibrous capsule in comparison to ultra-high-molecular-weight polyethylene (UHMWPE) (56).

1. Scanning Electron Microscopy

Representative implants were examined by scanning electron microscopy. Surfaces were examined with either an ISI-Super IIIA[1] or Cambridge Stereoscan[2] model S4-10 SEM.

As received, masked, and ion polished PTFE samples revealed macroscopically smooth surfaces. At low magnification the surfaces are characterized by parallel grooves of variable widths and spacing believed to be skive marks made by the manufacturer during final sizing (Figure 3). Occasional surface scratches are also present. At higher magnification, holes of varying shapes were observed and believed to be the result of imcomplete sintering during manufacturer (Figure 4). These holes ranged in size from 0.1 μ to 5.0 μ in diameter. Further investigation into the effects of ion polishing on PTFE surfaces revealed a slight roughening. Extremely smooth surfaces were produced on PTFE by glass pressing (discussed in section III C.3.a). Ion polishing of these surfaces exhibited multi-directional grooves when viewed by the back-scattered electron (B.S.E.) mode on the ISI-Super IIIA S.E.M. (Figures 7 and 8).

---

1. International Scientific Instruments, Inc. Los Angeles, CA.

2. Cambridge Instrument Co., Cambridge, England.

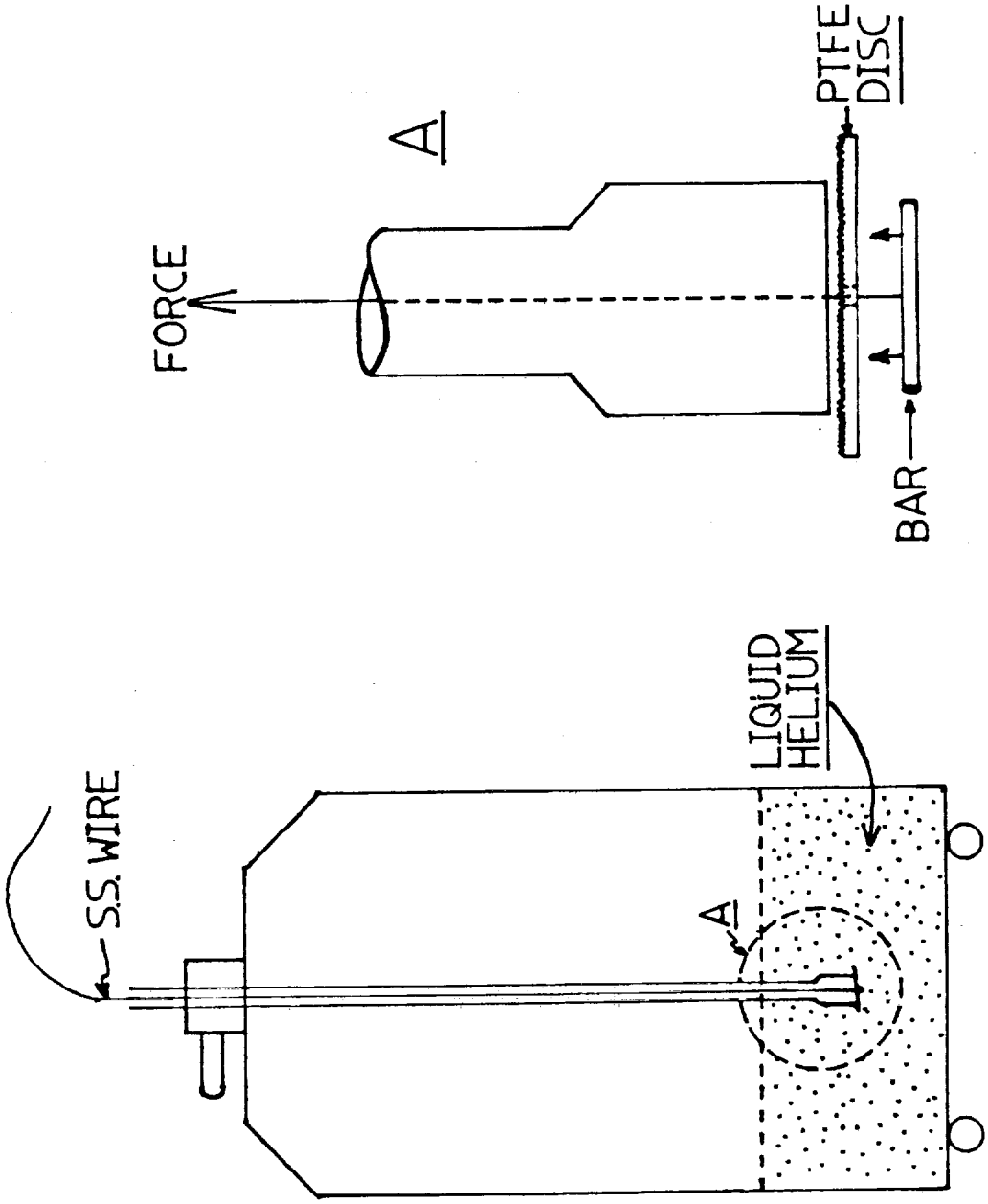

FIGURE 2. APPARATUS FOR FREEZE-FRACTURING PTFE

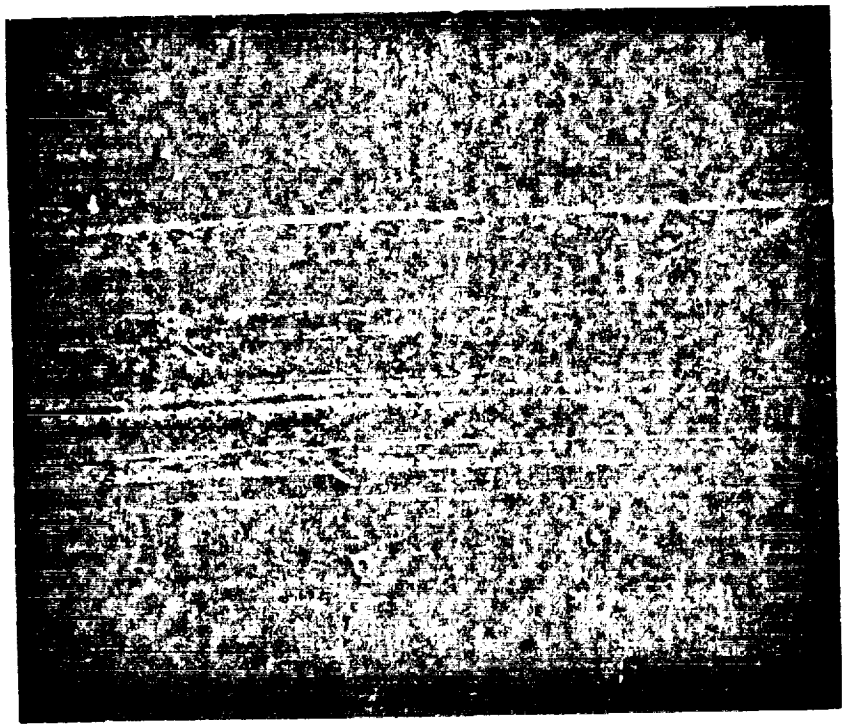

Figure 3. Surface of as received PTFE (100X).

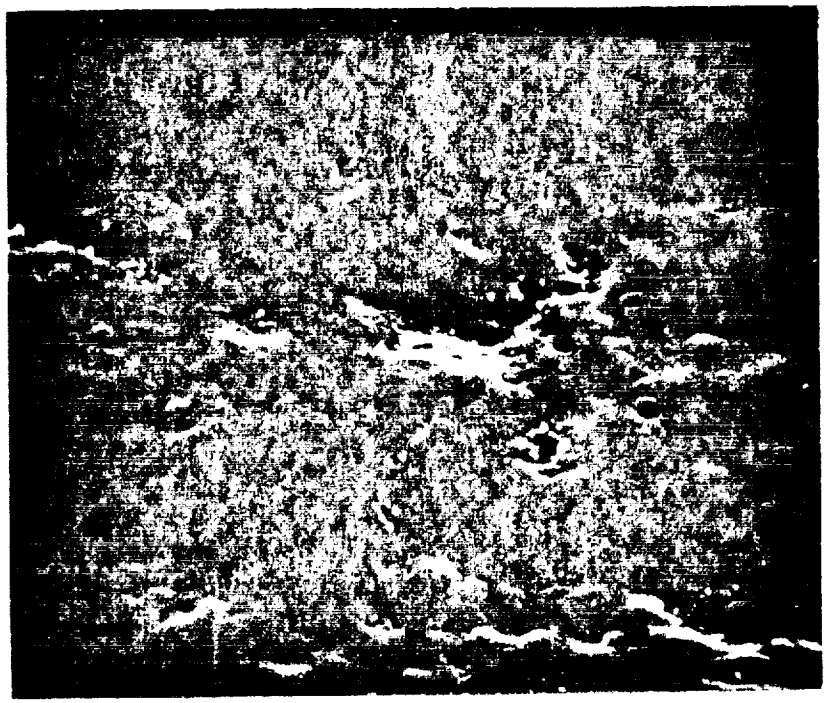

Figure 4. Microscopic pits on "as received" PTFE (5000X).

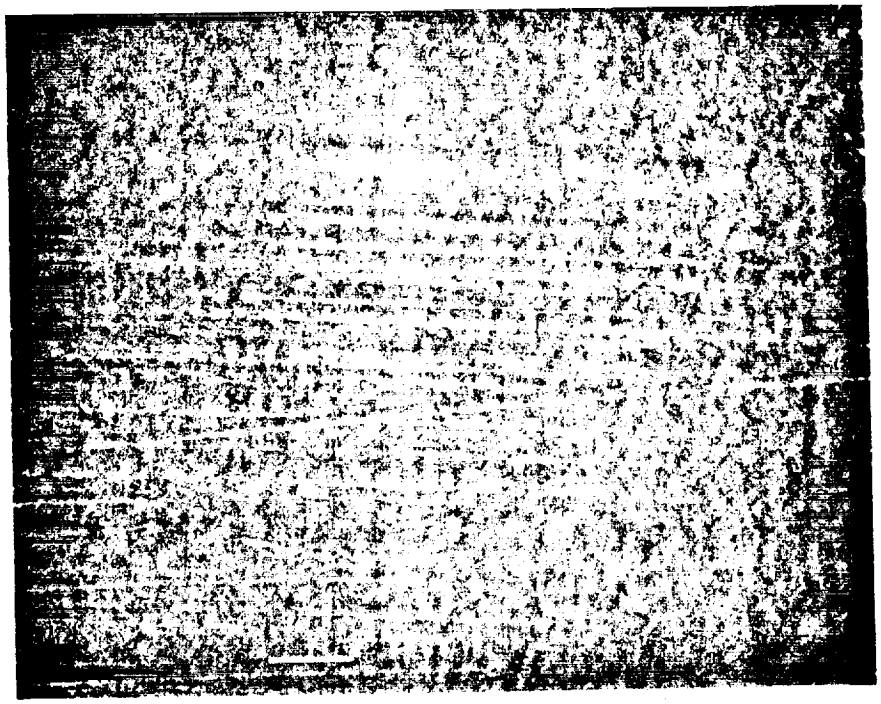

Figure 5. Surface of "ion polished" PTFE (160X).

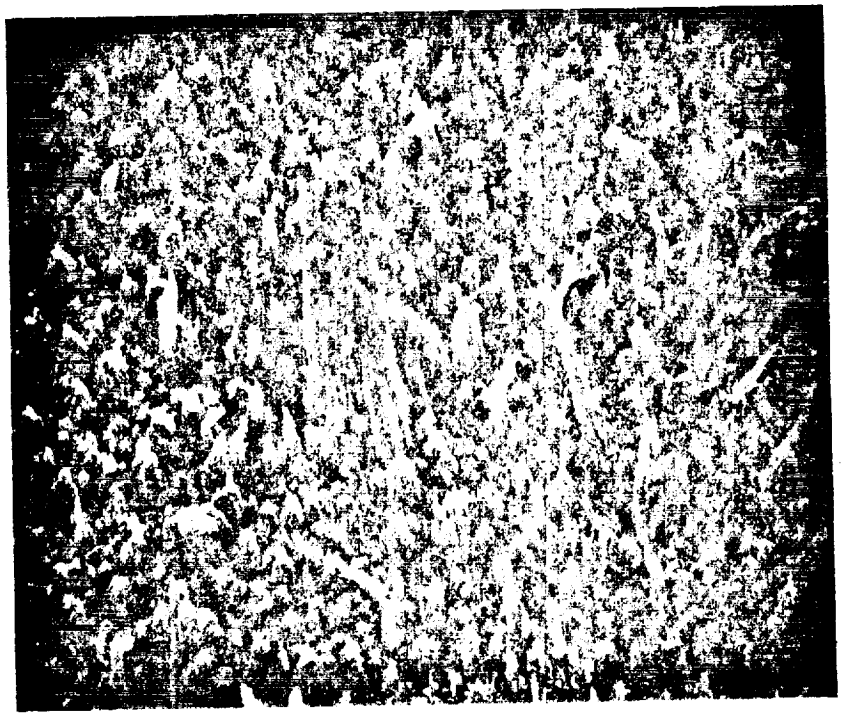

Figure 6. Surface of ion beam textured PTFE (500X).

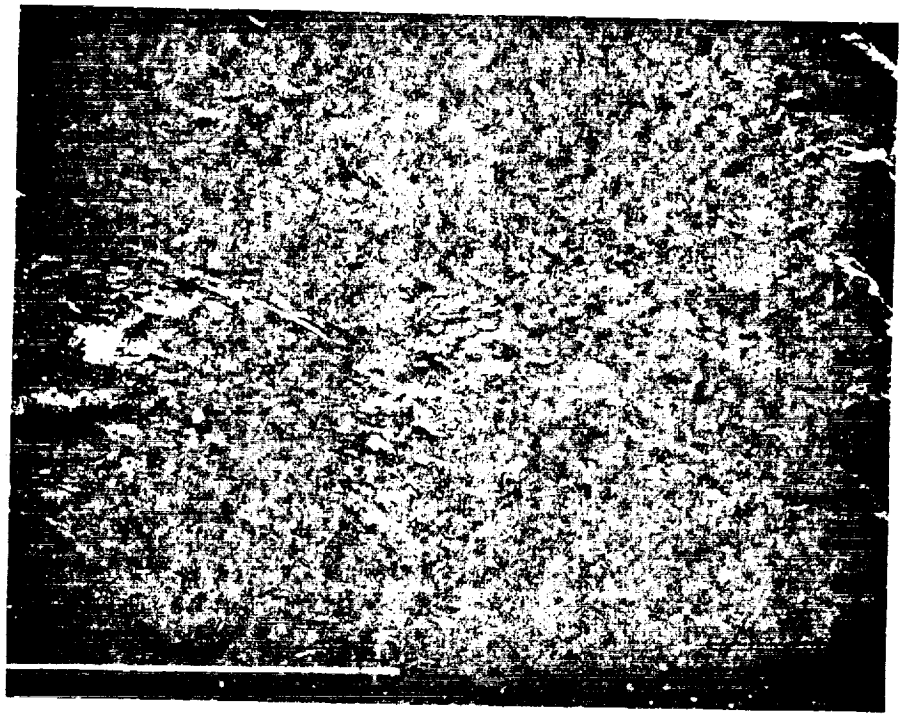

Figure 7. PTFE surface which has been heat pressed between glass slides (800X).

Figure 8. Glass-pressed PTFE which has been "ion polished" (800X).

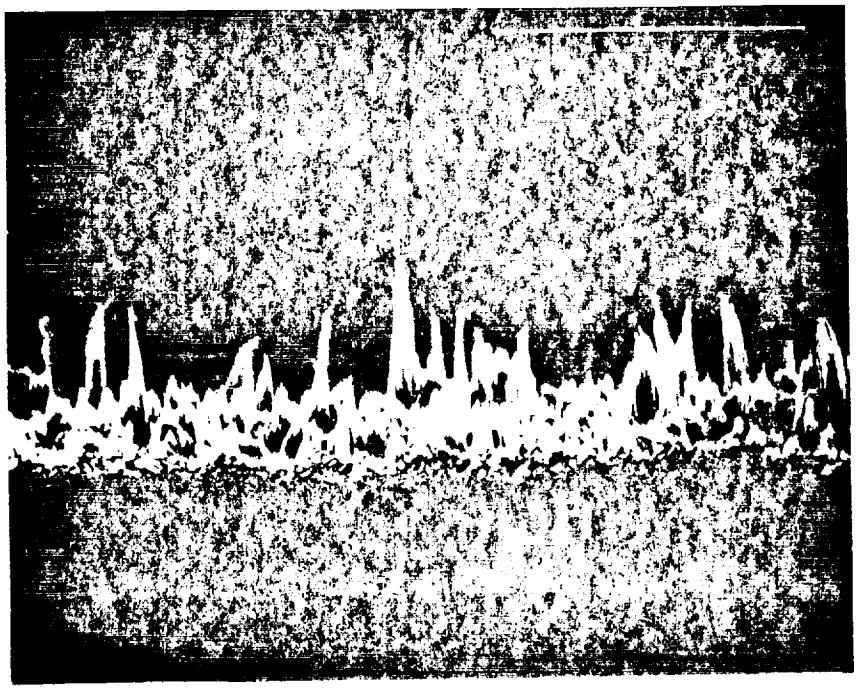

Figure 9. Cross-sectional view of ion beam textured PTFE (560X).

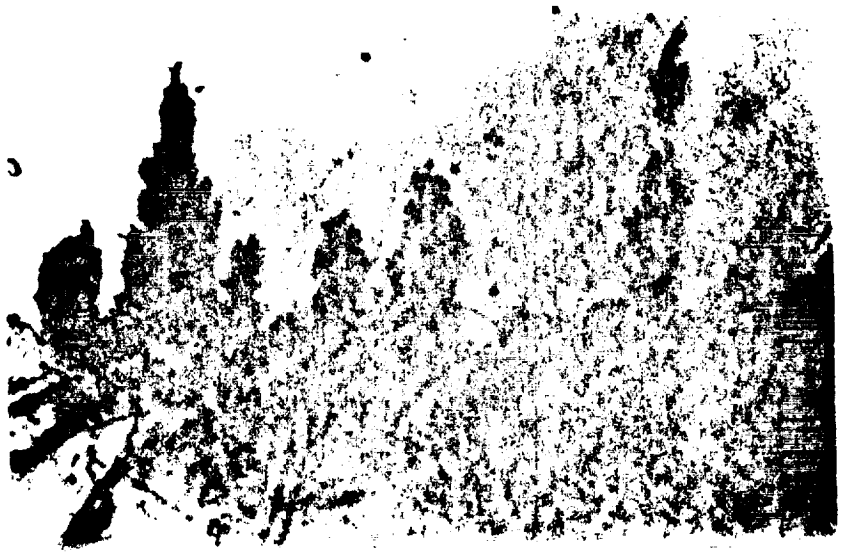

Figure 10. Cross-section of textured PTFE which has been embedded in epoxy (930X).

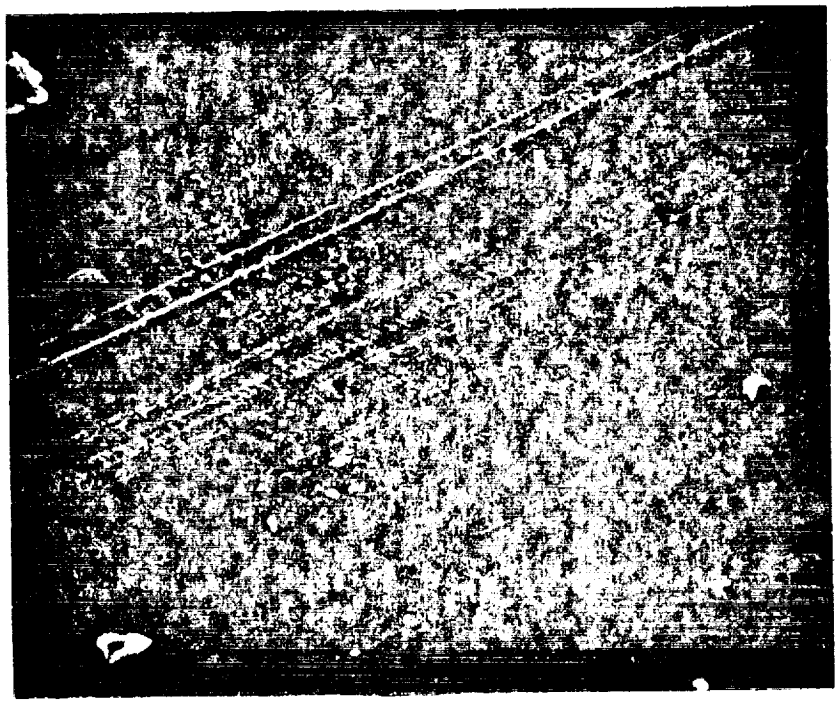

Figure 11. Surface of as received Delrin (500X).

Figure 12. Surface of "ion polished" Delrin (1600 X).

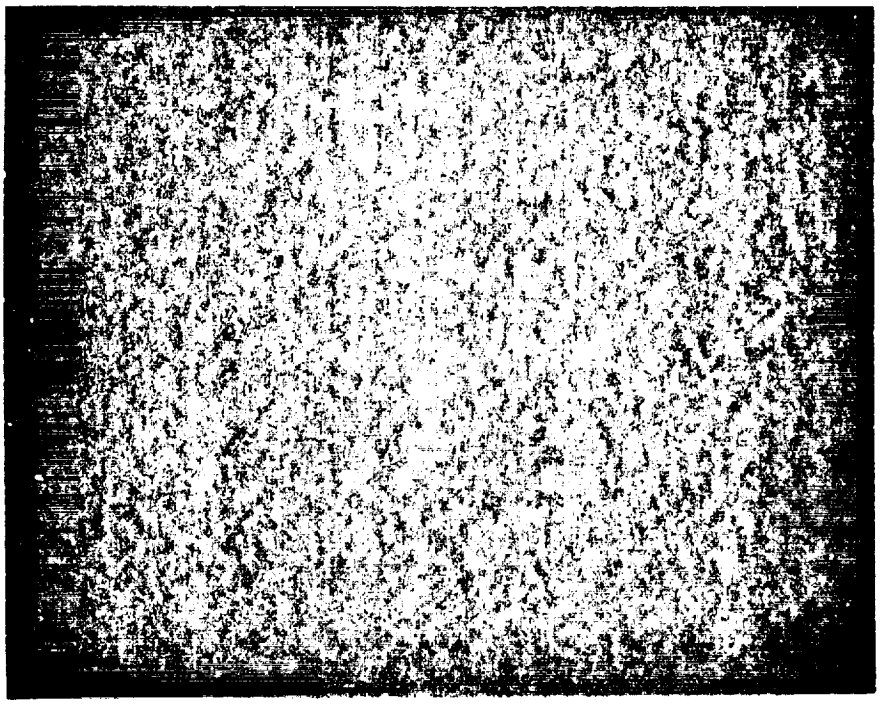

Figure 13. Delrin surface which has been heat pressed between glass slides (750X).

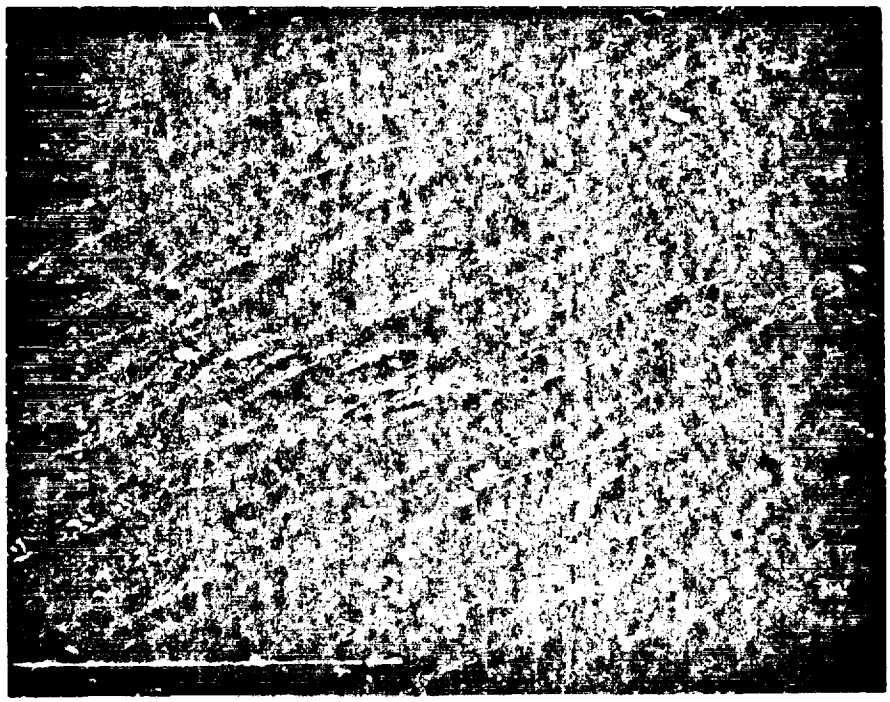

Figure 14. Glass pressed Delrin surface which has been "ion polished" (750X).

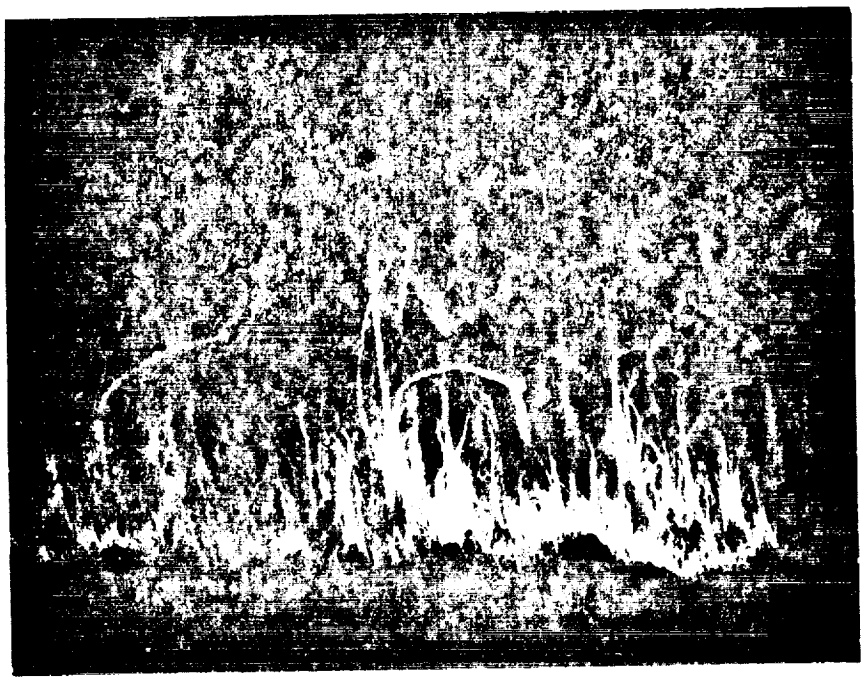

Figure 15. Cross-sectional view of ion textured Delrin (800X).

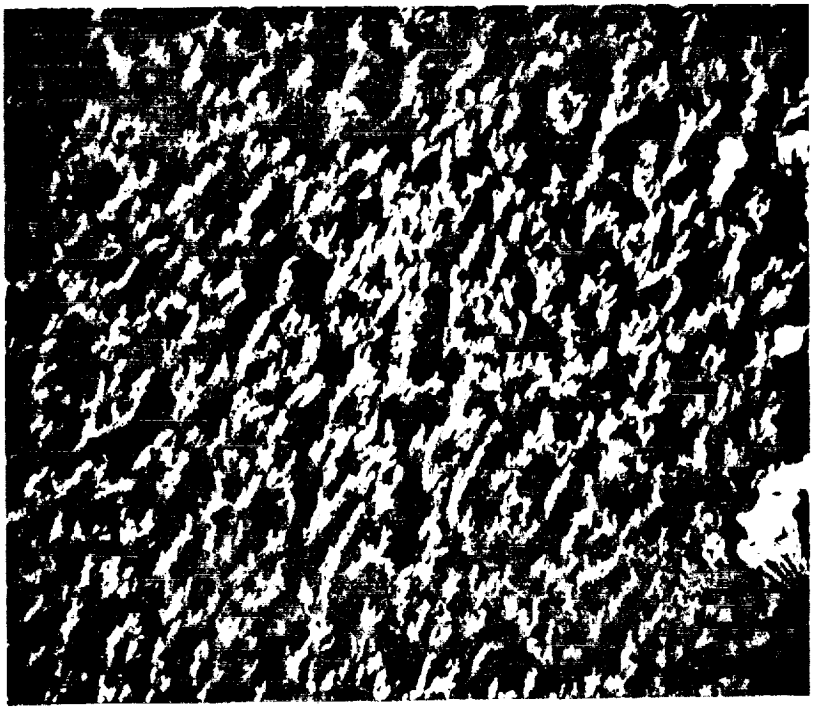

Figure 16. Surface of ion beam textured Delrin (2000X).

The surface of textured PTFE (Figure 6) was characterized by the presence of conical spikes of variable height and width (further quantification will be described subsequently). No gross pattern was observed, however, rows of spikes were occasionally seen and believed to have resulted from surface scratches. This surface was also present on the textured half of $\frac{1}{2}$ textured/$\frac{1}{2}$ masked samples.

As received, masked, and ion polished, Delrin samples were also macroscopically smooth, although ion polished samples had a "dull" finish. Low magnification of these samples revealed surface scratches probably produced by handling (Figure 11). Higher magnification of ion polished samples revealed surface "pores" approx. 0.1 to 0.5 μ in diameter (Figure 12). A roughening effect due to ion polishing was again exhibited on glass-pressed and ion polished glass-pressed Delrin surfaces (Figures 13 and 14).

The surfaces of textured Delrin had the appearance of coral (Figure 16). The projections were typically hair-like with a uniform shaft as viewed from the surface. Areas were observed where the hair structures had been "matted down" probably as a result of handling. The textured side of $\frac{1}{2}/\frac{1}{2}$ samples was similar to completely textured samples.

2. Cross-sectional Analysis of Textures

Random samples of ion beam etched Delrin and Teflon samples were chosen for texture quantification. Cross-sections were obtained by three methods: (1) embedding sections in epoxy and then sectioning and polishing, (2) freeze fracture, and (3) cutting with a razor blade.

Delrin and PTFE samples were placed on edge in 1.5 in. bakelite

ring forms containing uncured Hysol (Dexter Corp., Olean, N.Y.) epoxy media. After curing at room temperature for 24 hours, the epoxy blocks were cut in a plane normal to the sample surface so that the cross section at the disc diameter was exposed. The cross section surface was abraded en bloc with wet/dry silicone carbide papers in the following order: 180, 240, 320, 400, 600. This surface was thin polished on a Beuhler Polimet using 14 μ, 6 μ, 0.3 μ, and 0.05 μ metallographic polish. The polished cross-sections were examined by reflected light, Nomarski interference contrast microscopy on a Zeiss Ultraphot II microscope.

Textured PTFE cross-sections could be observed by this method. Representative areas of the texture were photographed at 300X. The following parameters were measured: spike height, base width of the spike, and the radius of curvature of the spike tip. Using three samples and approximately seven areas per sample, results for PTFE were obtained. These results are listed in Table 6.

Textured Delrin could not be deliniated from the surrounding epoxy by this method. An attempt was made to improve the relief between Delrin and epoxy by dissolving the epoxy with methylene chloride. This method was without success.

Freeze fractures were performed on textured Delrin and PTFE. Delrin samples were immersed in a Dewar flask containing liquid nitrogen (-196°C), extracted quickly and fractured by bending. PTFE was fractured in liquid helium (-268°C) using the apparatus shown in Figure 2. The difficulty of this method presented a need for an alternative. By placing a razor blade in a vice, PTFE discs could

TABLE 6. RESULTS OF TEXTURE ANALYSIS FOR TEFLON AND DELRIN
(Average Value ± S.D.)

MATERIAL	TEXTURE PARAMETERS	EPOXY SECTIONS	FREEZE FRACTURE	RAZOR SECTIONS
TEFLON[1]	Height (μ)	18.6± 9.8	4.7 ± 3.5	12.1 ± 7.1
	Base Width (μ)	6.7 ± 3.1	1.1 ± .5	4.5 ± 1.1
	Tip Radius (μ)	.2 ± .1	.2 ± .1	.1 ± .1
DELRIN	Heigth (μ)	N.A.	31.0 ± 12.1	N.A.
	Shaft Width (μ)	N.A.	1.0±.5	N.A.
	Tip Radius (μ)	N.A.	.08 ± .11	N.A.

1. There are noticably differences in texture dimensions between samples. Although the ion beam etching process is controllable, minor variations in beam parameters may vary the texture dimensions considerably.

be pushed onto the blade edge (textured side up) to obtain cross-sections of quality comparable to freeze fractures. The sliced sections were in effect better, because the problem of an uneven fracture surface was alleviated.

When a particular cross-sectioning technique could be applied, three samples were analyzed. The results are presented in Table 6.

3. Surface Changes Caused by Ion Beam Sputtering

a. Surface Elemental Compositon

The relative surface elemental content of ion beam treated and untreated samples was determined by Ion Scattering Spectroscopy (ISS) through the generosity of M.W. Feralli (Lord Corporation, Erie, PA.) This method permits elemental characterization by determining the fractional energy loss of a ^{3}He ion beam when it collides with the atoms of a sample. Since ^{3}He is very light, the target surface is essentially undisturbed by the analysis, and information is recorded only about the uppermost few atomic monolayers of the surface. It is the surface composition that is important when analyzing the tissue response at a material interface, not the bulk elemental composition which may be determined by more deeply penetrating analysis techniques.

Two samples of each surface treatment were analyzed. Samples were cleaned and autoclaved in the same manner as implant specimens. A .2 x .2 mm. area of each sample was scanned using a 2500 eV ^{3}He beam for 150 seconds. A .2 x .2 mm. area produces reasonable spatial averaging while a scanning time of 160 seconds assures little surface disturbance (63). Results are presented in Table 7.

The ion beam process appears to slightly enhance the F content

TABLE 7. SURFACE ELEMENTAL ANALYSIS OF TEFLON AND DELRIN SAMPLES USING ION SCATTERING SPECTROSCOPY

MATERIAL	SURFACE TREATMENT	RESULT
Teflon	As Received	A suppressed C peak along with the large F peak indicated a surface monolayer of F.
	Masked	Slight contamination was present, the contaminants were O, Al, and either Cu or Zn; source of contaminants was not determined.
	Textured	C peak was slightly broadened, indicating the F content of the monolayer is enhanced.
	Ion Polished	F content was slightly enhanced, some contanimation was present (K, Na).
Delrin	As Received	C and O are indicated in first monolayer.
	Masked	Similar to as received sample.
	Textured	The amount of C and O at the surface is slightly reduced, could be interpreted as enhanced H at the surface.
	Ion Polished	Similar to textured sample.

of Teflon surfaces and slightly reduce the C and O content of Delrin surfaces, according to ISS. Overall, ISS data indicates the texturing process introduces very little elemental alterations of the surfaces of either Teflon and Delrin outside of inconsistent contamination. This contamination could be a result of handling, cleaning, or autoclaving.

ESCA analysis of Teflon and Delrin reveal slightly different results (243). The F/C atom ratio at the Teflon surface was reduced slightly. Delrin shows a decrease in the O/C ratio at the surface from 0.75 to 0.16. The discrepancy between ISS and ESCA data may result from differences in surface penetration. Both analytical methods must be interpreted with some caution when considering a roughened surface.

b. Contact Angle Analysis

Contact angle measurements were used to determine the surface energy of the materials tested in this study and resolve the surface energy into its polar and London dispersion force components. The experimental technique employed was identical to that of Van Kampen (222), Parks (156), and Helmus (89). Due to slight curvature of the 1 cm. PTFE and Delrin discs, a thicker sample (1/8 in.) of the same materials was found more suitable for the analysis. All samples were processed in the ion beam, cleaned, and autoclaved in the same manner as the implant specimens.

The diagnostic liquids used were: distilled water (2 x, de-organified), glycerol, ethylene glycol, benzyl alcohol, 1-methylnapthalene, n-butyl acetate, ethanol, and n-heptane. All liquids were

TABLE 8.

THE CONTACT ANGLE LIQUIDS - DISPERSION AND POLAR COMPONENTS OF THE SURFACE TENSION (222).

Liquid	γ_1^d	γ_1^p	γ_1
1. Water	21.8 dynes/cm.	51.0 dynes/cm.	72.8 dynes/cm.
2. Glycerol	37.0	26.4	63.4
3. Ethylene Glycol	31.9	15.8	47.7
4. Benzyl Alcohol	36.6	2.4	39.0
5. Methyl Napthalene	38.7	0	38.7
6. n - Butyl Acetate	22.5	2.7	25.2
7. Ethanol	17.5	5.2	22.7
8. n - Heptane	20.3	0	20.3

of spectroscopic grade. The surface tension and surface energy components of the diagnostic liquids are listed in Table 8.

Contact angle measurements were made in a constant temperature-constant humidity room (20°C, 50% R.H.). A 20 µl drop of liquid was placed on the test material in air. The advancing angle was measured on both sides of circular drops only. Back lighting provided adequate delination of the drop profile while angle measurements were made with a goniometer telescope. Addition of another 20 µl provided 2 more measurements of the advancing angle. The receding angle was obtained by decreasing the drop volume until the periphery of the drop just recedes. Two samples of each material were tested to give the average angles listed in Tables 9 and 11. Contact angles could not be obtained for textured samples of either PTFE or Delrin due to wicking (106).

A surface without adsorbed molecules, chemical heterogeneity or surface roughness greater than 0.5 µ should not exhibit contact angle hysteresis (106). Others suggest the surface roughness must be less than 0.1 µ for hysteresis to be absent (73,74). In the experimental set-up used, a hysteresis of greater than 6° was considered significant due to a $\pm$ 3° error inherent in the goniometer measurement (89,222). All PTFE samples displayed a large hysteresis (see Table 9). Intuitively, this should not occur because PTFE is chemically homogeneous and adsorbs ions with difficulty. It was assumed that the skived surface as seen in Figure 3 was responsible for producing the hysteresis. Supporting this hypothesis, internal reflection was noticed underneath higher viscosity liquids due to

trapped air in the grooves. This produces a composite effect, creating surface heterogeneity (106).

To alleviate any physical heterogeneity on PTFE that might cause hysteresis, the following method was employed to produce "glass-like" surface:

- cut strips of material (3.2 x 7.5 x 0.6 cm)
- clean glass slides (2 per piece of material) in detergent ultrasonically
- heat press samples between glass slides at 10,000 psi and 300°F for 18 hours

These surfaces were treated in the appropriate beam environment and used for contact angle measurements. The data in Table 10 was obtained from the glass pressed samples and used in the surface energy analysis. The hysteresis observed with ion polished PTFE was attributed to a slight roughening of the surface described in Section III.C.1.

Commercially produced molded surfaces of Delrin were analyzed in the same manner as PTFE. The contact angles for these surfaces are listed in Table 11. Hysteresis existed for all Delrin samples and was ascribed to small scratches on as received and control samples. Sharp edges have been described as an important factor in contact angle hysteresis (152). The hysteresis observed on ion polished samples was again assigned to a roughening effect by the process (see Figure 14). An attempt to heat press Delrin between glass slides resulted in a decrease in the polar component and increase in the dispersion component of the surface energy. This observation

TABLE 9.

ADVANCING AND RECEDING CONTACT ANGLES MEASURED IN DEGREES FOR PTFE

	Diagnostic Liquids[a]								
SURFACE TREATMENT	1.	2.	3.	4.	5.	6.	7.	8.	
As Received	114	113*	105*	72*	76	30	30	15	Advancing Angles
Ion Polished	89	77*	77*	52*	54	32	17	wets	
Masked	108	117*	109*	75*	73	34	34	15	
As Received	110	89*	83*	60*	59	29	23	wets	Receding Angles
Ion Polished	60	62*	48*	22*	52	wets[b]	wets	wets	
Masked	107	100*	86*	56*	63	29	28	wets	

a - Liquids are summarized in Table 8.

b - Liquid spreads on surface.

* - Composite affect noticed.

TABLE 10.

ADVANCING AND RECEDING CONTACT ANGLES MEASURED IN DEGREES FOR GLASS PRESSED PTFE

SURFACE TREATMENT	Diagnostic Liquid[b] 1.	2.	3.	4.	5.	6.	7.	8.	
As Received	107	98	87	74	71	45	36	9	Advancing[a] Angles
Ion Polished	102	95	79	73	60	29	34	wets	
Masked	107	98	88	76	68	45	37	6	
As Received	107	96	85	70	70	45	35	5	Receding Angles
Ion Polished	85	76	55	53	32	wets	wets	wets	
Masked	106	98	88	74	71	44	36	5	

a. Values used for the surface energy analysis.

b. Liquids summarized in Table 8.

TABLE 11.

ADVANCING AND RECEDING CONTACT ANGLES MEASURED IN DEGREES FOR DELRIN

SURFACE TREATMENT	Diagnostic Liquid[a] 1.	2.	3.	4.	5.	6.	7.	8.	
As Received	67	71	55	11	11	wets[c]	wets	wets	Advancing[b] Angles
Ion Polished	64	66	40	wets	wets	wets	wets	wets	
Masked	66	71	54	11	11	wets	wets	wets	
As Received	52	33	21	wets	wets	wets	wets	wets	Receding Angles
Ion Polished	wets	wets	wets	wets	wets	wets	wets	wets	
Masked	56	37	22	wets	wets	wets	wets	wets	

a. Liquids are summarized in Table 8.

b. Used for energy analysis.

c. Liquid spreads on surface.

was not understood and may have resulted from contamination. Surface energy analysis was therefore performed on the original non-heat pressed samples.

Computational methods of Nyilas (148) and Kaelble (107) were used in the analysis of the dispersion and polar force contributions. This method assumes that the total surface energy may be expressed solely as a sum of polar and dispersion forces and that other force components, such as hydrogen and Π-bonding, may be included in the polar force component (222). Some have suggested a possible need for adding hydrogen bonding forces as a third and separate component (7).

The reversible work of adhesion may be expressed as follows (107,272):

$$W_a = \gamma_s + \gamma_{lv} - \gamma_{sl} \qquad (1)$$

γ_s = surface tension of the solid under vacuum

γ_{lv} = liquid surface tension in equilibrium with its vapor

γ_{sl} = interfacial tension between solid and liquid

Young's equation relates the forces existing at a drop of liquid in equilibrium with a solid (65,106,152).

$$\gamma_{sv} = \gamma_{sl} + \gamma_{lv} \cos \theta \qquad (2)$$

This equation may be rearranged and substituted into equation (1) to give:

$$W_a = \gamma_s - \gamma_{sv} + \gamma_{lv} (1+\cos \theta) \qquad (3)$$

The quantity $\gamma_s - \gamma_{sv}$ is the spreading pressure and is usually expressed as π (106). For non-wetting liquids and for surfaces whose predominant energy component is dispersion forces, $\pi = 0$ (64,73,106).

Fowkes has shown the interfacial surface tension, γ_{sl}, to be (64):

$$\gamma_{sl} = \gamma_s + \gamma_{lv} - 2\,(\gamma_s^d \gamma_l^d)^{\frac{1}{2}} - 2\,(\gamma_s^p \gamma_l^p)^{\frac{1}{2}} \qquad (4)$$

and the work of adhesion to be:

$$W_a = 2\,(\gamma_s^d \gamma_l^d)^{\frac{1}{2}} + 2\,(\gamma_s^p \gamma_l^p)^{\frac{1}{2}} \qquad (5)$$

The superscripts refer to the polar (p) and dispersion (d) components of the surface tension of the solid (s) and liquid (l). By equating equations (5) and (3), assuming $\pi = 0$, and dividing by 2, equation (6) is derived (89):

$$\frac{W_a}{2} = (\gamma_s^d \gamma_l^d)^{\frac{1}{2}} + (\gamma_s^p \gamma_l^p)^{\frac{1}{2}} = \gamma_{lv}\,(1 + \cos\theta)/2 \qquad (6)$$

The dispersion and polar components of the liquid are known, leaving the dispersion and polar components of the solid as unknowns. From a pair of liquids, the following set of equations may be written:

$$\left.\begin{aligned} (W_a/2)_i &= (\gamma_l^d)_i^{\frac{1}{2}}\,(\gamma_s^d)^{\frac{1}{2}} + (\gamma_l^p)_i^{\frac{1}{2}}\,(\gamma_s^p)^{\frac{1}{2}} \\ (W_a/2)_j &= (\gamma_l^d)_j^{\frac{1}{2}}\,(\gamma_s^d)^{\frac{1}{2}} + (\gamma_l^p)_j^{\frac{1}{2}}\,(\gamma_s^p)^{\frac{1}{2}} \end{aligned}\right\} \qquad (7)$$

Equation (7) can be rearranged into standard determinant form (107):

$$\gamma_{sij}^d = \frac{\begin{vmatrix} (W_a/2)_i & (\gamma_l^p)_i^{\frac{1}{2}} \\ (W_a/2)_j & (\gamma_l^p)_j^{\frac{1}{2}} \end{vmatrix}^2}{D_{ij}^2} \qquad (8)$$

$$\gamma^{p}_{sij} = \begin{vmatrix} (\gamma^{d}_{l})^{\frac{1}{2}}_{i} & (W_a/2)_i \\ (\gamma^{d}_{l})^{\frac{1}{2}}_{j} & (W_a/2)_j \end{vmatrix}^2 \Big/ D^2_{ij} \qquad (9)$$

$$D_{ij} = \begin{vmatrix} (\gamma^{d}_{l})^{\frac{1}{2}}_{i} & (\gamma^{p}_{l})^{\frac{1}{2}}_{i} \\ (\gamma^{d}_{l})^{\frac{1}{2}}_{j} & (\gamma^{p}_{l})^{\frac{1}{2}}_{j} \end{vmatrix} \qquad (10)$$

γ^{p}_{sij} and γ^{d}_{sij} were averaged over paired combinations of diagnostic liquids. This average has been termed, the composite surface free energy function (CSFEF)(48). Paired combinations were calculated for an absolute value of D greater than 10 (89) and thus decrease the probability of inconsistencies in the calculations (107). When hysteresis was insignificant, advancing and receding angles were averaged. When hysteresis did exist, only advancing angles were used (162).

The critical surface tension, γ_c, was determined for each surface by applying linear regression to cos θ vs. $1/(\gamma_l)^{\frac{1}{2}}$ (74). Table 12 summarizes the results.

Summary

The ion beam and the ion beam environment do not alter to a statistically significant degree, the surface energy components of the materials tested. The γ_c measurements for as received, and masked samples of Teflon and Delrin are in close agreement with published values (7,64,156,162). The slight increase in γ_c for Teflon and Delrin may be a result of the slight roughening caused by the

TABLE 12. RESULTS OF SURFACE ENERGY ANALYSIS OF TEFLON AND DELRIN

(ergs/cm^2)

MATERIAL	SURFACE TREATMENT	$\bar{\gamma}^p \pm$ S.D.	$\bar{\gamma}^d \pm$ S.D.	$\bar{\gamma}_c \pm$ S.D.	R*
Teflon	As Received	.4 ±.2	18.1 ± 1.8	20.2	.99
	Masked	.3 ±.3	18.1 ± 2.3	20.2	.996
	Ion Polished	.8 ±.4	18.6 ± 3.3	22.2	.981
Delrin	As Received	39.1 ± 9.3	2.6 ± 2.4	37.6	.925
	Masked	38.8 ± 7.8	3.0 ± 2.5	37.7	.917
	Ion Polished	33.4 ± 5.3	5.9 ± 4.0	39.4	.911

*. R=Correlation Coefficient for Linear Regression of cos θ vs. $1/(\gamma_1)^{\frac{1}{2}}$ used to determine γ_c.

"ion polishing" process. The correlation coefficients indicating the linearity of cos θ vs. $1/(\gamma_1)^{\frac{1}{2}}$ are less for Delrin than for Teflon. This may be a result of strong H-bonding interactions causing deviation from the expected linearity. The largest deviations from these regressions occur with water whose γ_1^d component has not been completely agreed upon (222).

4. Formaldehyde Release from Delrin

The polyoxymethylene chain is completely linear and consists exclusively of oxymethylene links. Hydroxyl groups are the most common end group. The polyoxymethylene chain is stable to base, but is slowly cleaved by acid. Hydroxyl end groups are attacked by either acid or base. Following chain cleavage or end group attack, depolymerization occurs via an unzipping reaction which can occur in either acid or basic media (27). Depolymerization gives monomer (formaldehyde) as the sole produce (27,56). Formaldehyde is a known toxic substance.

The polymer chains within Delrin have been end blocked with appropriate groups (27) by the manufacturer to prevent hydrolysis and subsequent unzipping. However, formaldehyde is released from Delrin, and is believed to be a leaching of monomer trapped within the polymer.

The amount of formaldehyde released from Delrin was determined by a colorimetric method described by Stone(200). Two samples were tested - textured and as received. A 5.0 x 1.0 x 0.3 cm. strip of each sample was placed in a vial containing 20 ml. of 2 x distilled deorganified water. The vial was sealed and left at room temperature

for 3 weeks. At the end of this time period, the water was tested for the presence of formaldehyde. Formaldehyde undergoes a reaction with chromotropic acid (1,8 - dihydroxynaphthalene 3,6 - disulfonic acid) in the presence of concentrated sulfuric acid (90% or higher) to form a purple color (see appendix A for procedure). The absorbancy of the elluant from the textured, as received, and a water control was measured on an American Optical Spectrophotometer at 520 nm. Calibration was obtained by diluting formaldehyde of known concentration (35%) by factors of 10^{-4}, 5×10^{-5}, 10^{-5}, 5×10^{-6}, 10^{-6}, 5×10^{-7}, and 10^{-7}, and then processing by the same colorimetric procedure.

The same samples were reimmersed in 20 ml. of fresh water and retested by the above procedure after 3 weeks. This entire procedure was repeated for a third and final 3 weeks.

The data is presented in Figure 17. The textured Delrin released formaldehyde at a greater rate than the smooth surface. This could be a result of either increased surface area, increased sites for hydrolytic attack caused by chain scission, or a combination of these factors. The release kinetics for both samples is first order, indicating possibly a diffusion limited process. By 9 weeks, the amount of formaldehyde detected was similar for both samples. If release rates from previous work (56) are extrapolated and averaged for a 3 week period, the predicted value is very close (within 10%) to the value obtained experimentally for the 3 week as received sample.

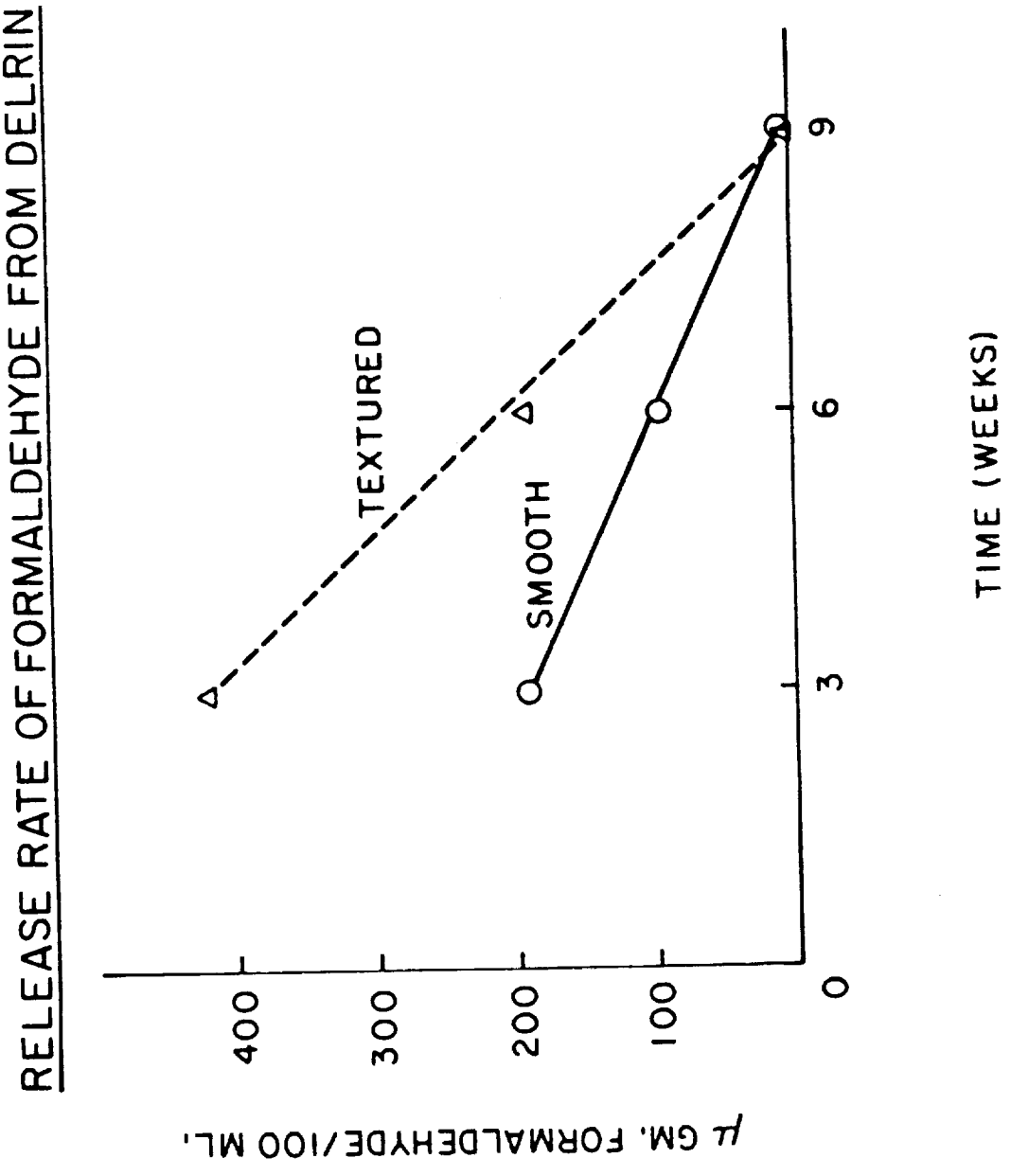
RELEASE RATE OF FORMALDEHYDE FROM DELRIN
TEXTURED
SMOOTH
400
300
200
100
0
3
6
9
μ GM. FORMALDEHYDE/100 ML.
TIME (WEEKS)

FIGURE 17

D. In Vivo Methods

1. Sample Preparation for Implantation

All implant samples were cleaned and sterilized in the same manner. Samples were received from NASA with the treated surfaces face up. The samples were then placed in a PTFE cage which was of small enough inner dimensions to prevent the samples from turning over, thus maintaining orientation. Samples were left in the PTFE cages during all cleaning processes. Samples were cleaned ultrasonically in acetone for 15 minutes. This was repeated with fresh acetone. Samples were then cleaned ultrasonically with ethanol (95%) for 15 minutes, which was again repeated with fresh ethanol. The samples were rinsed ultrasonically in 2 x distilled H_2O for 5 min., placed in fresh 2X distilled H_2O and autoclaved for 30 to 45 min. Samples were left (covered) in the autoclaved water until implantation.

2. Implantation Procedure

a. Animals

Sprague-Dawley male rats (Zivic-Miller) were individually caged prior to and after surgery. The animals weighed from 250 to 400 gm. at surgery and were maintained on standard rat pellets (Purina) and water ad libidum.

b. Anaesthesia

At the time of implant surgery, the animal was anaesthetized with anaesthesiagrade ether (Squibb). When voluntary movements had ceased, the animal was removed from the vessel and prepared for surgery. The proper level of anaesthesia was maintained by the use

of a nose-cone containing ether-soaked gauze. The level of anesthesia was monitored by observing the breathing pattern, eye color, and extent of bronchial congestion.

c. Surgical Preparation

After the rats were carefully clipped with fine-bladed animal clippers, the skin was thoroughly scrubbed with phisohex^{R} soap and shaved with a surgical prep blade at the areas of incision. The skin was then rinsed with Zepharin^{R} chloride solution (1:750) and rescrubbed with Betadine^{R}. All instruments were maintained in a tray of Zepharin choride solution.

d. Implantation

Implant samples were removed from the autoclave vessel and placed in zepharin chloride solution prior to implantation. A 1.5 cm. incision was made perpendicular to the spinal column in each of 4 quadrants of the dorsal surface. A subcutaneous pocket was prepared by blunt dissection and the specimens inserted immediately adjacent to the facia of the intercostal musculature. Sample discs were placed in the pocket with the surface of interest facing down. Shams (subcutaneous pockets without implants) were performed to observe the normal healing response. The implants were distributed among the sites such that each surface condition was at one point implanted in each quadrant. This eliminated the effect of implant location in the analysis (108). The incision was closed with 2 or 3 stainless steel wound clips (9 mm. autoclip), and covered with Betadine.

3. Sample Retrieval and Preparation

After the implant had been in place for the intended time period, the animal was sacrificed by ether overdose. The wound clips were removed, and the animal was shaved. The skin over the dorsal surface was resected at the level of the skeletal muscle underlying the implant. The pelts were fixed in either formalin or glutaraldehyde, or frozen, depending on the observation technique to be used.

a. Light Microscopy

The pelt containing the implants was placed in either 10% buffered formalin (pH 7.4) or 2.5% glutaraldehyde buffered with sodium cacodylate (pH 7.4). After fixation for 7 to 14 days, each implant was removed from the pelt en bloc. The block of tissue containing the sample disc or sham site was cut into thirds and placed in vials containing formalin (if fixed in same) or .2M cacodylate buffer (if fixed in glutaraldehyde). These sections were embedded in parafin, cut, and stained with, hemotoxylin and eosin (H and E) and Masson's trichrome stains using standard histological techniques. All histology sections came from within 1.5 mm. of the implant disc diameter. These sections represented the primary source for microscopic analysis which will be described subsequently. Extra samples were placed in vials containing the appropriate solution (formalin or cacodylate buffer) and stored at 4°C for future reference if additional samples were needed for analysis.

b. Enzyme Histochemistry

The type and number of cells responding to the presence of an

implant can be evaluated by standard histological preparations, but this does not take into account changes in cell function. Application of enzyme histochemistry to the study of cell function offers the only means available for examining enzyme systems associated with particular cells and their activity (185). Because certain enzyme systems are associated with a particular cell type, the investigator does not have to rely solely on the subjective morphologic evaluation of the cell types in judging the tissue response (182-187).

Three enzyme systems were investigated. Acid phosphatase is the most prominent hydrolase found in association with macrophages and FBGC's. Alkaline phosphatase is typically associated with neutrophil activity, and succinic dehydrogenase (SDH) is an indicator of cell metabolic activity and level of energy utilization (140,182,187).

Because fixation reduces or inactivates the enzyme activity, frozen sections were employed. For these applications, the cryostat microtome is essential. PTFE was sufficiently soft to be left in the frozen tissue and cut on the cryostat, but Delrin was too hard and had to be removed from the tissue.

After the pelt containing the samples were resected, a 1.2 x 1.2 cm. block of tissue containing the disc was cut out. If Delrin was present, an incision was made at the edge of the implant so that the disc could be carefully extracted. The tissue block was then frozen quickly by immersion into isopentane (2-methyl-butane) cooled in liquid nitrogen. The frozen tissue block was transferred to a vial and stored in dry ice while being transported to a storage

freezer (-60°C). Frozen sections (approximately 10 μ thick) were cut on an American Optical Cryo-Cut cryostat microtome. Sections were stored at -60°C until stained. The staining procedures are outlined in appendices B, C, and D.

c. Scanning Electron Microscopy

Samples reserved for scanning electron microscopy were fixed en bloc with 2.5% buffered glutaraldehyde. After fixation, the inferior capsule was cut along the edge of the implant and carefully retracted to prevent disturbance of biological tissue at the implant surface. The implants were carefully reimmersed into glutaraldehyde. SEM examination requires dehydration of biological specimens which was accomplished by critical point drying. Freon 13 (monochorotrifluoroethane, T_c = 29°C, P_c = 39 atm.) was used for this process. The following procedure was used:

. Equilibrate specimens for 30 min. in each of the following solutions:

Ethanol - 50%, 70%, 90%, 100%, 100%

Freon 113 - 50%, 70%, 90%, 100%, 100%

. After last change to 100% Freon 113 (trichlorotrifluoroethane), critical point dry from Freon 13.

. Store dried specimens in dissicator until needed

Samples were examined with either a Cambridge Steroscan Model S4 10, or an ISI - Super III A SEM.

d. Transmission Electron Microscopy

Transmission electron miscoscopy (TEM) was utilized to observe the ultrastructural details of cells in the immediate vicinity of the

implant surface. This technique allows identification of cell type and structural details not discernable with optical microscopy.

Textured and smooth (as received or masked) samples of 1, 4, and 8 week implants of Delrin and PTFE were selected for TEM. The following preparation was used:

. Implants were fixed en bloc in 2.5% glutaraldehyde (buffered with sodium cacodylate) at 4°C for approximately 7 days.

. Tissue blocks (containing sample discs) were transferred to .2M cacodylate buffer at 4°C.

. Specimens (1.5 x 2.5 mm) were cut from inferior capsule so that tissue/material interface was maintained (preserved in all samples except smooth PTFE implants)

. Specimens were post-fixed with 1% O_sO_4 in 0.2M cacodylate buffer for 2 hr. at 4°C.

. Rinse in .2M carodylate buffer for 15 min. x 3.

. Rinse in distilled H_2O for 5 min.

. Dehydrate by equilibrating specimens for 15 min. in each of the following: Ethanol - 50%, 70%, 80%, 90%, 100%, 100%

. Place in: ethanol/propylene oxide (1:1) for 30 min.
propylene oxide for 30 min.
propylene oxide/epon (1:1) for 1 hr.
(Epon = Epon A/Epon B = 1/1)

. Place in Epon overnight at room temperature in the dark.

. Place specimens in Epon (A/B = 1/1) + 1.5% DPM - 30 and cure at 37°C for 2 days followed by 45°C for 2 days and 60°C for 2 days.

The blocks were trimmed and thick sections (1 μ) were cut and stained with toluidine blue to identify areas of interest. Thin sections (approximately 900 Å) were cut on the ultramicrotome using a diamond knife. Specimens were picked up on Cu or Ni grids and stained for 30 min. with uranyl acetate and 30 min. with lead citrate. Specimens were examined on either a JOEL 101-B or Philips 201C electron microscope.

E. Evaluation Methods for Light Microscopy

Four parameters were evaluated from the parafin sections of the tissue surrounding the implant materials: the capsule thickness, the number of specific cell types, the cell density, and the degree of vascularization. Only the inferior capsule and tissue were considered. All counts and measurements were performed on fields selected randomly in the middle one third of the tissue section to eliminate any problem of edge effects (135). All counts and measurements were made at 400 X with a Nikon model L-Ke microscope using a grid in the occular lens. An average of 3 implants were examined for each data point.

1. Capsule Thickness

The fibrous capsule was defined as the newly formed layer of collagen adjacent to the implant and was measured in microns to the nearest 5 μ. Cells that remained attached to the implant upon sectioning were not included. The capsule was not always clearly definable. Often a row of capillaries adjacent to the exterior of the capsule aided in the identification of the line of demarcation. Trichrome stain also aided in capsule delineation. At least 4 capsule

measurements were made for each of two sections per implant.

2. Differential Cell Counts

By use of a superimposed grid image, it was possible to count cells within a specified reaction zone parallel to the implant surface. The 200 x 200 μ grid was divided into 10 μ squares (at 400X). This grid was placed over the capsule. Only those cells within the capsule and within the 200 μ grid boundary were counted. This counting zone was termed the "field". Cells attached to the implant were not counted. This was repeated until a total of one hundred cells had been counted. Each one hundred cell analysis constituted one differential cell count. One differential cell could was performed on each of two sections per implant. By counting 100 cells per count, the types of cells could be averaged as a percentage. In the case of a sham site or an implant not having a fibrous capusle, the field was taken as a 200 x 200 μ area adjacent to the implant or within the connective tissue where the blunt dissection had been performed. Adipose tissue was excluded from the field of interest, so in some situations, the area being quantified was less than 200 x 200 μ. An attempt was made to distinguish between seven types of cells.

a. Polymorphonuclear Leukocytes (PMN, poly, neutrophil)

This cell, active in early inflammation and phagocytosis or micro-organisms, is identifiable by a lobulated nucleus with several connected segments (2-5). The cytoplasm is slightly amphophilic(22,44,126,247).

b. Fibroblasts

The fibroblast is typically large and ovoid when actively producing intercellular materials. The nucleus is large with prominent nucleoli and the cytoplasm is slightly eosinophilic. A quiescent fibroblast (fibrocyte) is spindle shaped with a tapering eosinophilic cytoplasm. The nuclei are elongated and darkly staining (44,247). The fibroblast and fibrocyte were considered as the same cell during cell counts.

c. Macrophages

The macrophage has a more rounded nucleus that is smaller and more darkly staining than the fibroblast. When actively phagocytic, the cytoplasm is more heterogeneous than the fibroblast and appears "foamy". This was the distinguishing characteristic used during cell counts. Monocytes were counted as macrophages as well. These cells have a reniform nucleus with scant, slightly basophilic cytoplasm (22,44).

d. Lymphocytes

Lymphocytes in fixed tissue, are from 5-8 μ and have a large, spherical intensely staining nuclei that occupies almost the entire cell (44,247).

e. Plasma Cells

Plasma cells are the principle producer of antibodies. They are from 10 to 30 μ in diameter, ovoid with an eccentric nucleus, and have an intensly basophilic cytoplasm. The nuclear chromation is distributed in coarse clumps that tend to be spaced around the periphery of the nucleus producing a "cartwheel" pattern, helpful in identification of the cell.

f. Eosinophils

The nucleus of the eosinophil is a thick irregular ring (22) with an eosinophilic center. Eosinophilic granules are present in the cytoplasm. The cell is typically 9-12 μ in diameter.

g. Mast Cells

Mast cells not identifiable with H and E stain, are from 20 to 30 μ in diameter and filled with basophilic granules which often obscure the cell nucleus.

3. Cell Density

The area in square microns required to count 100 cells was averaged for each sample and expressed as cells/10^4 μ^2.

4. Cross-Sectional Area of Blood Vessels

The number of blood vessels and their diameter were counted in each field. When a fibrous capsule was present, only those vessels within the capsule itself or within 10 μ of the periphery were considered. The total cross-sectional area of blood vessels for each field was compiled and averaged over the number of fields viewed per sample. Diameters of vessels were rounded to the nearest 10 μ.

5. Enzyme Activity

The degree of enzyme activity for SDH, acid phosphatase, and alkaline phosphatase was measured semi-quantitatively. The sections were viewed at 100X. The intensity of stain at the implant surface was graded between 0 and ++++.

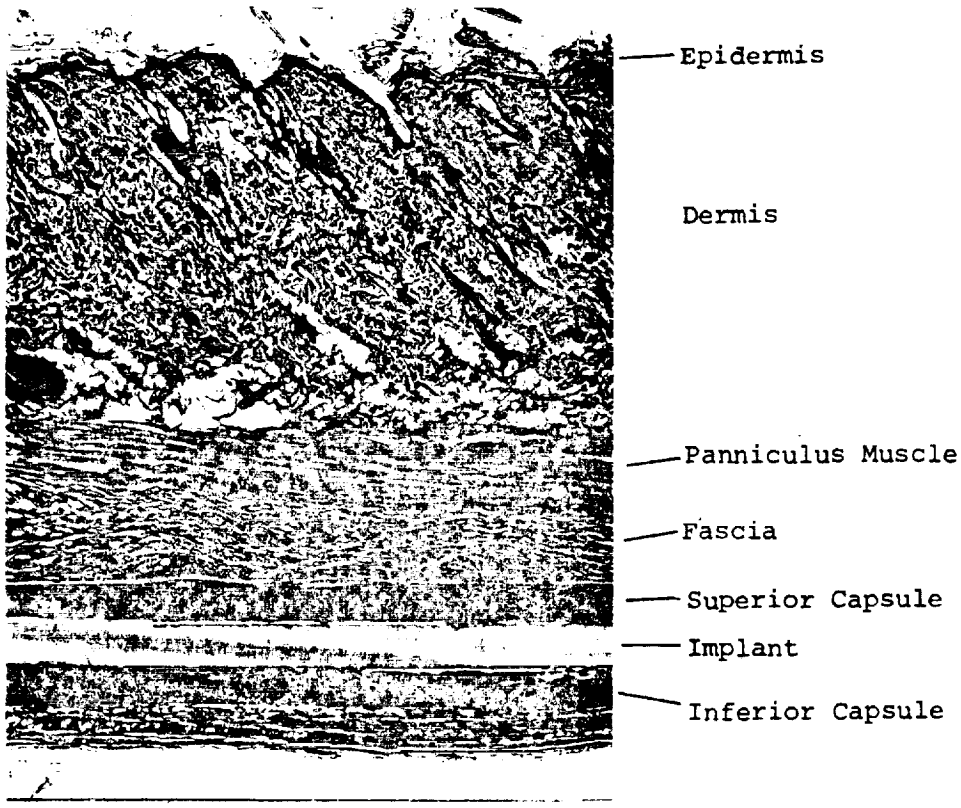

Figure 18. Location of Implant Disc Within Subcutaneous Tissue

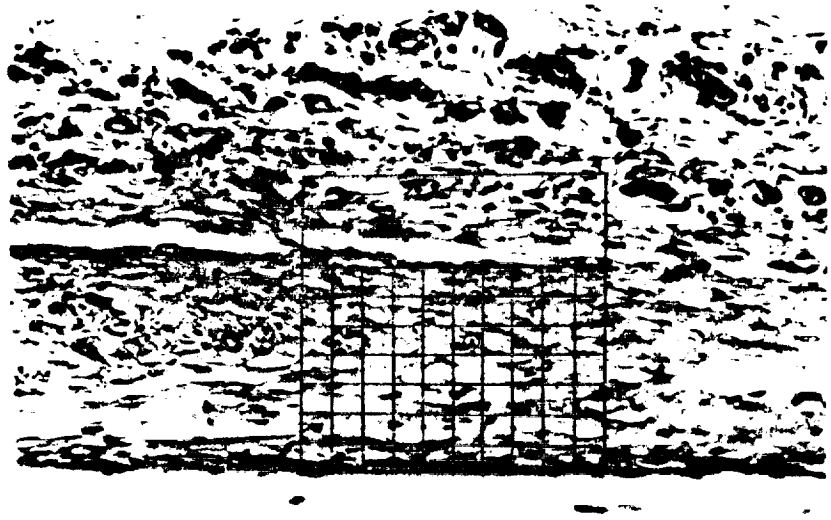

Figure 19. A Representative Area used for Measurements. The "field" is that area which is gridded (200X).

CHAPTER IV. HISTOPATHOLOGY-EXPERIMENTAL RESULTS

A. Optical Microscopy

A minimun of two tissue sections from each implant were analyzed according to the parameters outlined in Section III.E. Each data point on a graph represents the average of pooled data from a minimum of two implants with three being an average. Samples with associated infection, sterile abscesses, or wound dehiscence were not considered in the analysis. Averages and their respective 95% confidence intervals for each data point are presented in a table format. Significance of data was determined by use of the Student's t-test.

1. PTFE (Figures 20-24)

At 1 day all PTFE implants are covered by a layer of substance assumed to be exudate. This layer stains positively for fibrin or mucopolysaccharide with trichrome stain. Monocytes are occasionally embedded in this proetin coating. Textured samples have more exudate surrounding the sample. No difference is detected in the number and pattern of PMN accumulation during the acute reaction in any of the samples. By 3 days the textured interface has many mononuclear cells-both monocytes and macrophages-adhering to the texture. This layer of cells extends no more than 3 cell diameters away from the interface. At this time, occasional binucleated cells are observed. These cells are thought to be fused mononuclear cells. The cells at the textured interface have a large cytoplasmic to nuclear ratio, appearing "swollen" or "plump". By 7 days the textured surfaces are covered by large sheets of FGBC's having

a thickness of approximately 2 cell diameters. This sheet of fused cells was present up to 8 weeks. The cells associated with interfacial contact with smooth surfaces were flattened from the third day on.

Although parafin sections for light microscopy suggest that cells adjacent to the textured interface lie on top of the projections, thick 1 μ epoxy sections indicate that interfacial cells completely invaginate the interstices of the texture.

A fibrous capsule was not clearly definable until the 7 day measurement in all samples. The capsule thickness on all samples increases at a maximum rate between 7 and 21 days after which the rate decreases considerably. The decrease in capsule thickness between 21 and 28 days for the masked surface was not statistically significant. At 8 weeks, the decreased capsule thickness associated with textured surfaces is statistically significant. The capsule adjacent to a textured interface is reduced approximately 30% from the smooth surfaces. No consistent difference in collagen density within the capsule was discernable between smooth and textured samples.

Differential cell counts of the tissue adjacent to the inferior surface of the implants reveals that there is no difference between the PTFE surfaces investigated. All samples display a typical acute response with neutrophils present at one day, but only occasionally observed after day 3. Macrophages show a maximum number at 3 days and subsequently show a steady decline. The fibroblast population responds in an almost mirror image to the macrophage population. As the

macrophages disappear, fibroblasts become more prominent. Lymphocytes were present in small numbers around all implants at all time periods. Eosinophils, and basophils were seen only occasionally while plasma cells were never observed.

There is no difference between smooth and textured PTFE surfaces with respect to cell density. The fact that masked surfaces respond similarly to textured surfaces eliminates any differences in cell density due to surface texture alone. The presense of an implant does increase the cell density above the surgical sham levels at all times up to 8 weeks.

No differences in the amount of vascularity associated with each surface treatment was detectable. Although the average values presented in Figure 22 suggest differences, the large confidence intervals associated with these measurements eliminate all significance. The large intervals arise from the fact that vessels are nonuniformly distributed and by randomly selecting fields, it is inevitable that areas will be measured where no blood vessels are seen. The large confidence intervals arise from pooling very small numbers with very large values of cross-sectional area obtained from just a few blood vessels.

The textured side of $\frac{1}{2}/\frac{1}{2}$ PTFE samples indicate a slight reduction in capsule thickness at 8 weeks, but not of the magnitude seen with corresponding fully textured and masked samples. All other measurements indicate no significant difference between the responses of the textured and smooth sides of $\frac{1}{2}/\frac{1}{2}$ samples. The enlarged mononuclear cells which eventually form a layer of fused cells are seen only in

association with the textured surface.

Fibrin or mucopolysaccharides were present in the capsule at all times as indicated by the trichrome stain. However, it is not possible to differentiate between fibrin or mucopolysaccharide with this stain. The amount of this substance decreases with implant time.

2. Delrin (Figures 25-29)

As with the PTFE, all Delrin samples were initially coated with a layer of exudate. Monocytes and macrophages are seen at the textured interface at 3 days, with an occasional multinucleated cell also present. By 7 days the textured surfaces are covered by a layer of fused cells which are 2 to 3 cell diameters in thickness. Swollen cells with large cytoplasmic to nuclear ratios are seen occasionally at textured interfaces up to 7 days. Thick 1 μ epoxy sections demonstrate that the interstices of the Delrin texture are completely invaginated by cellular processes. In comparison to PTFE, interfacial cells in contact with smooth surfaces are not as flattened. No fused cells are seen on non-textured Delrin samples. Interfacial cells on all samples, however, have foamy cytoplasms and pale staining nuclei at times greater than 7 days.

A fibrous capsule is not clearly definable until the 7 day measurement. The smooth and textured interfaces develop similar capsules up to the 28th day. At 56 days, the capsule adjacent to textured interfaces is decreased in thickness by approximately 50% from smooth interfaces.

Differential fell counts within specified fields reveal no differences between surface treatments. As with PTFE, neutrophils

present at day 1 are replaced by macrophages which reach a peak population at day 3. The macrophage population declines subsequently and is replaced by fibroblasts. The fibroblast population as a function of time, appears as the mirror image of the macrophage population. Lymphocytes were present in small numbers around all implants at all time periods. Eosinophils, and basophils were occasionally seen. Plasma cells were not observed.

There is no significant difference in cell density within the capsule associated with either smooth or textured surfaces. Adjacent to the cells adherent to each implant, there is a zone of numerous macrophages many of which have foamy cytoplasms and appear nonviable. This cytoplasmic character is similar to the cells adhering to the implant. This zone is present at all time periods starting at 7 days, and is typically 20 to 50 μ in thickness. As with PTFE, the presence of Delrin elevates the local cell density above normal tissue levels at all times investigated.

The amount of vascularity associated with Delrin implants is reduced from the surgical sham at 21 and 28 days, but is similar at all other times observed. No difference is detectable between textured and smooth surfaces.

The ½/½ samples reveal findings similar to the fully textured and masked counterparts. The textured side displays adhering and fusing mononuclear cells and a fibrous capsule reduced in thickness from that of the masked sides.

3. Material Comparison (Figures 30-34)

As received and textured samples of both Delrin and Teflon were

compared, no difference in capsule thickness is significant until day 56. At this time, the capsule for the PTFE samples is considerably thicker than that of the Delrin counterparts. Delrin samples generally exhibit a significantly greater cellular response than the PTFE samples. This difference in cell density is considerable from 27 to 56 days. No difference in vascularity can be seen until day 56. At this time, textured Delrin exhibits very little vascularity associated with the fibrous capsule in comparison to as received Delrin and all PTFE samples. Differential cell counts indicate no differences between the two materials.

4. Effect of Material Compliance (Figures 35-39)

Textured 50 μ PTFE samples do not reveal a decrease in capsule thickness at 56 days when compared to the 125 μ as received samples. No other differences between thin (125 μ and 50 μ) and thick 250 μ Teflon samples are distinguishable.

5. Enzyme Histochemistry (Figures 40-42)

Due to tissue disorientation brought about by removal of Delrin samples, only frozen sections of 250 μ PTFE samples could be analyzed for enzyme histochemistry. Interfacial cells of textured PTFE samples show an increase staining for succinic deyhdrogenase and acid phosphatase above smooth samples at time periods of 7 days and greater. All smooth PTFE samples (as received, masked, ion polished) responded similarly. The succinic deyhdrogenase activity persists at a high level for both smooth and textured samples up to the 56 day observation. The acid phosphatase, however, reveals a diminished activity from 28 to 56 days for both surfaces, but

TABLE 13. FIBROUS CAPSULE THICKNESS (MICRONS)

(Average Value ± 95% Confidence Interval)

		1 DAY	3 DAYS	1 WEEK	2 WEEKS	3 WEEKS	4 WEEKS	8 WEEKS	18 WEEKS
10 MIL PTFE	½/½ MASKED	0±0	0±0	20±8	80±18	103±4	147±35	232±31	
	½/½ TEXTURED	0±0	0±0	28±11	73±15	116±27	142±12	160±22	
	ION POLISHED	0±0	0±0	10±0	24±13	106±16	123±30	145±20	
	MASKED	0±0	0±0	15±5	51±15	101±22	63±25	177±15	
	TEXTURED	0±0	0±0	30±0	56±16	116±17	123±26	94±13	153±32
	AS RECEIVED	0±0	0±0	0±0	41±8	85±21	88±11	176±23	117±26
	SHAM								
10 MIL DELRIN	½/½ MASKED	0±0	0±0	24±5	95±20	94±30	105±10	173±4	
	½/½ TEXTURED	0±0	N.A.	20±0	N.A.	65±15	55±6	60±0	
	ION POLISHED	0±0	0±0	45±20	78±17	84±10	120±20	129±34	
	MASKED	0±0	0±0	30±5	74±12	90±21	67±8	101±9	
	TEXTURED	0±0	0±0	17±5	54±4	73±9	49±4	46±6	203±40
	AS RECEIVED	0±0	0±0	46±6	58±10	118±31	98±17	111±8	240±53
THIN PTFE	5 MIL AS REC.	0±0	0±0	13±9	24±7	59±19	119±15	140±24	
	2 MIL TEXT.	0±0	0±0	0±0	16±4	89±19	153±27	163±8	

TABLE 14. CELL DENSITY

(Number of cells per 100 X 100 micron area adjacent to implant)

(Average Value ± 95% Confidence Interval)

		1 DAY	3 DAYS	1 WEEK	2 WEEKS	3 WEEKS	4 WEEKS	8 WEEKS	18 WEEKS
10 MIL PTFE	½/½ MASKED	45.8±10.4	28.8±2.1	33.3± 0	29.9±6.8	24.4±1.1	15.3±1.4	23.0±6.1	
	½/½ TEXTURED	28.6±0	24.0±8.4	56.6± 8.4	37.6±6.0	28.6±6.4	14.8± .9	23.3±3.5	
	ION POLISHED	62.5±11.8	56.5±7.4	37.7±4.4	49.9±19.7	25.6±4.9	23.5±2.7	20.4±5.4	
	MASKED	44.9±6.4	40.5±9.9	70.2±5.0	47.1±8.0	31.3±3.8	19.4±4.6	17.1±1.4	
	TEXTURED	43.9±8.4	43.0±17.0	66.6±14.2	49.4±4.9	29.4±5.2	23.9±3.1	22.5±3.2	12.9±3.8
	AS RECEIVED	48.5±6.0	30.2±12.2	33.3±3.5	47.6±8.2	26.5±6.9	21.4±5.8	13.7±3.0	15.9±1.4
	SHAM	37.2±11.0	26.3±2.9	15.3±2.4	15.3±1.5	11.5±1.0	12.1±1.5	11.2±.7	
10 MIL DELRIN	½/½ MASKED	51.5±9.6	46.7±9.4	88.7±11.8	41.4±7.6	49.1±9.2	52.9±5.0	24.4±4.2	
	½/½ TEXTURED	69.0±4.9	N.A.	111.1±0	N.A.	44.6±7.1	61.8±12.4	43.0±2.8	
	ION POLISHED	56.4±7.4	24.6±7.2	59.5±23.4	43.3±14.3	45.7±4.8	36.5±5.5	28.7±8.7	
	MASKED	64.5±14.9	34.7±14.2	63.7±11.6	57.0±8.1	43.9±10.4	50.9±4.5	37.7±9.3	
	TEXTURED	63.5±21.8	68.7±19.1	97.6±41.4	56.7±10.7	37.6±6.9	55.9±15.3	56.2±9.8	22.4±1.4
	AS RECEIVED	72.7±7.8	42.0±12.0	66.7±8.7	39.4±4.9	22.6±5.2	46.4±8.5	43.1±4.3	18.3±4.3
THIN PTFE	5 MIL AS REC.	24.8±2.5	35.1±8.3	70.9±22.2	47.6±9.2	33.5±7.7	23.7±5.7	19.4±2.6	
	2 MIL TEXT.	50.8±19.1	32.3±8.2	44.4±9.0	71.4±16.1	25.2±4.4	19.8±4.3	17.7±2.4	

TABLE 15. CROSS-SECTIONAL AREA OF BLOOD VESSELS PER FIELD (u^2)

(Average Area ± 95% Confidence Interval)

		1 DAY	3 DAYS	1 WEEK	2 WEEKS	3 WEEKS	4 WEEKS	8 WEEKS	18 WEEKS
10 MIL PTFE	½/½ MASKED	13±23	0±0	0±0	128±222	687±264	383±206	723±239	
	½/½ TEXTURED	0±0	13±22	0±0	373±119	524±164	715±240	1149±622	
	ION POLISHED	0±0	157±64	79±81	83±46	183±148	118±137	157±126	
	MASKED	0±0	11±16	43±61	253±176	366±287	250±195	213±119	
	TEXTURED	9±17	22±39	10±17	17±20	202±112	504±179	353±158	137±52
	AS RECEIVED	13±23	0±0	0±0	79±63	98±43	10±17	573±256	170±121
	SHAM	177±263	351±351	183±145	180±83	540±126	403±115	331±82	
10 MIL DELRIN	½/½ MASKED	29±21	146±181	10±17	0±0	13±23	39±39	314±79	
	½/½ TEXTURED	20±34	N.A.	0±0	N.A.	26±19	128±155	157±111	
	ION POLISHED	101±72	105±201	59±52	45±39	67±31	51±71	242±177	
	MASKED	79±88	0±0	167±201	67±76	34±41	57±63	383±66	
	TEXTURED	31±35	283±288	17±29	18±20	79±69	35±24	54±41	432±248
	AS RECEIVED	0±0	63±113	13±15	50±73	148±151	105±68	402±86	245±133
THIN PTFE	5 MIL AS REC.	0±0	11±19	26±32	7±11	86±71	340±99	96±54	
	2 MIL TEXT.	0±0	0±0	14±16	13±22	70±73	628±443	216±285	

TABLE 16. PERCENT NEUTROPHILS

(Average Value ± 95% Confidence Interval)

		1 DAY	3 DAYS	1 WEEK	2 WEEKS	3 WEEKS	4 WEEKS	8 WEEKS	18 WEEKS
10 MIL PTFE	½/½ MASKED	37.8±5.1	10.0±1.0	0±0	0±0	0±0	0±0	0±0	
	½/½ TEXTURED	43.0±0	34.5±25.7	0±0	0±0	0±0	.3±.4	0±0	
	ION POLISHED	42.8±31.4	.5±.5	1.5±1.5	.3±.4	0±0	0±0	0±0	
	MASKED	15.3±5.5	5.3±3.7	0±0	1.3±.6	0±0	0±0	0±0	
	TEXTURED	20.0±5.8	33.0±32.5	.8±.8	0±0	.5±.5	0±0	0±0	0±0
	AS RECEIVED	35.3±3.5	15.5±12.9	0±0	0±0	0±0	0±0	0±0	0±0
	SHAM	10.5±10.9	.5±1.1	0±0	.3±.4	0±0	0±0	0±0	
10 MIL DELRIN	½/½ MASKED	18.5±5.9	8.3±6.5	.4±.4	0±0	0±0	0±0	0±0	
	½/½ TEXTURED	13.5±.5	N.A.	0±0	N.A.	.2±.3	0±0	0±0	
	ION POLISHED	33.5±17.9	9.3±8.3	1±1.2	0±0	.1±.2	.1±.2	.2±.3	
	MASKED	55.0±18.6	16.8±17.0	0±0	0±0	.3±.4	0±0	0±0	
	TEXTURED	28.0±15.9	35.5±34.0	0±0	0±0	0±0	0±0	0±0	0±0
	AS RECEIVED	11.8±7.1	1.8±3.0	0±0	0±0	0±0	.1±.2	0±0	0±0
THIN PTFE	5 MIL AS REC.	52.3±15.0	8.0±1.9	.3±.4	.3±.4	0±0	0±0	0±0	
	2 MIL TEXT.	72.3±12.9	16.8±17.4	.5±.5	0±0	0±0	0±0	0±0	

TABLE 17. PERCENT MACROPHAGES

(Average Value ± 95% Confidence Interval)

		1 DAY	3 DAYS	1 WEEK	2 WEEKS	3 WEEKS	4 WEEKS	8 WEEKS	18 WEEKS
10 MIL PTFE	½ MASKED / ½ TEXTURED	39.0±14.5	58.8±10.5	11.0±0	10.5±3.0	5.0±4.0	8.3±4.7	9.5±3.9	
		40.0±1.0	44.7±17.9	12.7±5.2	19.8±3.8	20.8±3.9	1.3±1.3	4.5±1.2	
	ION POLISHED	45.0±20.8	63.5±6.5	27.0±5.6	18.7±3.0	12.5±5.6	9.3±4.3	2.8±1.3	
	MASKED	59.8±14.4	46.8±5.1	10.8±1.8	30.5±9.1	14.3±3.3	5.8±3.7	2.7±2.1	
	TEXTURED	66.3±8.4	44.5±19.5	12.0±5.2	17.3±.9	15.8±7.7	3.1±1.3	2.2±1.2	4.0±.7
	AS RECEIVED	42.8±17.3	60.3±7.4	19.5±8.1	22.8±4.9	11.8±5.8	12.0±5.7	3.3±2.4	3.0±4.2
	SHAM	24.3±10.8	70.5±5.2	8.5±2.5	11.1±3.0	7.0±1.7	13.6±3.0	7.4±2.6	
10 MIL DELRIN	½ MASKED / ½ TEXTURED	38.8±11.6	56.3±6.9	14.6±4.0	2.0±1.9	7.8±1.6	6.5±3.0	9.5±3.0	
		30.0±11.0	N.A.	25.0±0	N.A.	5.8±3.5	7.0±5.0	13.0±2.0	
	ION POLISHED	25.8±4.8	59.0±11.2	15.3±.8	8.2±1.5	5.4±1.6	5.4±1.9	6.0±2.9	
	MASKED	28.3±10.2	62.3±10.9	26.8±17.3	4.5±.9	6.0±3.7	8.3±3.0	5.3±2.7	
	TEXTURED	43.0±13.9	53.8±32.9	17.5±8.5	4.8±3.3	1.8±1.2	10.0±1.9	5.0±2.9	5.8±1.5
	AS RECEIVED	41.3±8.8	70.3±9.6	11.7±4.1	5.3±1.9	6.3±1.7	5.9±1.7	5.7±1.0	7.5±3.6
THIN PTFE	5 MIL AS REC.	32.3±11.7	76.5±6.9	39.5±21.0	43.3±30.3	11.5±2.5	9.0±5.0	1.0±1.7	
	2 MIL TEXT.	21.8±9.4	64.5±14.4	39.5±12.0	50.5±23.9	8.3±1.3	6.8±4.8	7.5±5.5	

TABLE 18. PERCENT FIBROBLASTS
(Average Value ± 95% Confidence Interval)

		1 DAY	3 DAYS	1 WEEK	2 WEEKS	3 WEEKS	4 WEEKS	8 WEEKS	18 WEEKS
10 MIL PTFE	½/½ MASKED	20.8±11.3	27.5±10.5	89.0±0	87.8±3.9	92.0±3.9	88.8±5.0	89.3±4.7	
	½/½ TEXTURED	10.0±0	16.7±12.5	86.7±2.1	77.3±4.4	75.8±5.6	97.3±1.9	95.5±1.2	
	ION POLISHED	10.3±9.4	34.0±7.0	69.8±15.3	79.7±4.0	83.5±6.8	86.5±5.4	96.3±1.9	
	MASKED	19.8±16.5	44.5±6.7	89.3±1.8	65.5±8.7	84.0±2.9	93.0±3.2	96.5±2.3	
	TEXTURED	12.8±2.6	20.0±18.3	86.3±6.9	77.3±2.9	83.5±7.8	94.9±1.2	97.2±1.6	92.8±1.3
	AS RECEIVED	18.5±13.5	21.8±12.5	80.0±7.8	76.8±5.8	87.3±6.4	87.0±5.1	95.5±3.2	95.0±2.1
	SHAM	62.3±20.9	24.5±5.2	89.3±3.4	83.8±5.0	90.3±2.5	85.3±2.9	89.6±3.3	
10 MIL DELRIN	½/½ MASKED	37.3±11.6	28.8±14.2	84.0±4.8	97.3±1.9	92.0±1.9	91.5±1.0	89.5±1.0	
	½/½ TEXTURED	30.1±11.0	N.A.	74.0±0	N.A.	93.2±3.9	86.3±3.1	86.0±0	
	ION POLISHED	32.5±15.6	22.5±5.9	87.0±3.7	91.2±1.8	94.0±1.8	93.4±2.0	93.3±3.0	
	MASKED	12.3±7.6	17.5±5.4	73.0±20.9	95.3±1.3	93.0±3.8	90.7±3.0	91.8±2.9	
	TEXTURED	23.3±12.8	6.5±5.0	81.5±9.5	95.0±3.1	98.2±1.2	89.8±1.5	96.3±2.0	42.8±1.1
	AS RECEIVED	40.8±10.0	20.3±4.5	86.5±4.7	94.0±2.5	92.0±2.8	93.6±1.8	94.3±2.2	90.5±3.6
THIN PTFE	5 MIL AS REC.	11.8±7.8	12.0±7.4	56.8±23.3	53.8±30.8	88.5±1.1	89.8±4.7	97.0±3.5	
	2 MIL TEXT.	3.8±3.3	14.3±13.8	58.5±10.2	49.5±23.9	89.5±2.1	92.8±4.8	89.5±5.5	

TABLE 19. PERCENT LYMPHOCYTES

(Average Value ± 95% Confidence Interval)

		1 DAY	3 DAYS	1 WEEK	2 WEEKS	3 WEEKS	4 WEEKS	8 WEEKS	18 WEEKS
10 MIL PTFE	½/½ MASKED	2.5±2.2	4.0±1.0	0±0	.5±.4	3.0±1.0	2.5±.5	.5±.7	
	½/½ TEXTURED	5.0±0	4.2±1.4	.7±.9	1.5±1.3	2.0±2.9	1.3±1.3	0±0	
	ION POLISHED	1.5±2.6	2.0±0	1.5±.5	.8±.9	2.0±2.0	1.3±.8	.8±1.2	
	MASKED	4.0±4.0	3.5±1.1	0±0	2.8±1.2	1.5±1.5	1.0±1.2	.7±.6	
	TEXTURED	2.8±1.4	2.5±2.6	1.0±1.2	3.8±1.5	0±0	1.8±1.3	.7±.7	
	AS RECEIVED	3.3±1.6	2.5±2.2	.5±.9	.5±.9	.3±.4	1.0±.8	1.3±1.0	2.0±2.1
	SHAM	3.0±1.2	4.0±2.1	2.0±1.2	4.8±2.0	2.8±2.1	2.0±.9	2.4±1.1	3.3±1.8
10 MIL DELRIN	½/½ MASKED	5.5±1.8	5.0±4.2	.8±.6	0±0	.3±.4	2.0±2.0	1.0±1.0	
	½/½ TEXTURED	9.0±2.0	N.A.	1.0±0	N.A.	.8±.3	1.3±1.1	1.0±1.0	
	ION POLISHED	8.3±2.8	8.3±5.6	1.0±.7	.7±.9	.5±.3	1.1±.5	.3±.5	
	MASKED	4.3±1.8	3.0±2.5	2.8±2.3	.3±.4	.8±.8	.3±.4	2.3±1.5	
	TEXTURED	5.8±2.9	6.5±2.7	1.0±1.0	.3±.4	0±0	.3±.4	.3±.4	1.5±.5
	AS RECEIVED	5.0±2.9	7.8±6.0	1.8±.9	.8±.8	1.3±.9	.4±.4	0±0	2.0±1.2
THIN PTFE	5 MIL AS REC.	3.3±2.6	3.5±1.1	3.5±3.8	2.8±.4	0±0	1.3±1.1	2.0±1.9	
	2 MIL TEXT.	1.8±.8	2.0±.7	1.5±1.5	0±0	1.3±.4	.5±.5	3.0±0	

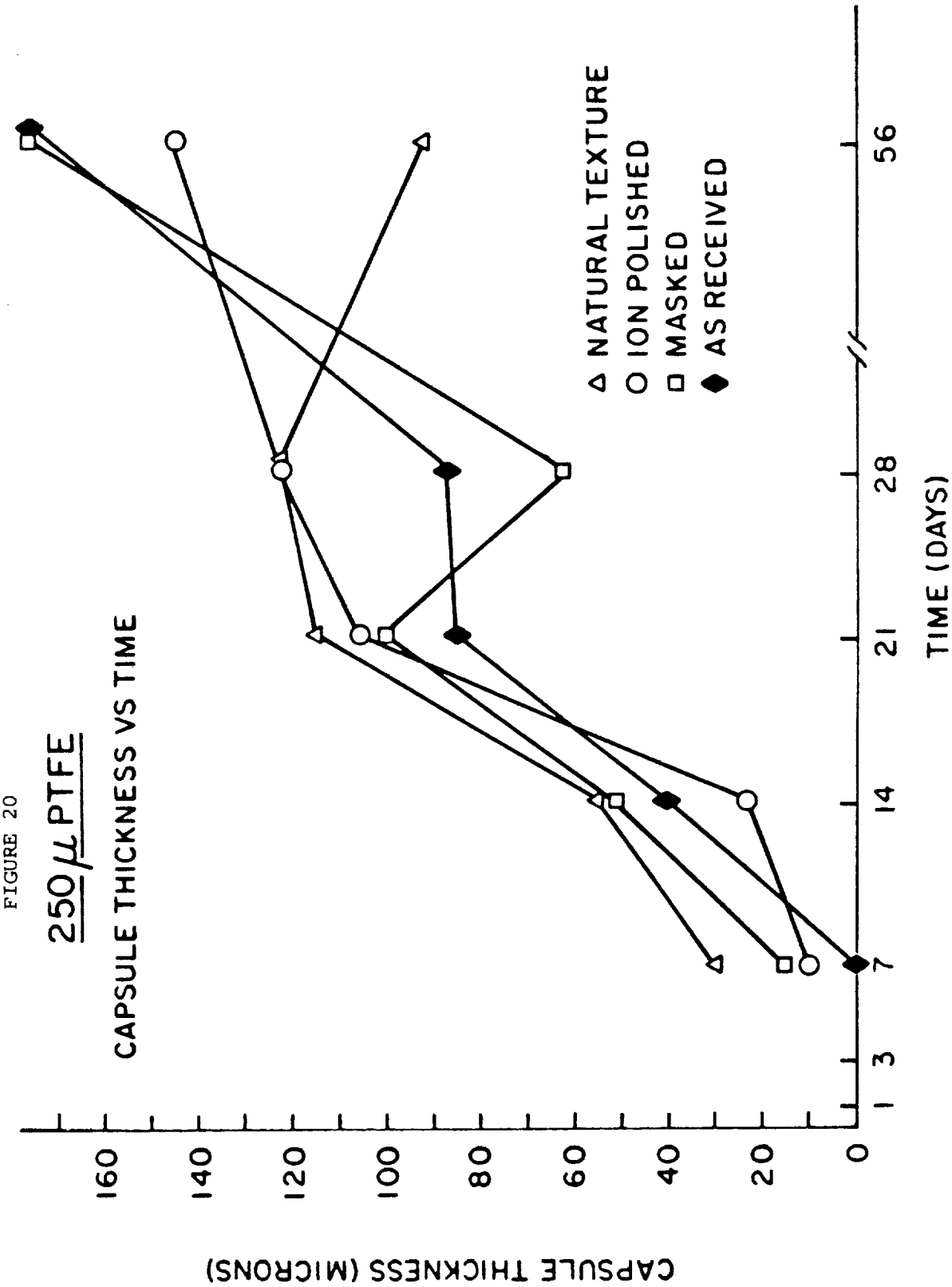
250 μ PTFE
CAPSULE THICKNESS VS TIME
Δ NATURAL TEXTURE
○ ION POLISHED
□ MASKED
◆ AS RECEIVED
CAPSULE THICKNESS (MICRONS)
TIME (DAYS)
0
20
40
60
80
100
120
140
160
1
3
7
14
21
28
56

FIGURE 20

FIGURE 21

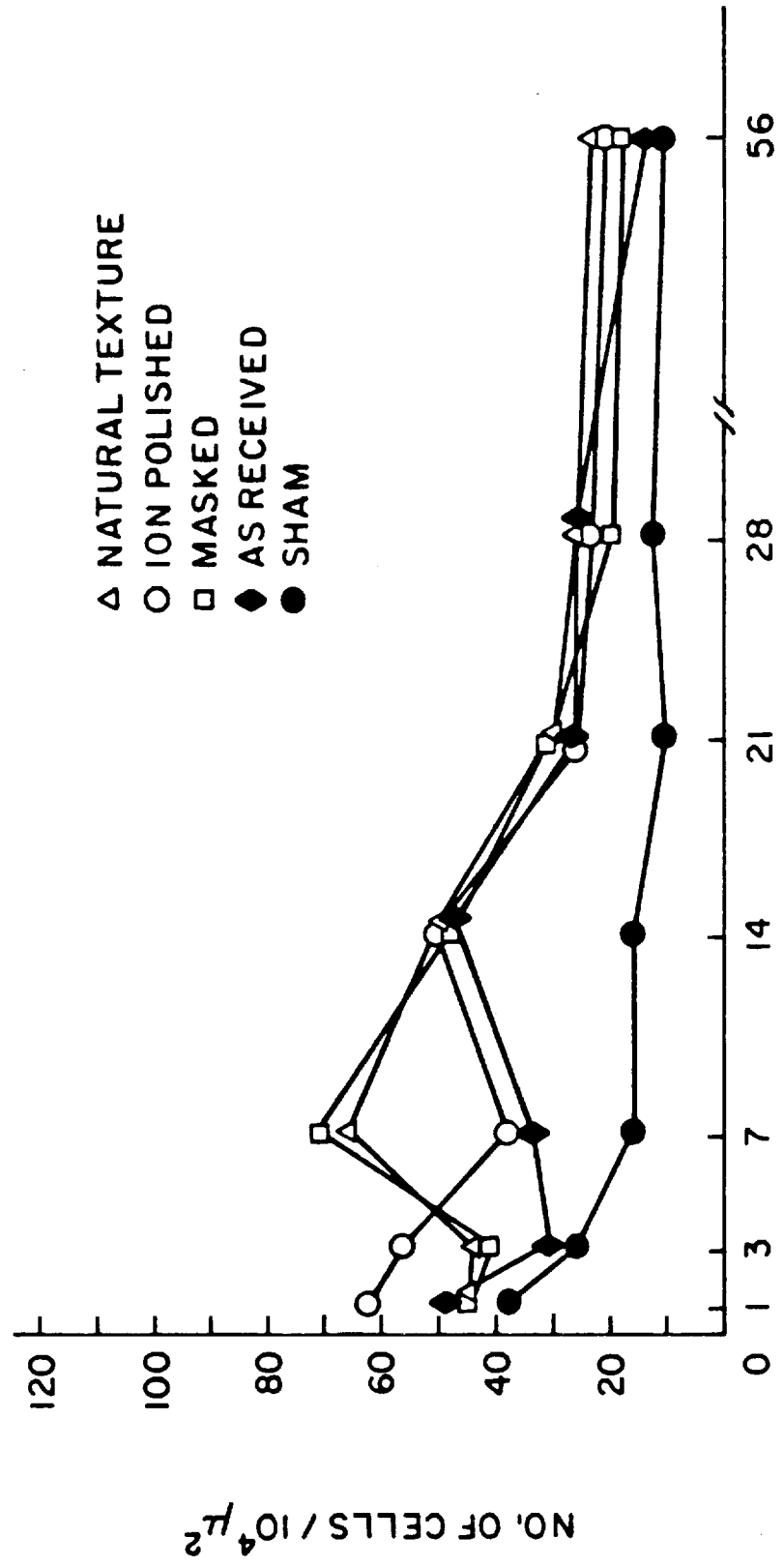
250 μL PTFE
CELL DENSITY VS TIME
△ NATURAL TEXTURE
○ ION POLISHED
□ MASKED
◆ AS RECEIVED
● SHAM
NO. OF CELLS / $10^4 \mu^2$
120
100
80
60
40
20
0
1
3
7
14
21
28
56
TIME (DAYS)

FIGURE 22

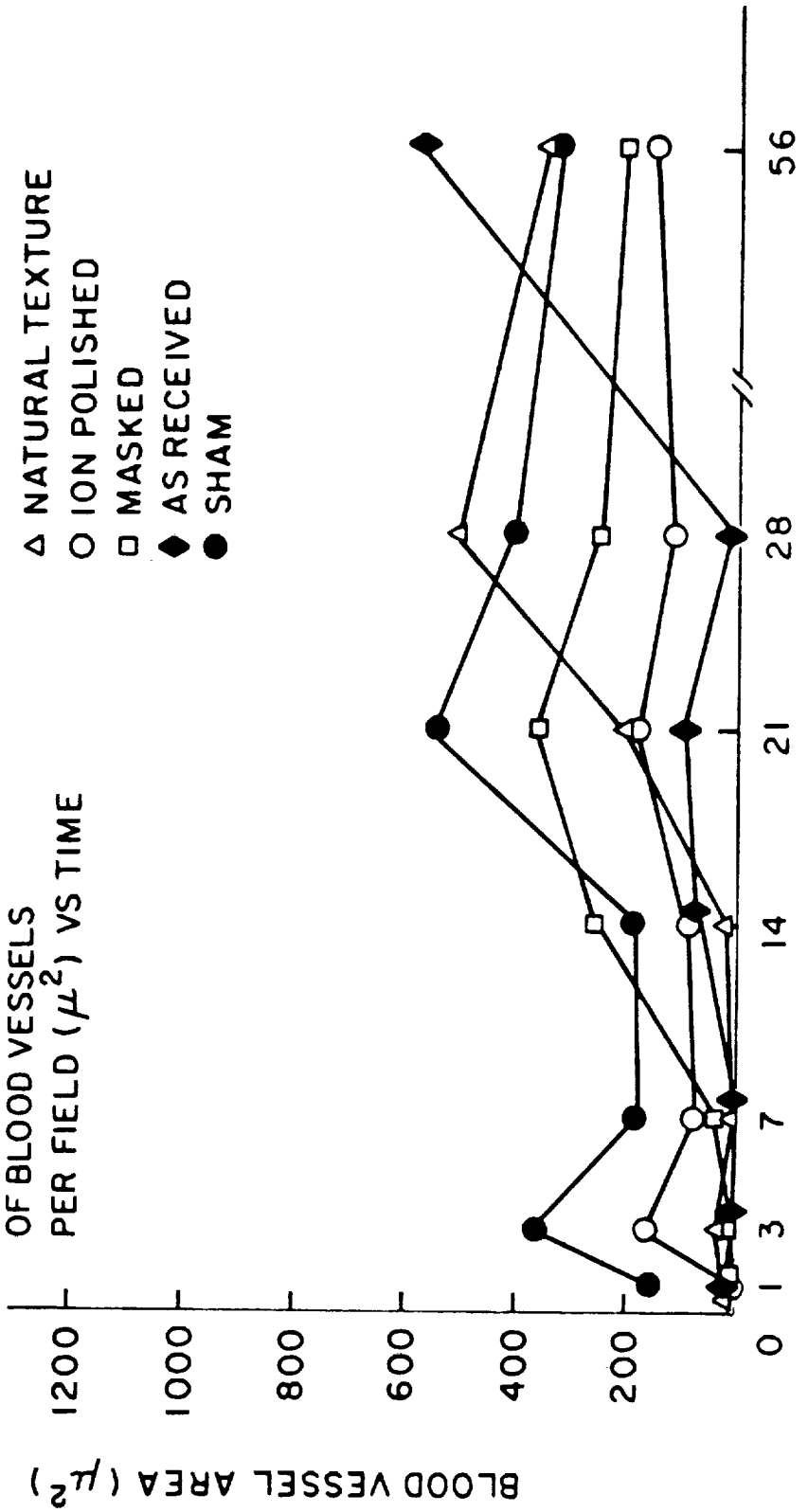
250μ PTFE
CROSS-SECTIONAL AREA
OF BLOOD VESSELS
PER FIELD (μ²) VS TIME
△ NATURAL TEXTURE
○ ION POLISHED
□ MASKED
◆ AS RECEIVED
● SHAM
BLOOD VESSEL AREA (μ²)
1200
1000
800
600
400
200
0
1
3
7
14
21
28
56
TIME (DAYS)

FIGURE 23

250 μ PTFE

PERCENT MACROPHAGES VS TIME

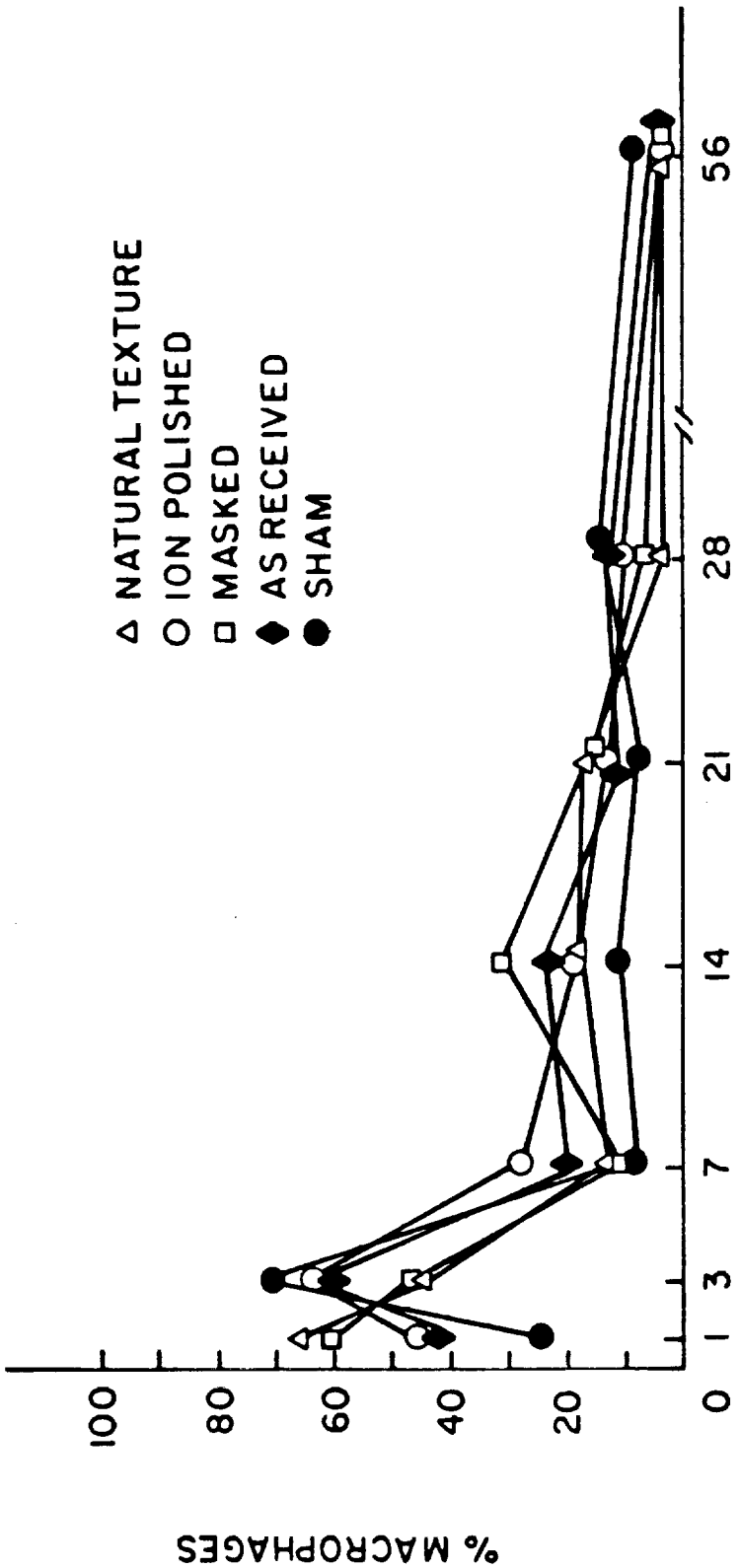

FIGURE 24

250 μ PTFE

PERCENT FIBROBLASTS VS TIME

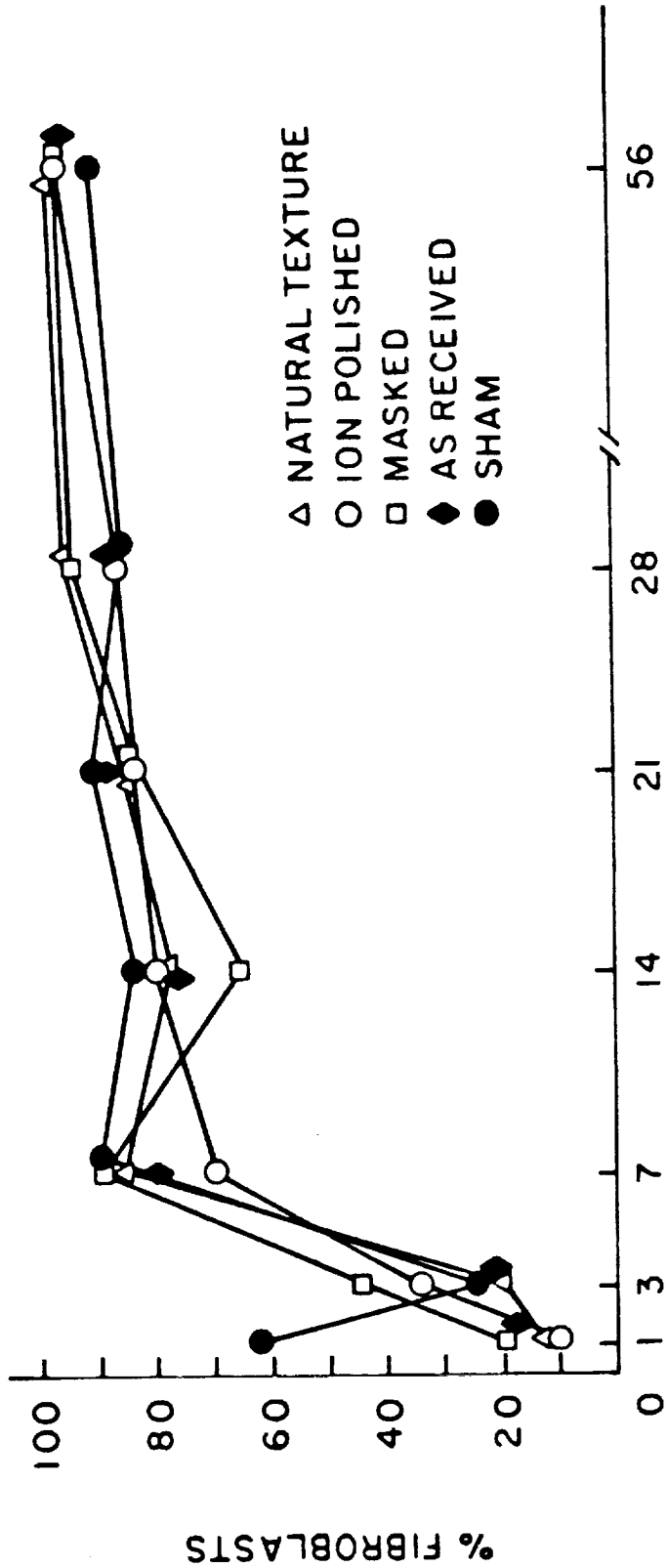

FIGURE 25

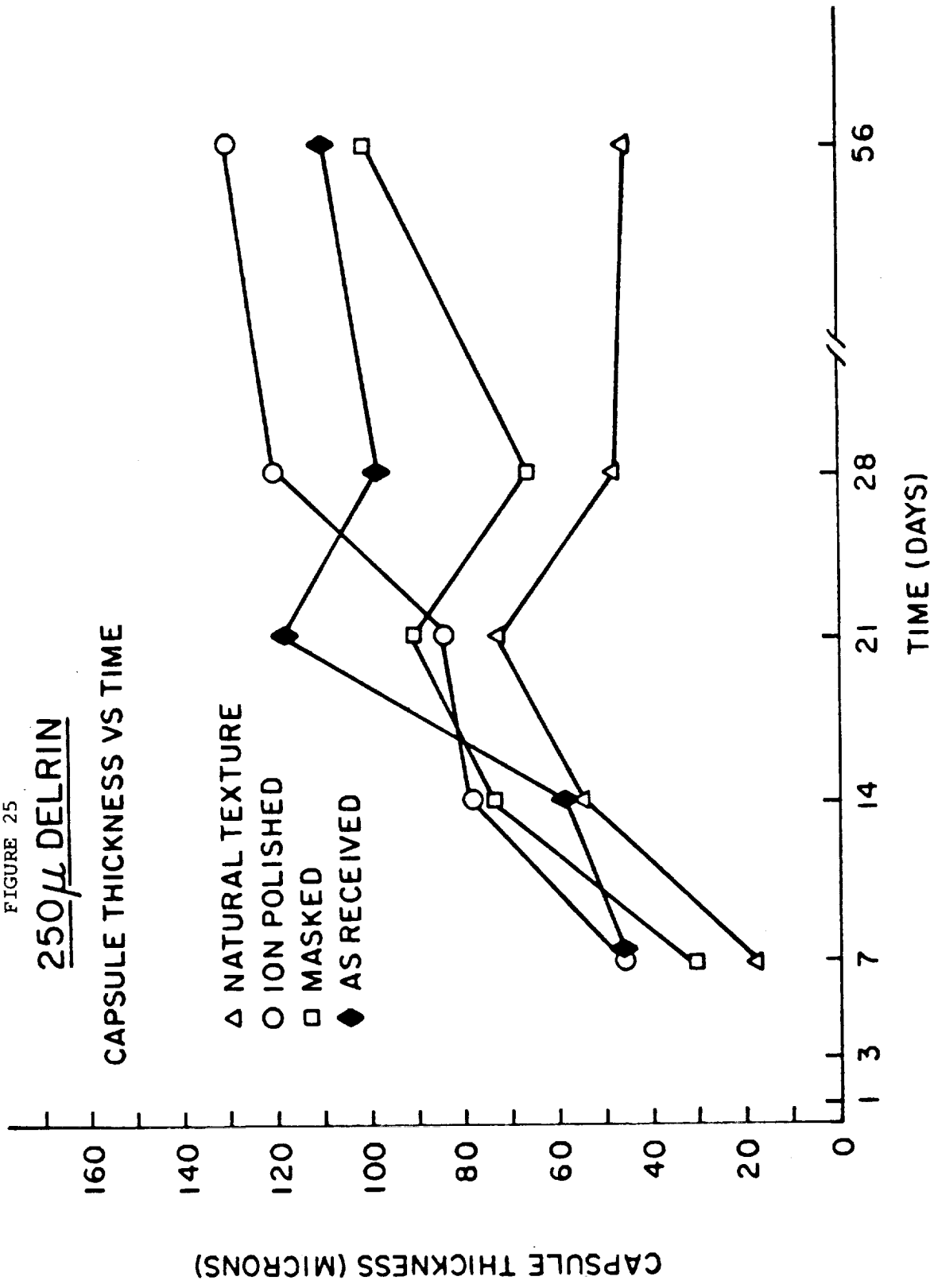
250μ DELRIN
CAPSULE THICKNESS VS TIME
△ NATURAL TEXTURE
○ ION POLISHED
□ MASKED
◆ AS RECEIVED
CAPSULE THICKNESS (MICRONS)
160
140
120
100
80
60
40
20
0
1
3
7
14
21
28
56
TIME (DAYS)

FIGURE 26

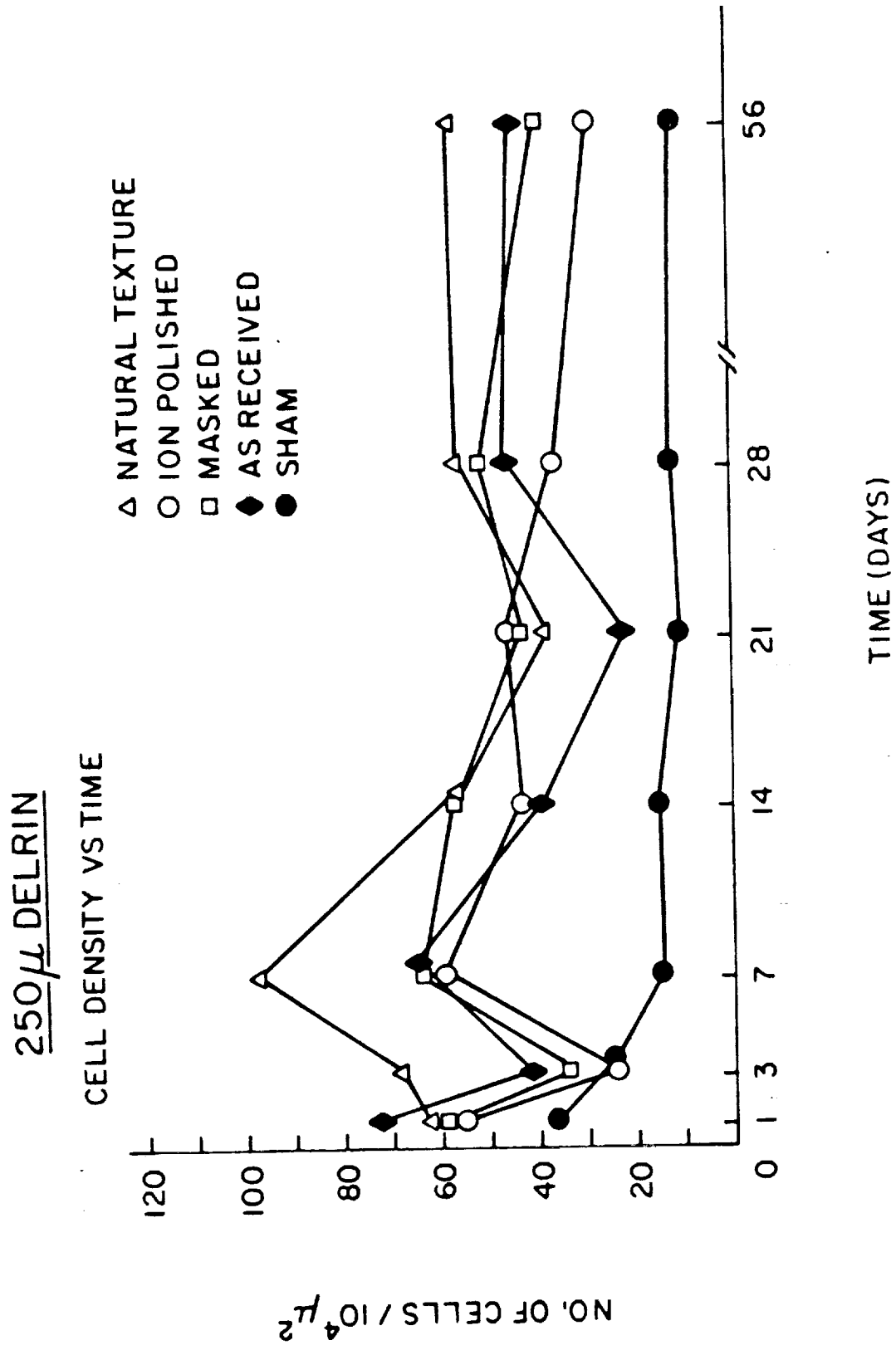
250μ DELRIN
CELL DENSITY VS TIME
△ NATURAL TEXTURE
○ ION POLISHED
□ MASKED
◆ AS RECEIVED
● SHAM
NO. OF CELLS / $10^4 \mu^2$
120
100
80
60
40
20
0
1
3
7
14
21
28
56
TIME (DAYS)

FIGURE 27

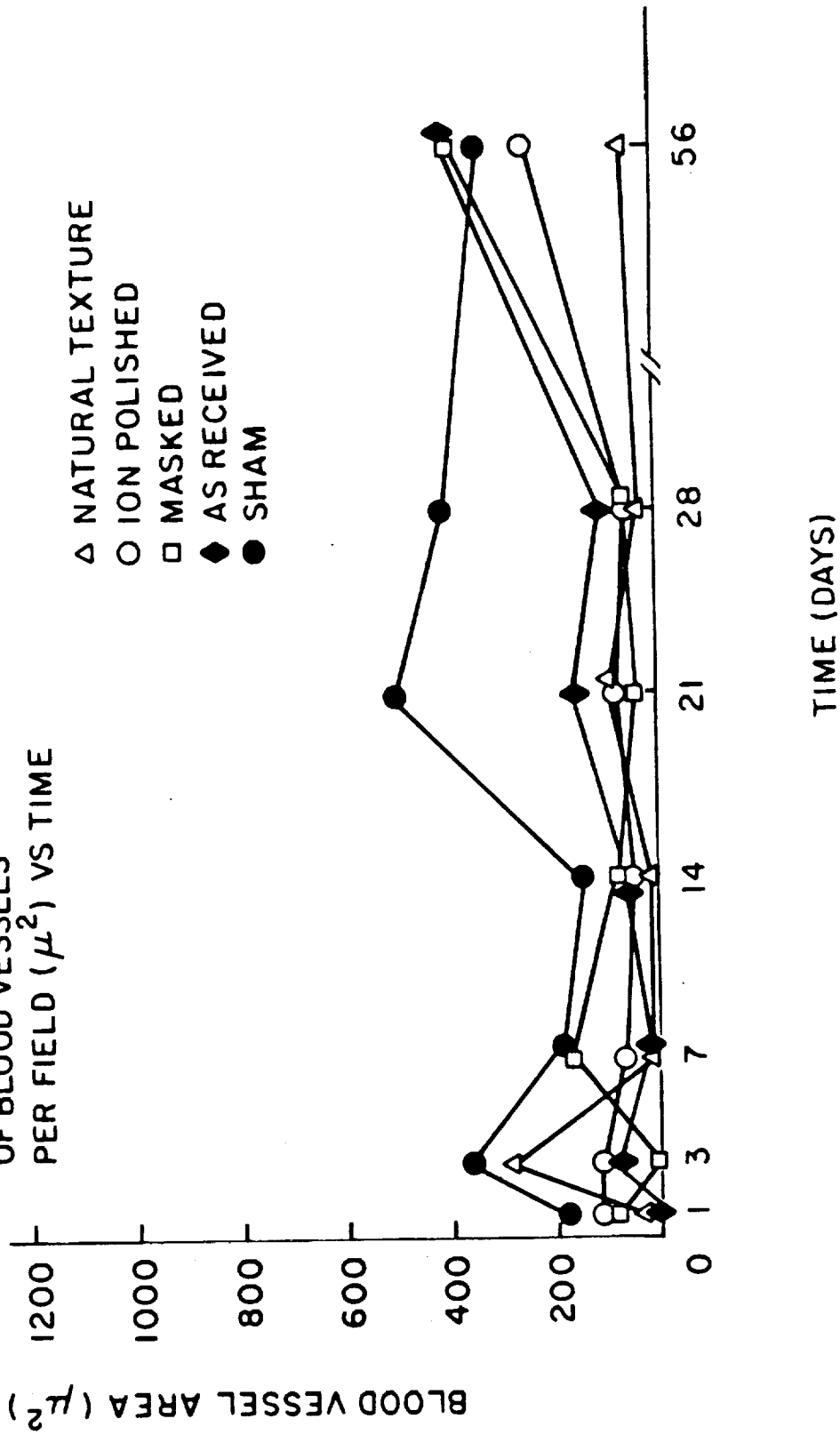
250μ DELRIN
CROSS-SECTIONAL AREA
OF BLOOD VESSELS
PER FIELD (μ²) VS TIME
△ NATURAL TEXTURE
○ ION POLISHED
□ MASKED
◆ AS RECEIVED
● SHAM
BLOOD VESSEL AREA (μ²)
1200
1000
800
600
400
200
0
1
3
7
14
21
28
56
TIME (DAYS)

FIGURE 28

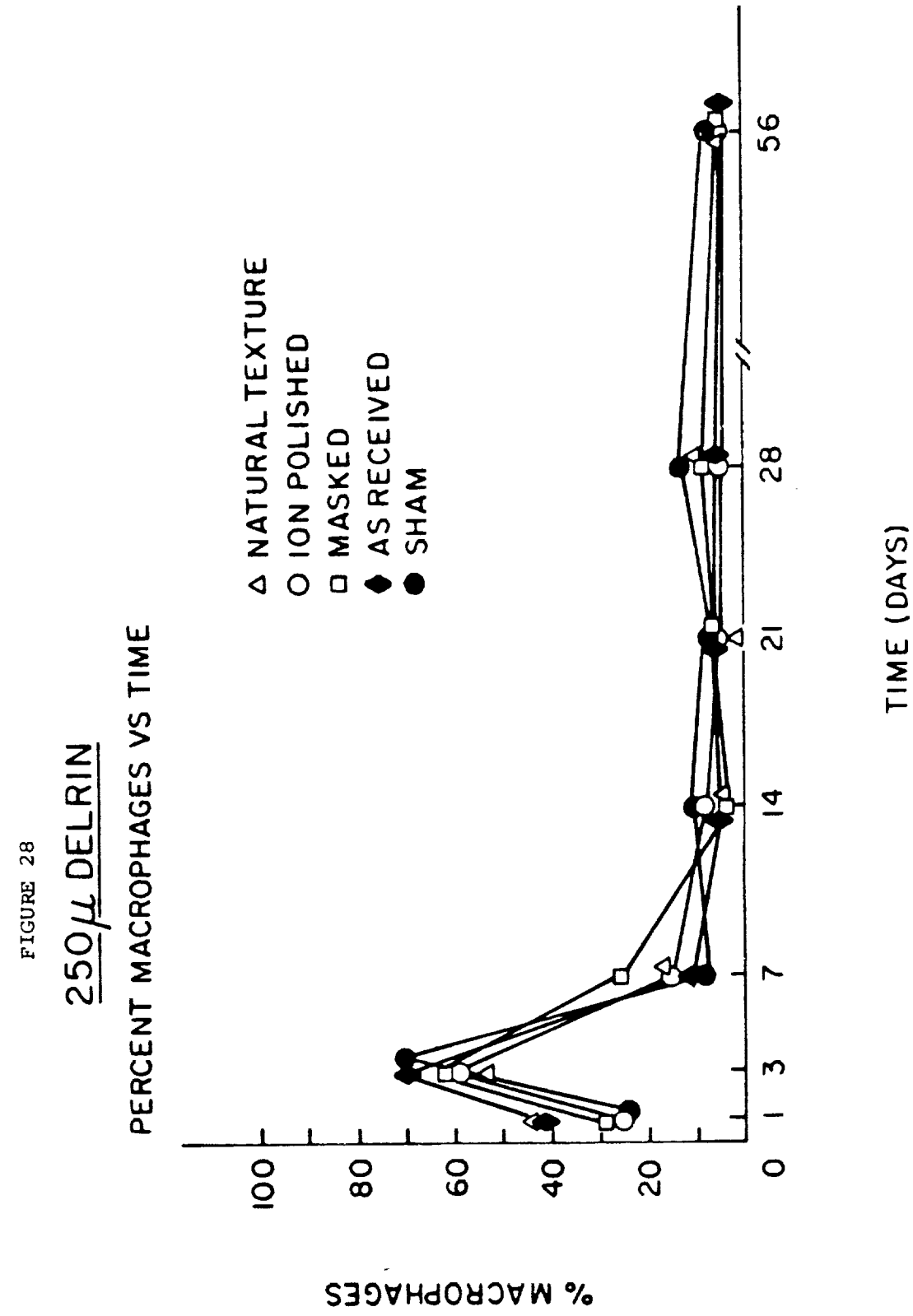
250μ DELRIN
PERCENT MACROPHAGES VS TIME
△ NATURAL TEXTURE
○ ION POLISHED
□ MASKED
◆ AS RECEIVED
● SHAM
% MACROPHAGES
100
80
60
40
20
0
1
3
7
14
21
28
56
TIME (DAYS)

FIGURE 29

250μ DELRIN

PERCENT FIBROBLASTS VS TIME

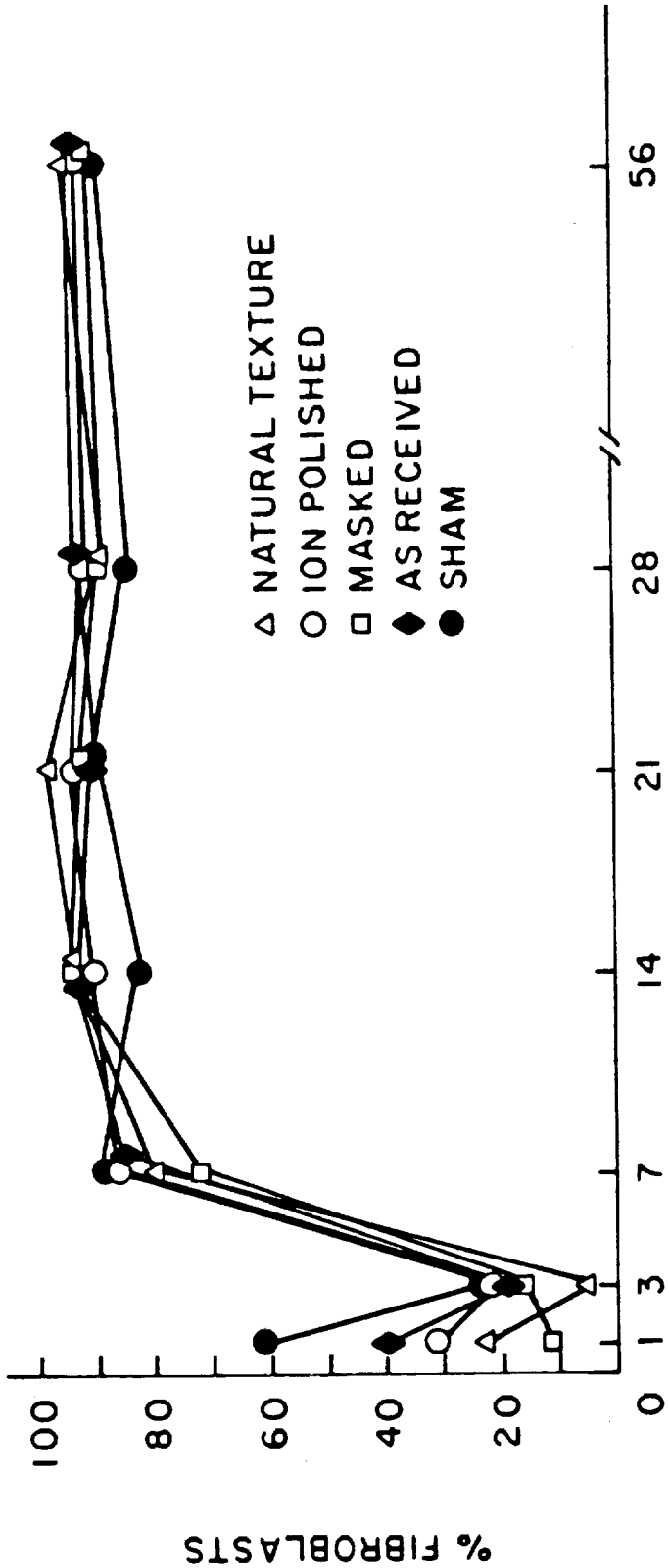

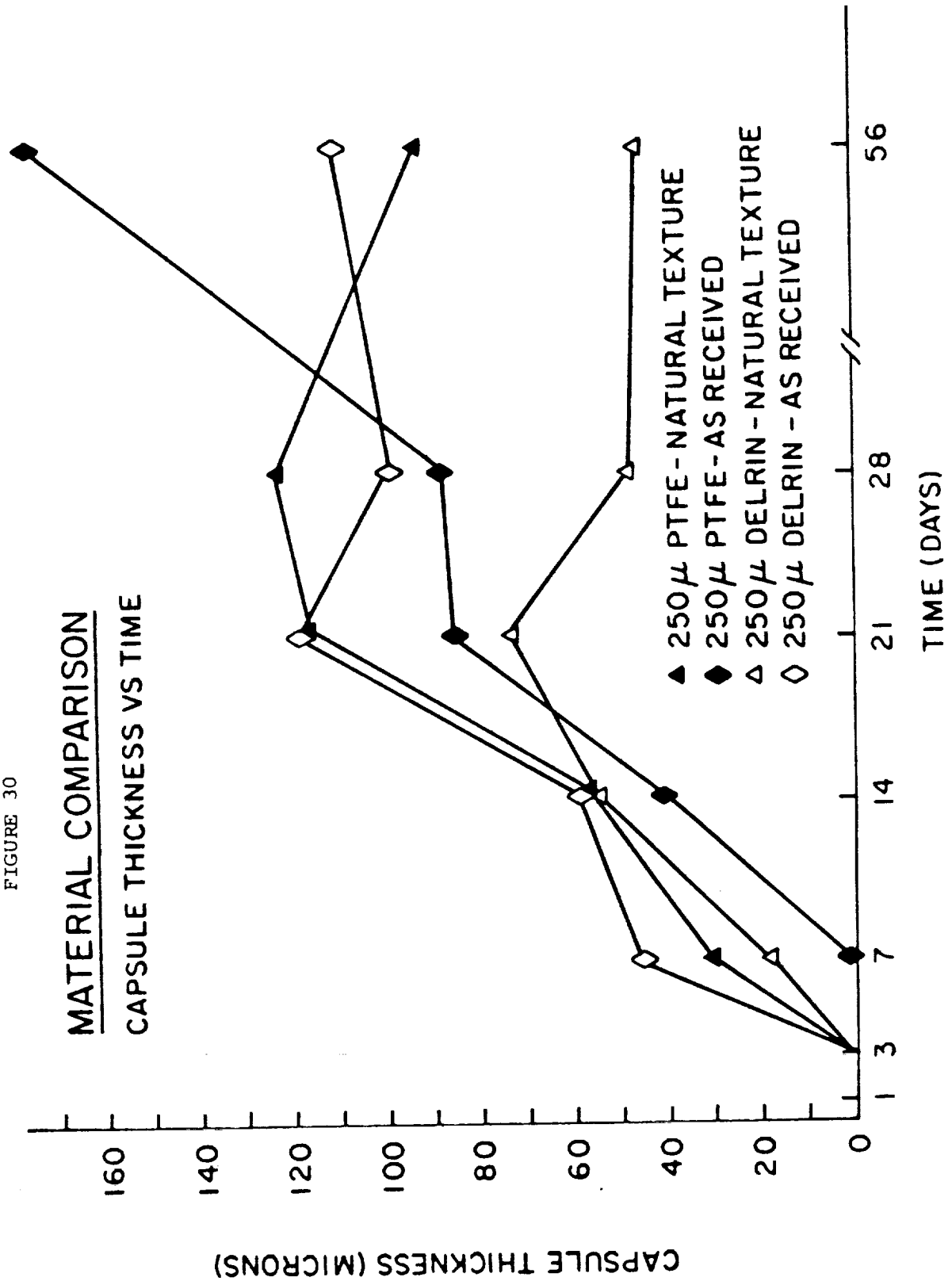
MATERIAL COMPARISON
CAPSULE THICKNESS VS TIME
▲ 250μ PTFE - NATURAL TEXTURE
● 250μ PTFE - AS RECEIVED
△ 250μ DELRIN - NATURAL TEXTURE
◇ 250μ DELRIN - AS RECEIVED
CAPSULE THICKNESS (MICRONS)
TIME (DAYS)
0
20
40
60
80
100
120
140
160
1
3
7
14
21
28
56

FIGURE 30

FIGURE 31

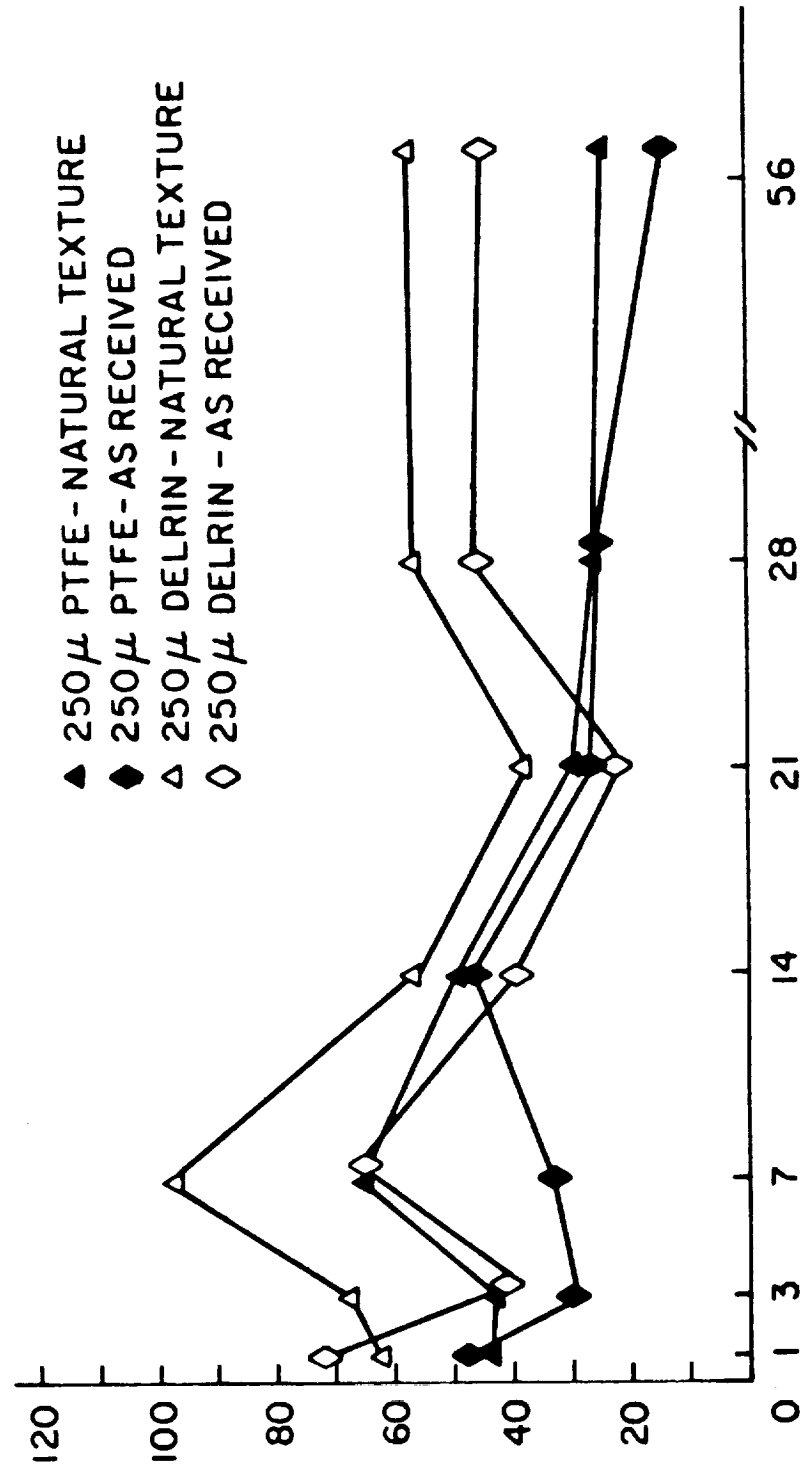
MATERIAL COMPARISON
CELL DENSITY VS TIME
▲ 250μ PTFE - NATURAL TEXTURE
● 250μ PTFE - AS RECEIVED
△ 250μ DELRIN - NATURAL TEXTURE
◇ 250μ DELRIN - AS RECEIVED
NO. OF CELLS / $10^4 \mu^2$
120
100
80
60
40
20
0
1
3
7
14
21
28
56
TIME (DAYS)

FIGURE 32

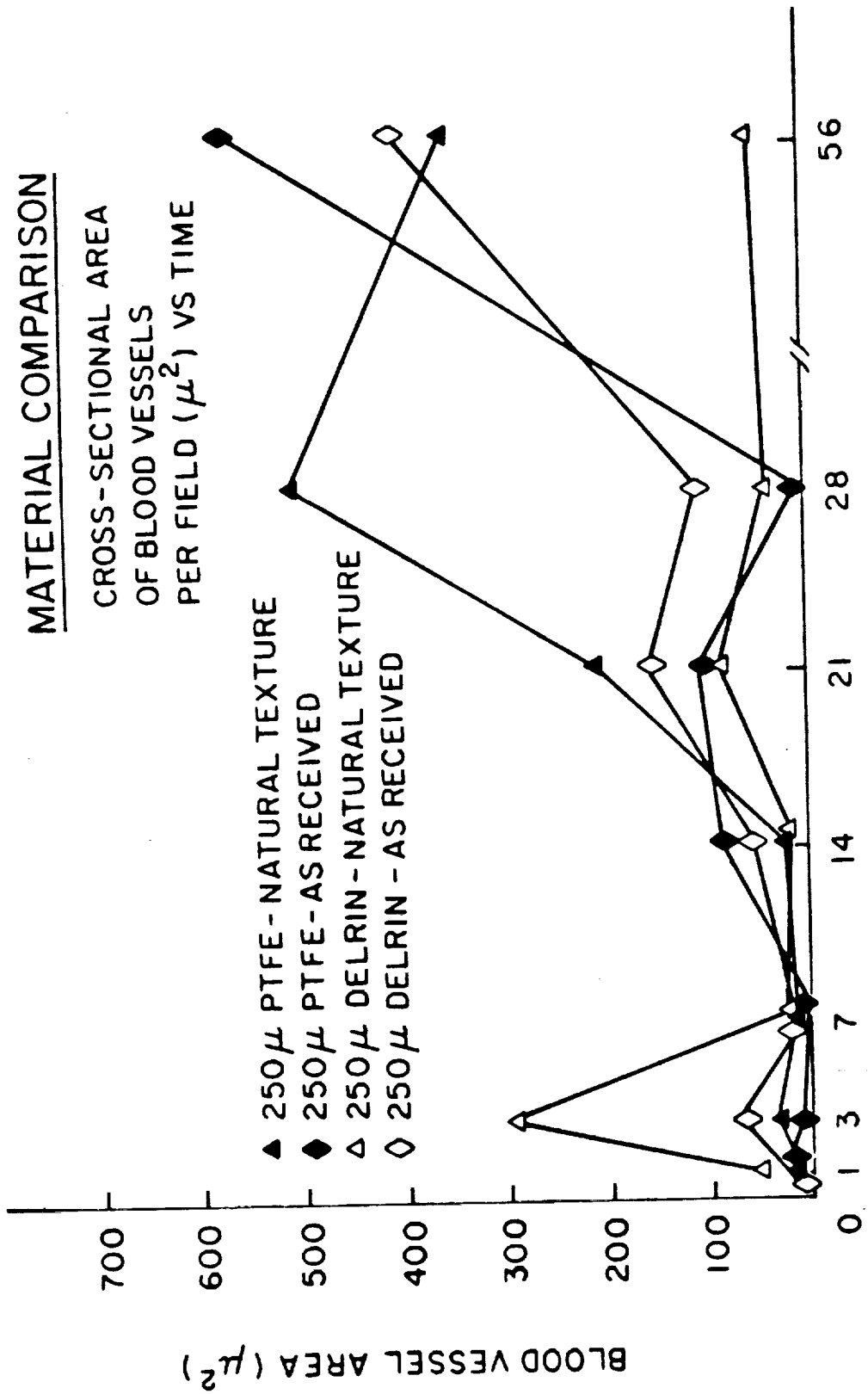
MATERIAL COMPARISON
CROSS-SECTIONAL AREA
OF BLOOD VESSELS
PER FIELD (μ^2) VS TIME
▲ 250μ PTFE-NATURAL TEXTURE
● 250μ PTFE-AS RECEIVED
△ 250μ DELRIN-NATURAL TEXTURE
◇ 250μ DELRIN-AS RECEIVED
BLOOD VESSEL AREA (μ^2)
700
600
500
400
300
200
100
0
1
3
7
14
21
28
56
TIME (DAYS)

FIGURE 33

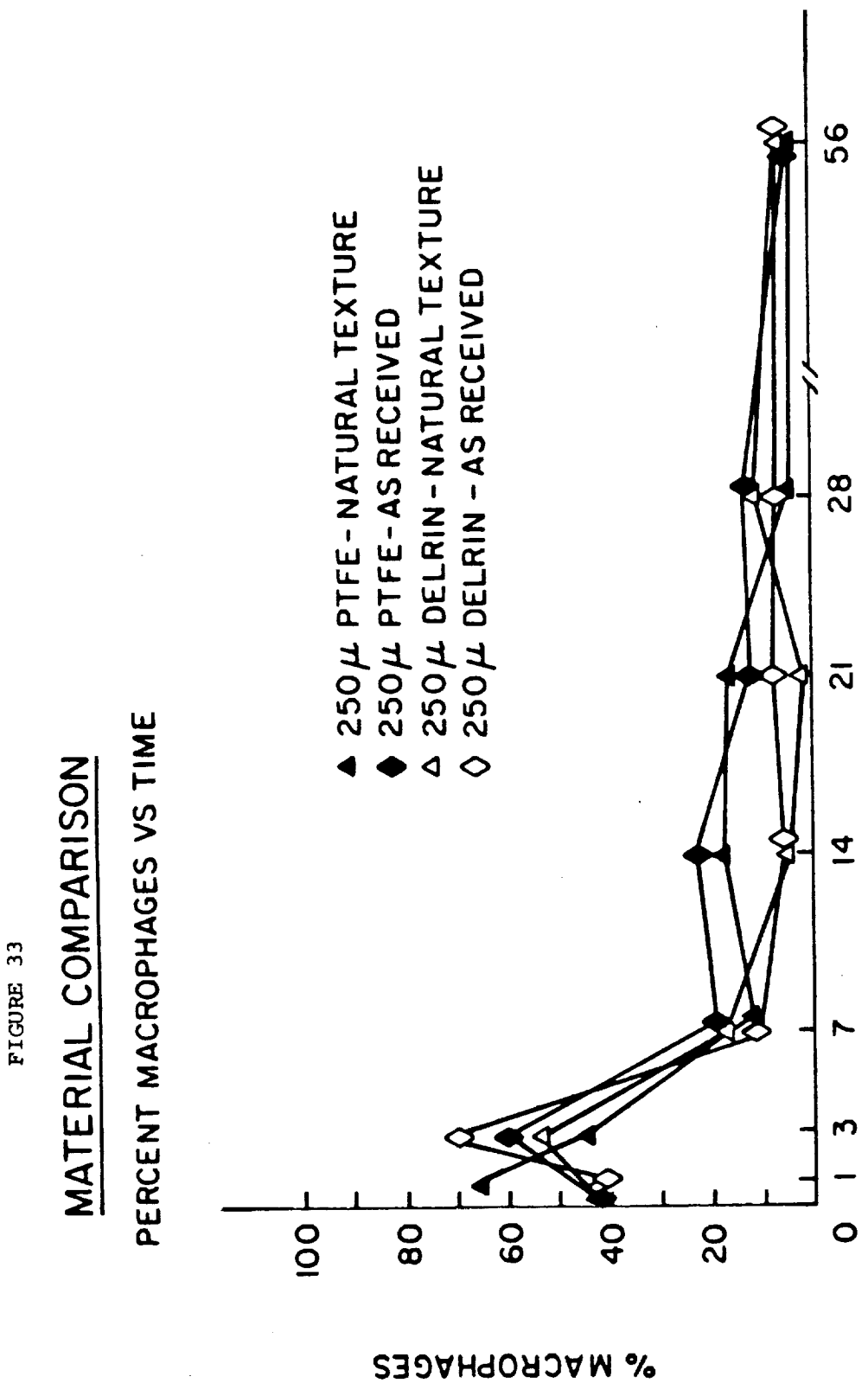
MATERIAL COMPARISON
PERCENT MACROPHAGES VS TIME
▲ 250μ PTFE - NATURAL TEXTURE
◆ 250μ PTFE - AS RECEIVED
△ 250μ DELRIN - NATURAL TEXTURE
◇ 250μ DELRIN - AS RECEIVED
% MACROPHAGES
100
80
60
40
20
0
1
3
7
14
21
28
56
TIME (DAYS)

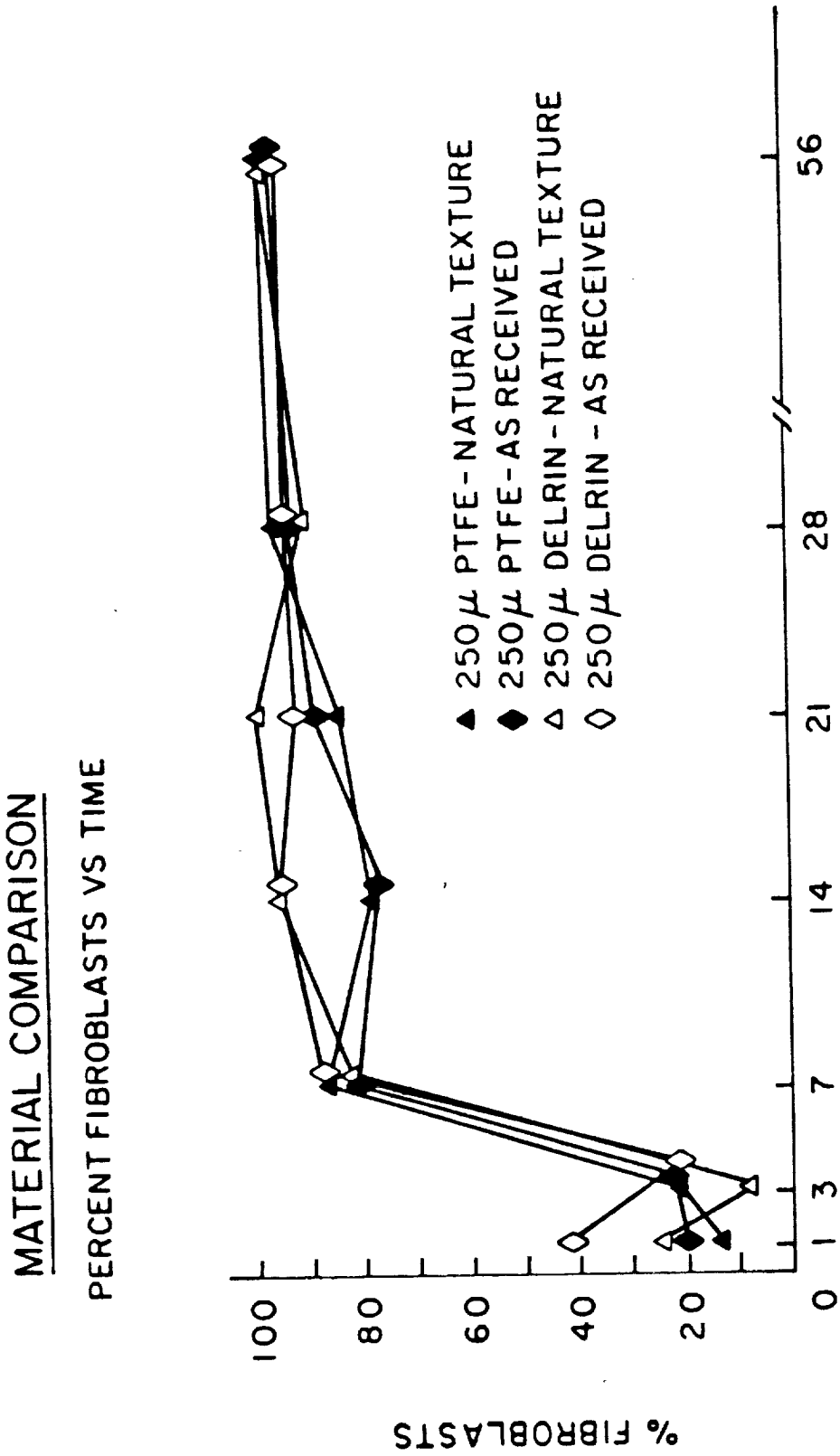
MATERIAL COMPARISON
PERCENT FIBROBLASTS VS TIME
▲ 250μ PTFE - NATURAL TEXTURE
● 250μ PTFE - AS RECEIVED
△ 250μ DELRIN - NATURAL TEXTURE
◇ 250μ DELRIN - AS RECEIVED
% FIBROBLASTS
100
80
60
40
20
0
1
3
7
14
21
28
56
TIME (DAYS)

FIGURE 34

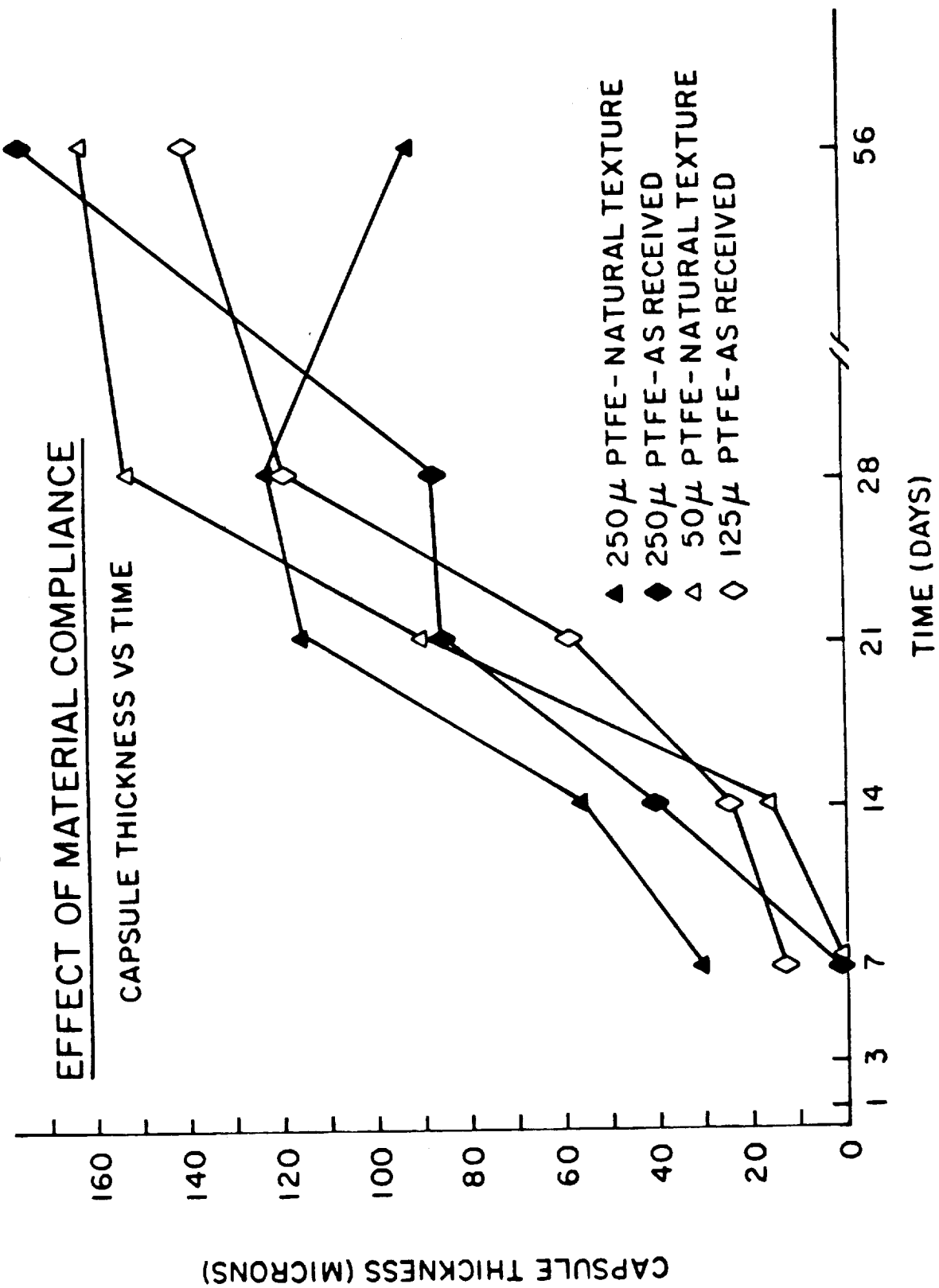
EFFECT OF MATERIAL COMPLIANCE
CAPSULE THICKNESS VS TIME
▲ 250μ PTFE-NATURAL TEXTURE
◆ 250μ PTFE-AS RECEIVED
△ 50μ PTFE-NATURAL TEXTURE
◇ 125μ PTFE-AS RECEIVED
CAPSULE THICKNESS (MICRONS)
160
140
120
100
80
60
40
20
0
1
3
7
14
21
28
56
TIME (DAYS)

FIGURE 35

FIGURE 36

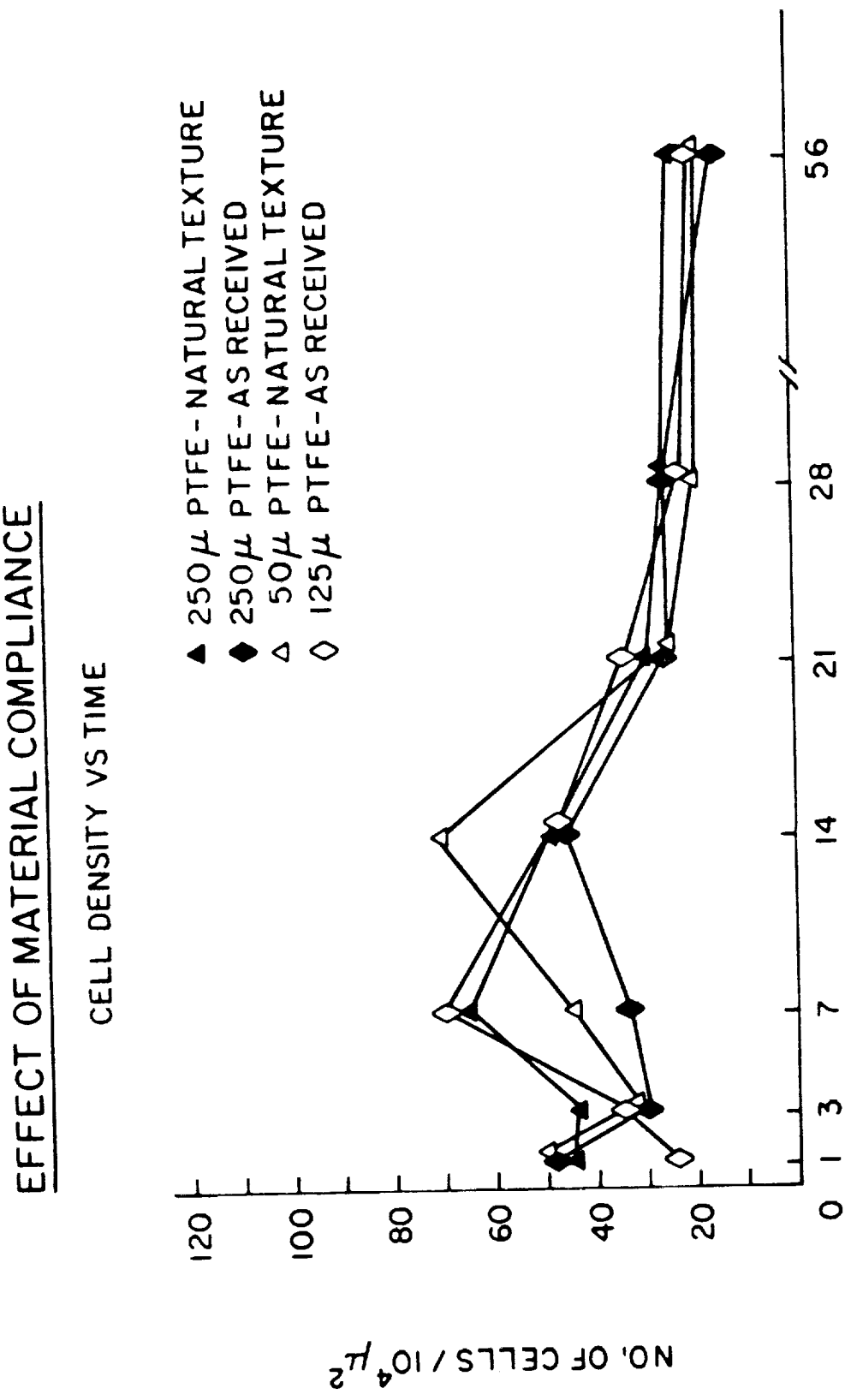
EFFECT OF MATERIAL COMPLIANCE
CELL DENSITY VS TIME
▲ 250μ PTFE-NATURAL TEXTURE
◆ 250μ PTFE-AS RECEIVED
△ 50μ PTFE-NATURAL TEXTURE
◇ 125μ PTFE-AS RECEIVED
NO. OF CELLS / 10⁴ μ²
120
100
80
60
40
20
0
1
3
7
14
21
28
56
TIME (DAYS)

FIGURE 37

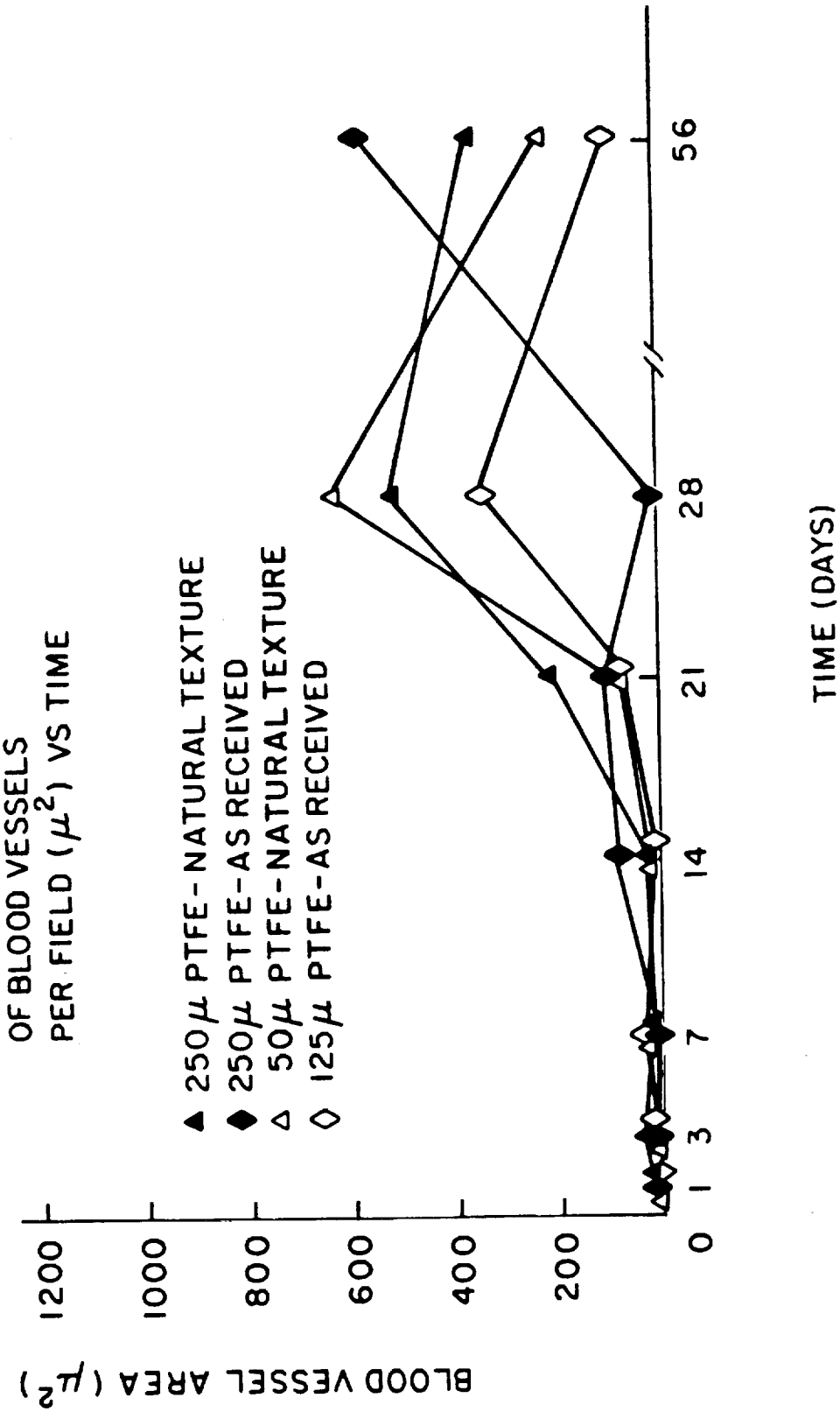
EFFECT OF MATERIAL COMPLIANCE
CROSS-SECTIONAL AREA
OF BLOOD VESSELS
PER FIELD (μ^2) VS TIME
▲ 250μ PTFE-NATURAL TEXTURE
◆ 250μ PTFE-AS RECEIVED
△ 50μ PTFE-NATURAL TEXTURE
◇ 125μ PTFE-AS RECEIVED
BLOOD VESSEL AREA (μ^2)
1200
1000
800
600
400
200
0
1
3
7
14
21
28
56
TIME (DAYS)

FIGURE 38

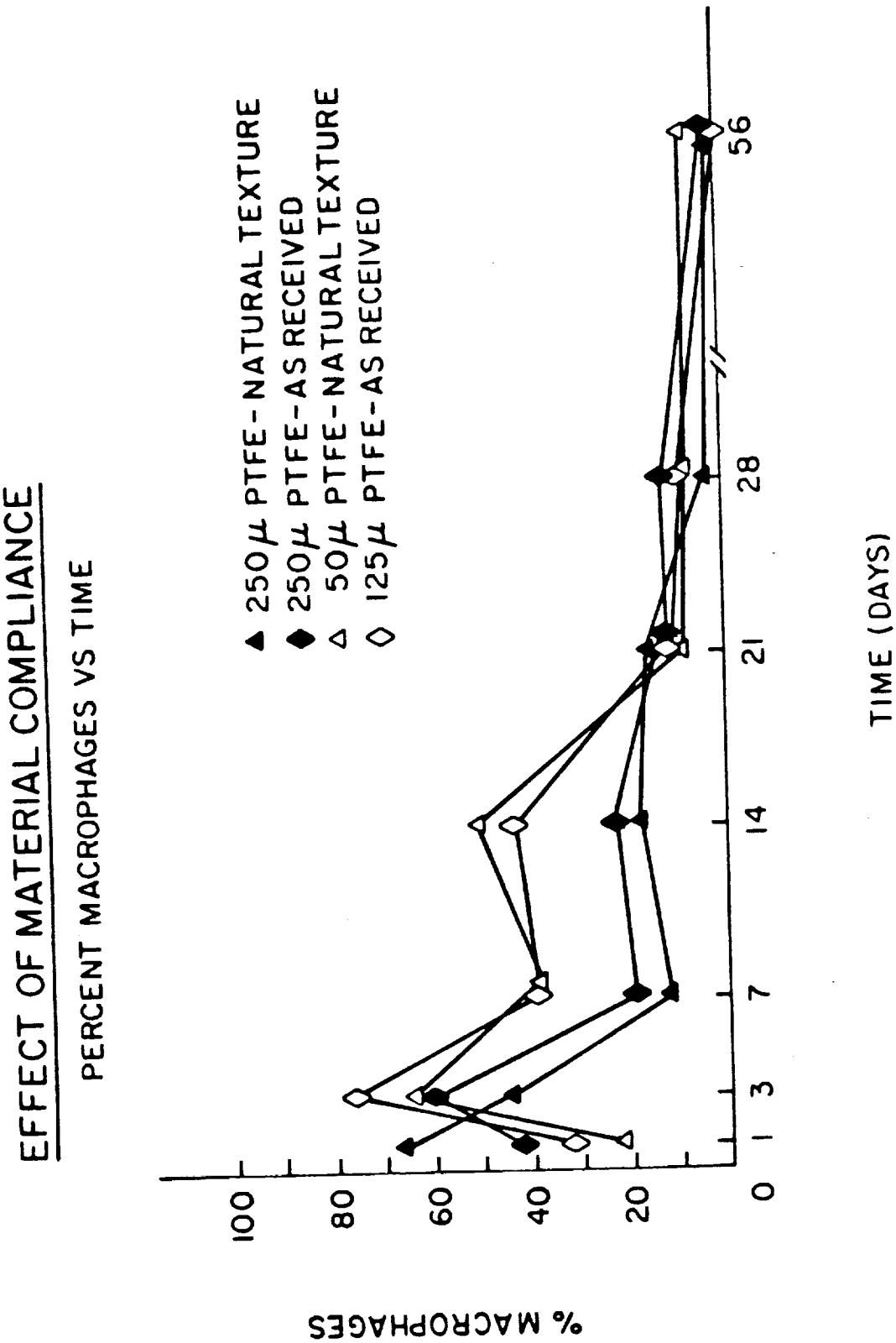
EFFECT OF MATERIAL COMPLIANCE
PERCENT MACROPHAGES VS TIME
▲ 250μ PTFE-NATURAL TEXTURE
◆ 250μ PTFE-AS RECEIVED
△ 50μ PTFE-NATURAL TEXTURE
◇ 125μ PTFE-AS RECEIVED
% MACROPHAGES
100
80
60
40
20
0
1
3
7
14
21
28
56
TIME (DAYS)

FIGURE 39

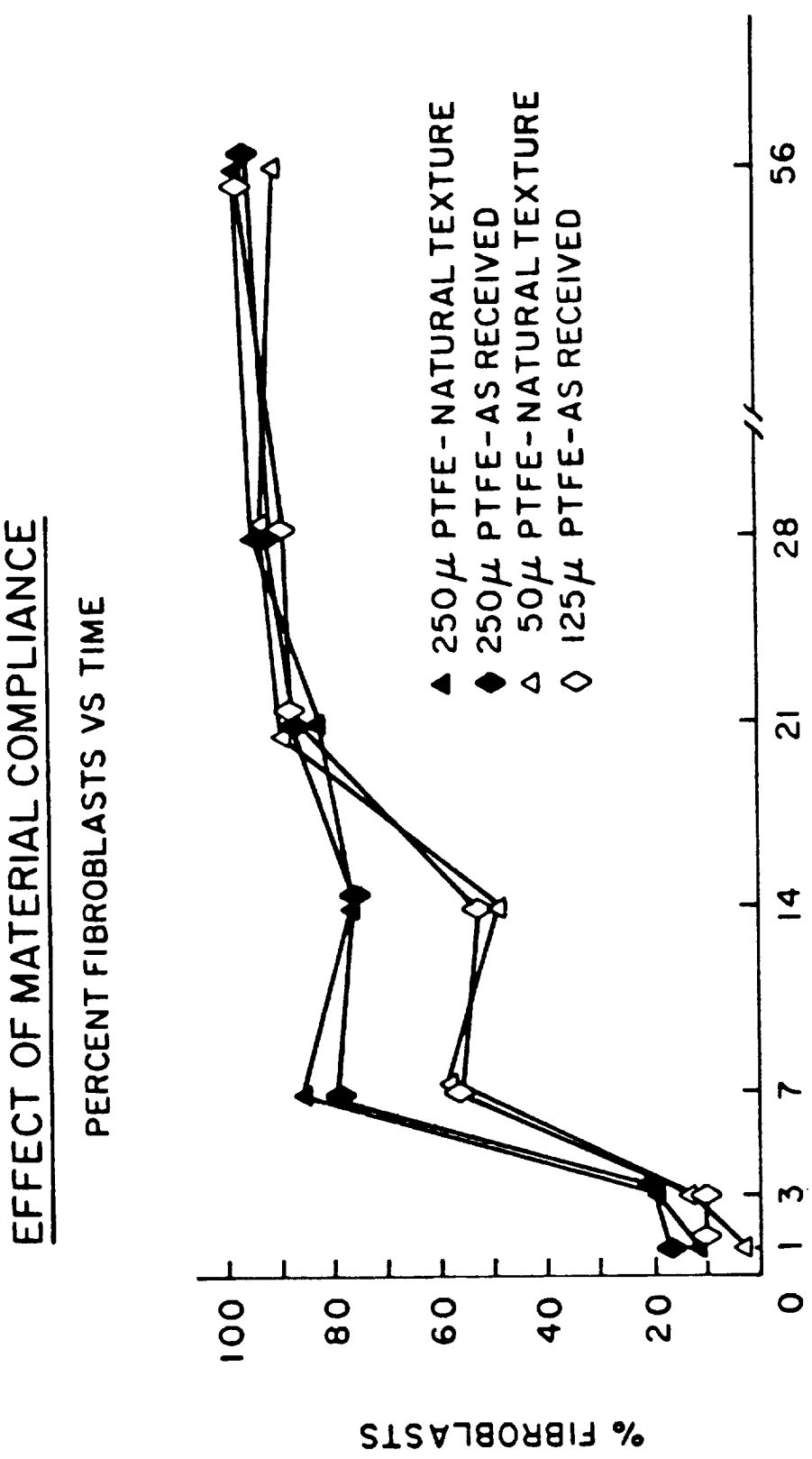
EFFECT OF MATERIAL COMPLIANCE
PERCENT FIBROBLASTS VS TIME
▲ 250μ PTFE-NATURAL TEXTURE
◆ 250μ PTFE-AS RECEIVED
△ 50μ PTFE-NATURAL TEXTURE
◇ 125μ PTFE-AS RECEIVED
% FIBROBLASTS
100
80
60
40
20
0
1
3
7
14
21
28
56
TIME (DAYS)

FIGURE 40

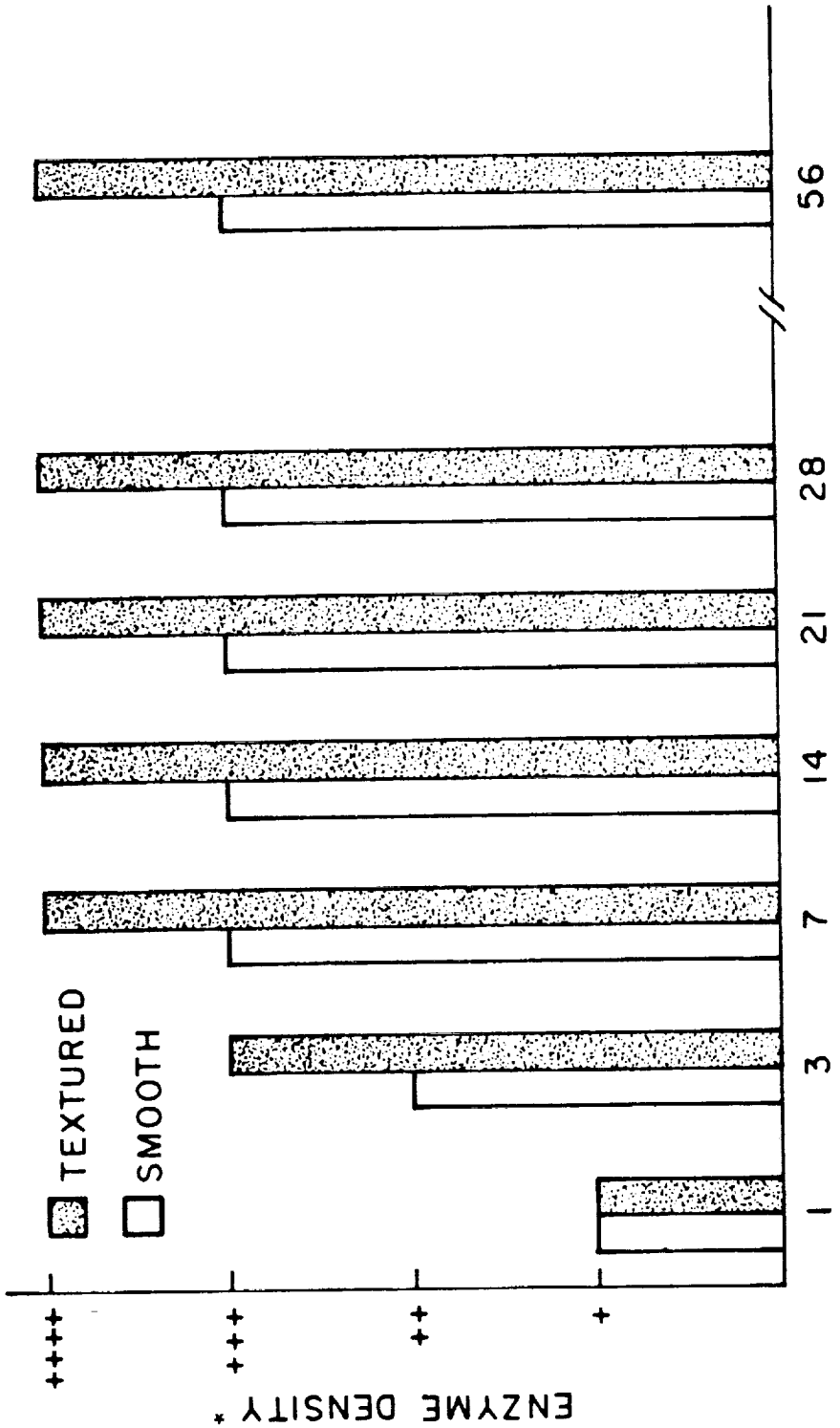

*Standards for (++++) and (+) were selected and used for comparison. A grade of (++++) was assigned to a slide having the most intensely staining interfacial cells. A grade of (+) was assigned to a slide having the least staining at the interface. A qualitative assessment was made to grade (++) and (+++). A minimum of 2 samples was analyzed for each data point.

FIGURE 41

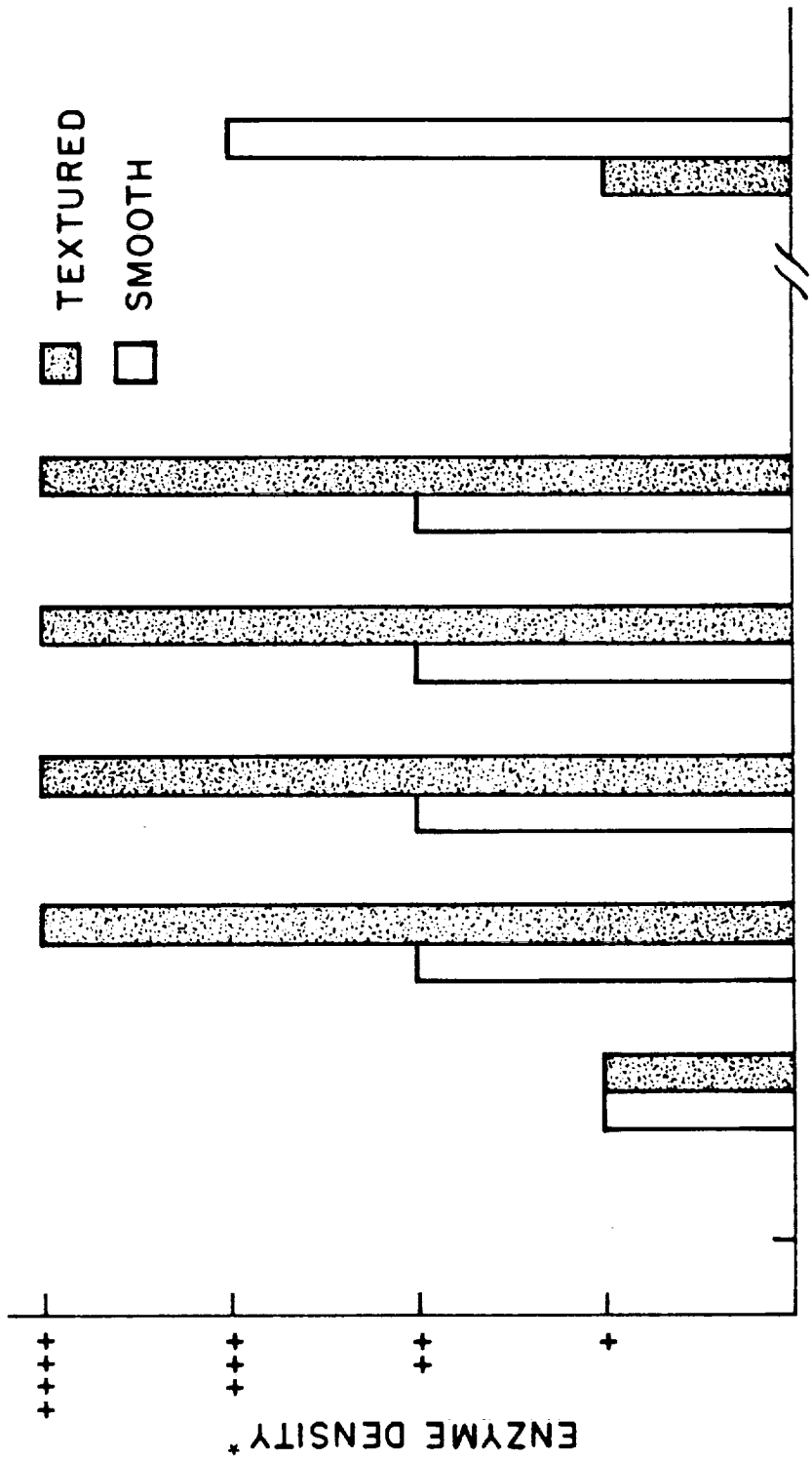

*Standards for (++++) and (+) were selected and used for comparison. A grade of (++++) was assigned to a slide having the most intensely staining interfacial cells. A grade of (+) was assigned to a slide having the least staining at the interface. A qualitative assessment was made to grade (++) and (+++). A minimum of 2 samples was analyzed for each data point.

FIGURE 42

250μ PTFE **ALKALINE PHOSPHATASE** ACTIVITY VS TIME

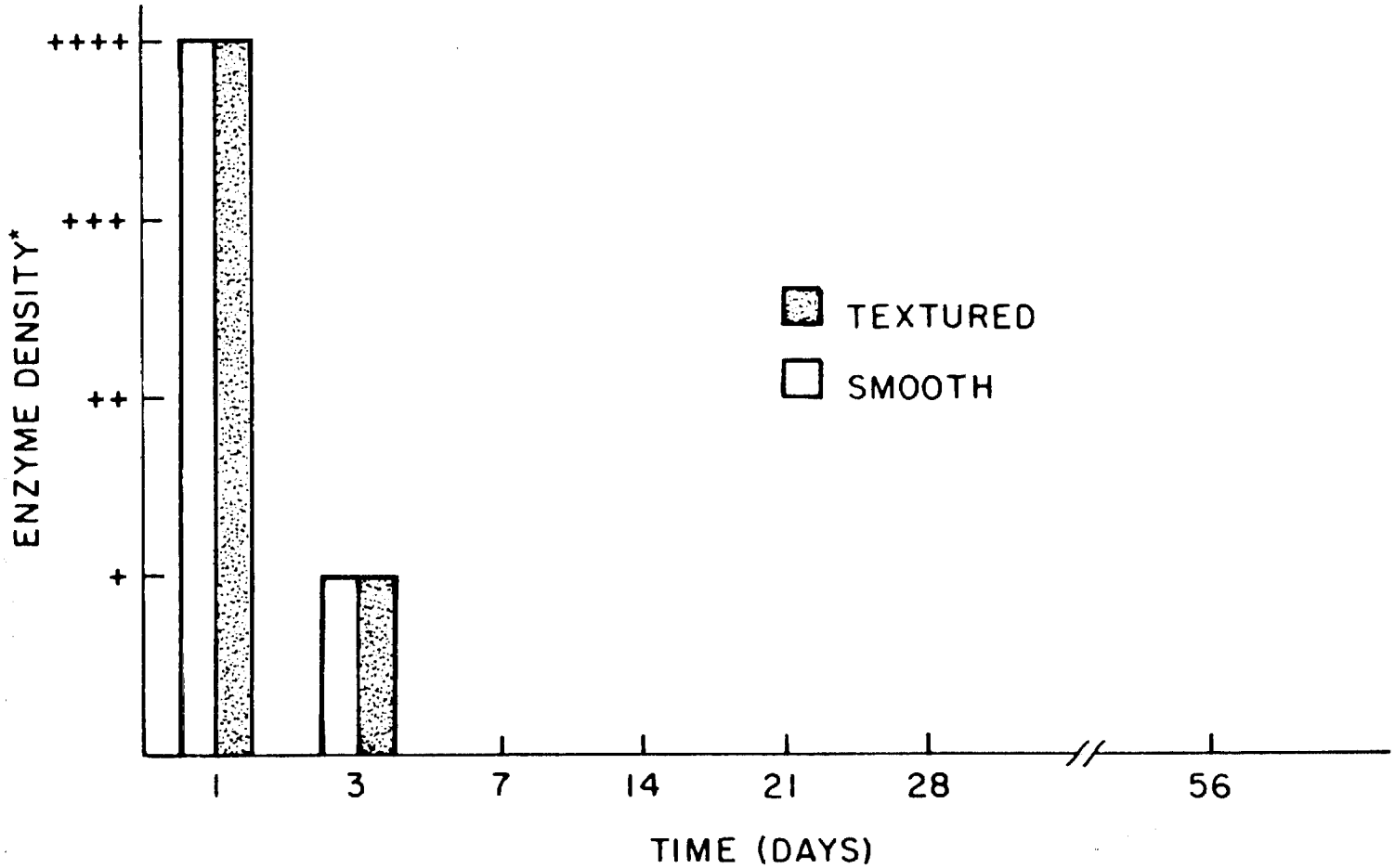

*Standards for (++++) and (+) were selected and used for comparison. A grade of (++++) was assigned to a slide having the most intensely staining interfacial cells. A grade of (+) was assigned to a slide having the least staining at the interface. A qualitative assessment was made to grade (++) and (+++). A minimum of 2 samples was analyzed for each data point.

the increased staining on textured surfaces is maintained. No difference between smooth and textured surfaces can be seen with the alkaline phosphatase; both surfaces reveal a peak staining at 1 day which has subsided completely by day 7.

B. Scanning Electron Microscopy (Figures 43-47)

Samples were selected so that at least one implant of each surface treatment at each time period could be observed using scanning electron microscopy. Textured surfaces of both Teflon and Delrin revealed an increased adhesion of cells and biological material at all time periods. At times of 7 days and more, large biological masses could be seen on the textured surfaces with attached individual cells. These masses were assumed to be FBGC's. Smooth samples of both PTFE and Delrin were coated with a layer of substance believed to be protein with cells adhering to this layer. Smooth Delrin samples typically displayed an increased cell adhesion, which in many areas reached confluence, when compared with smooth PTFE samples, which revealed less cell adhesion with individual cells that were less spread. Within each material system, no difference could be distinguished between as received, masked, or ion polished samples.

C. Transmission Electron Microscopy

Smooth and textured samples of both Teflon and Delrin were processed and observed using TEM. Time periods of 1 week, 4 weeks, and 8 weeks were observed for each sample. All smooth samples were as received, except the 4 week Teflon sample. Textured and smooth samples at this time period were taken from a ½ textured/½ masked sample.

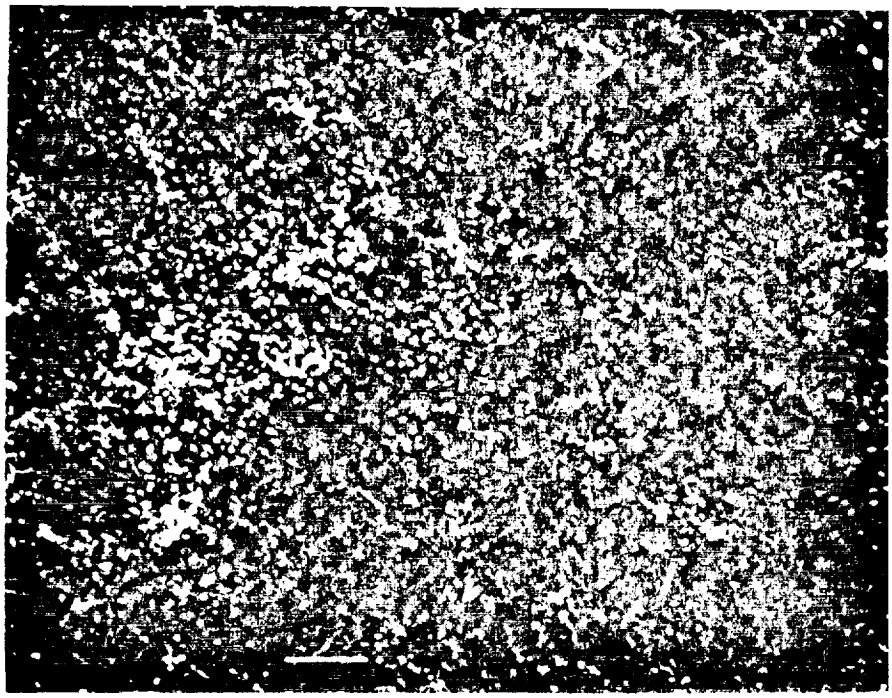

Figure 43. Surface of 1 day, textured Delrin (160X).

Figure 44. Surface of 1 day, as received Delrin. Note decreased cell adhesion in comparison to Figure 43 (160X).

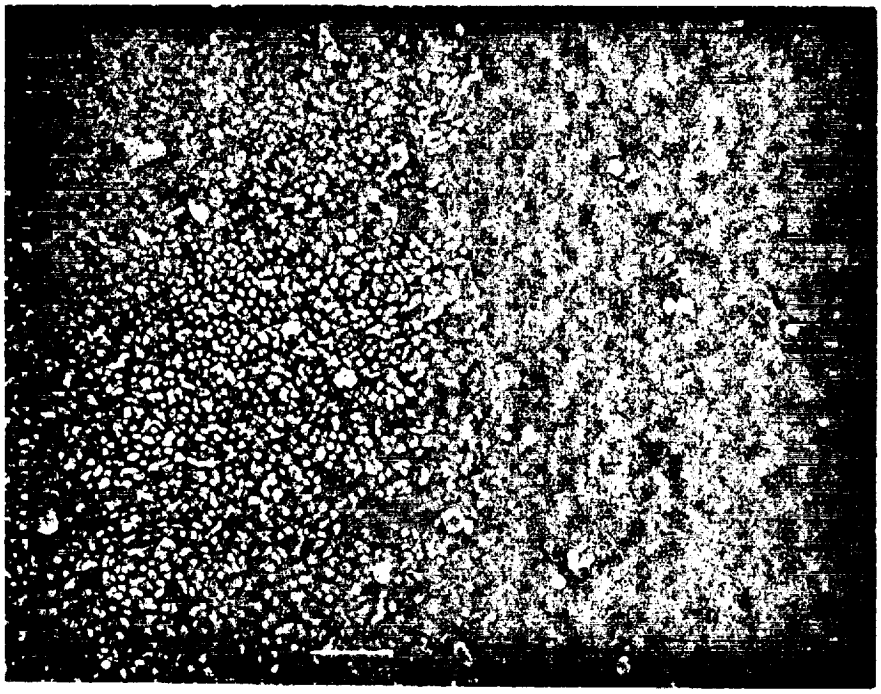

Figure 45. Surface of 3 day, ½/½ sample showing increased cell adhesion on textured side (160X).

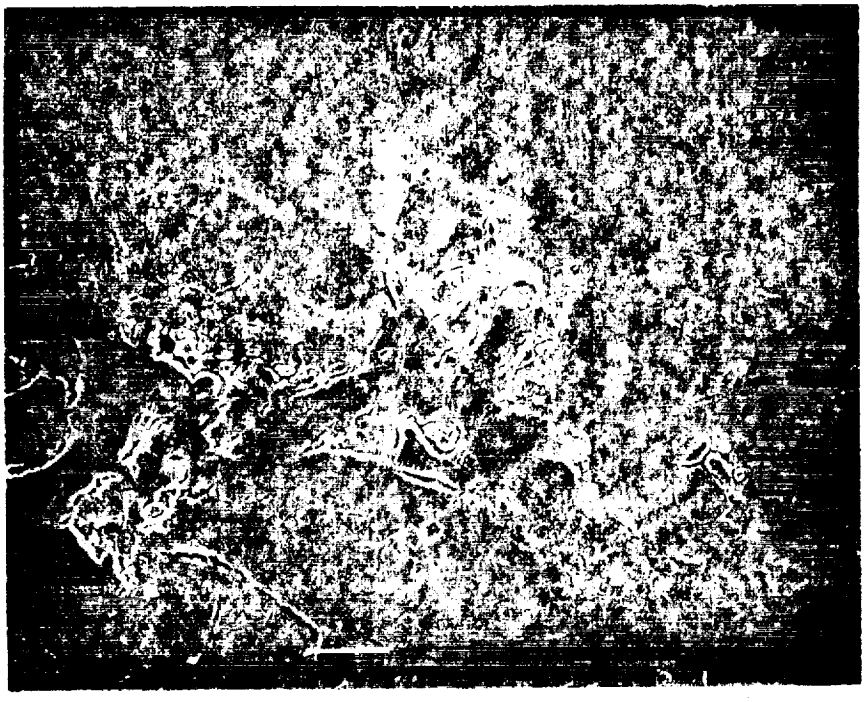

Figure 46. Surface of 4 weeks, as received Delrin (160X).

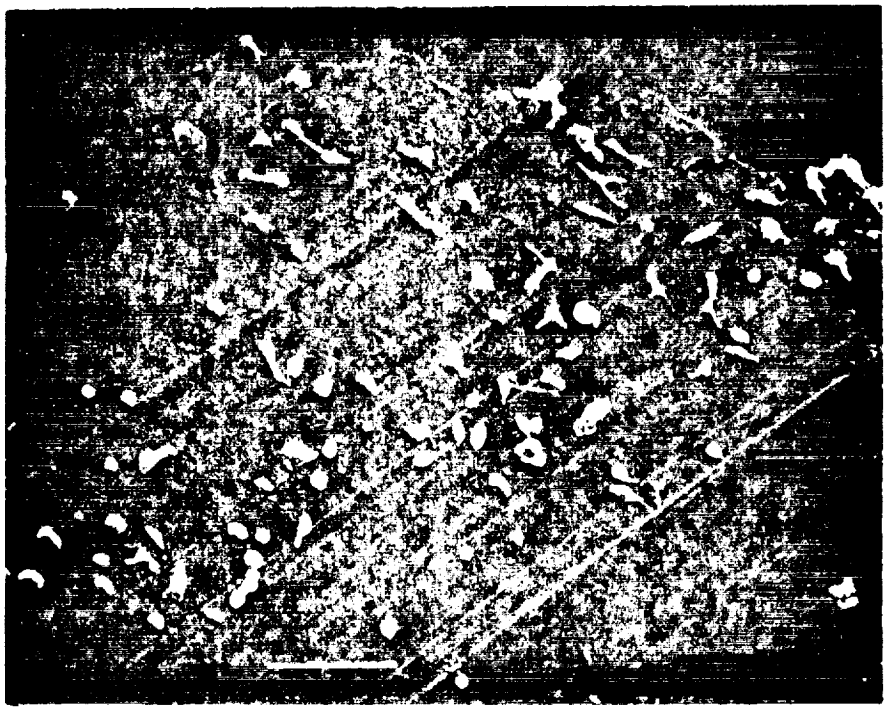

Figure 47. Surface of 4 week, as received PTFE. Note decreased tissue adhesion in comparison to Figure 46 (240X).

1. PTFE

At one week, many of the cells at the textured interface have fused to form FBGC's. Macrophages with numerous filopodia and vacuoles can be seen at or near the interface. There is a tendancy for filopodia to be on the side of the cell facing this material. The collagen within the fibrous capsule is layered in different directions. As received samples at one week reveal macrophages at the surface with fewer filopodia than the textured surface and few if any vacuoles. Collagen is sparse within the capsule.

At 4 weeks, the textured interfaces reveal mononuclear cells that are spherical and contain numerous filopodia and vacuoles. There is a high degree of interdigitation of filopodia between neighboring cells. The comparable smooth surface exhibits interfacial cells which are flattened with few vacuoles or filopodia.

Eight week textured surfaces reveal cells at the interface with a "foamy" appearance in the nucleus and cytoplasm. Cell borders are not well defined. The cytoplasm of interfacial cells contain numerous vacuoles and electron dense bodies, assumed to be lysosomes. The chromatin in the nucleus is unevenly distributed. Some of the elognated cells within the fibrous capsule which appear as fibrocytes under light microscopy are actually elongated macrophages. As received PTFE at this time displays flattened macrophages at the interface with few filopodia, and no vacuolozation. The capsule exhibits abundant collagen organized in layers, each layer in a different direction.

2. Delrin

At one week, as received samples exhibit monocytes and macrophages

at the interface with filopodia and a small amount of vacuolization. The textured sample at this time, reveals fused mononuclear cells (FBGC) immediately adjacent to the texture. These FBGC's contain numerous vacuoles and electron dense bodies assumed to be lysosomes. The nuclei within the FBGC's appear picnotic, with clumped chromation aggregating toward the nuclear envelope. Adjacent to the FBGC's are numerous nononuclear cells possessing very large numbers of filopodia interdigitating with neighboring cells. Beyond these cells are fibroblasts and occasionally elongated macrophages. Within the capsule of the 1 week smooth Delrin sample, a cell was observed having some of the features of a myofibroblast - abundant ER, convoluted nuclei, and collagen fibers running perpendicular to the axis of the cell.

Four week as received samples demonstrate interfacial cells with numerous vacuoles and lyosomal bodies within the cytoplasm and picnotic nuclei. These cells are very similar to those described for one week textured samples. Adjacent to these picnotic cells, going into the capsule, are macrophages with abundant filopodia. Occasionally, fibroblasts are adjacent to the interfacial macrophages.

Eight week samples do not reveal a remarkable difference from their respective 4 week samples. The interfacial cells of both the as received and textured samples exhibit characteristics associated with nonviable cells. The chromatin is aggregated and much of the nuclear space is clear. On textured samples, interfacial cells are fused, however, no fusion was observed at the smooth surface. Both 8 week samples reveal macrophages adjacent to the nonviable interfacial

cells with numerous filopodia. Phagocytosis of cellular debris can be seen.

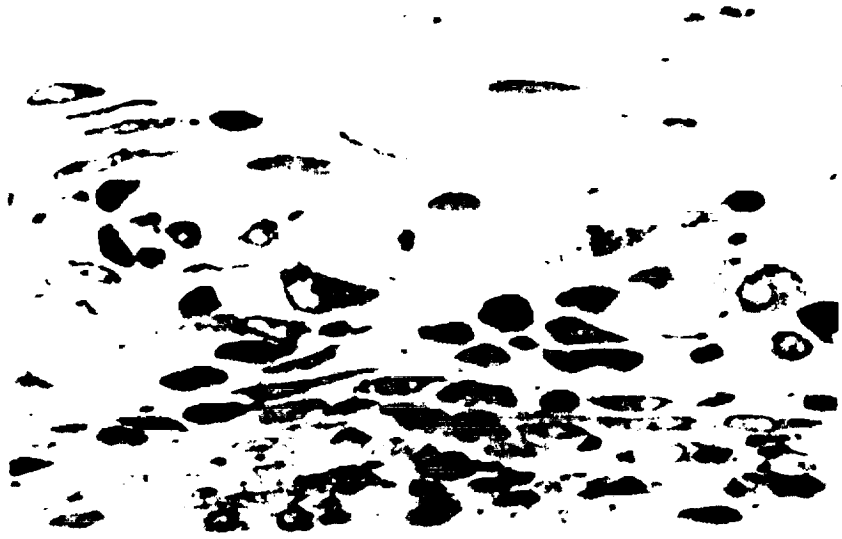

Figure 48. Tissue response to as received PTFE after 1 week implantation (material/tissue interface at bottom) (770X).

Figure 49. Mononuclear phagocytes adjacent to textured PTFE at 3 days (770X).

Figure 50. Interfacial region associated with textured PTFE at 1 week (material at bottom) (2000X).

Figure 51. Higher magnification of Figure 50. (5000X).

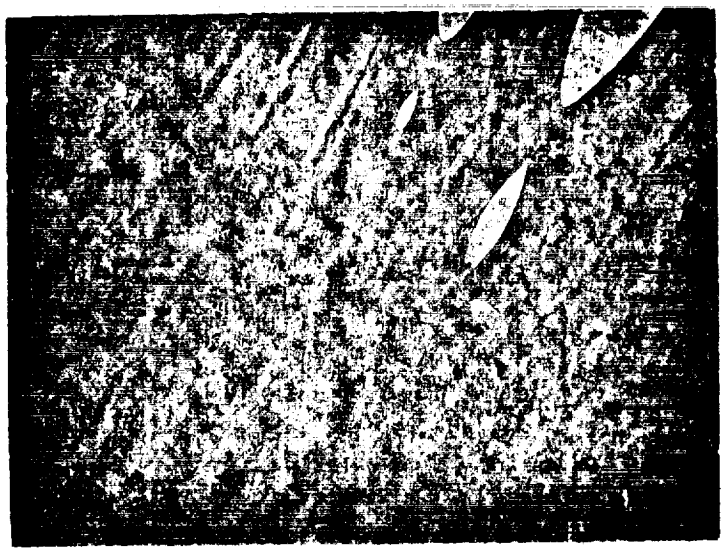

Figure 52. Interfacial cell associated with smooth (masked) PTFE at 4 weeks (3300X).

Figure 53. FBGC's adjacent to textured PTFE (4 weeks) (770X).

Figure 54. Cell having large cytoplasmic to nuclear ratio adjacent to textured PTFE (4 weeks) (770X).

Figure 55. Interfacial cells associated with textured PTFE at 4 weeks (2000X).

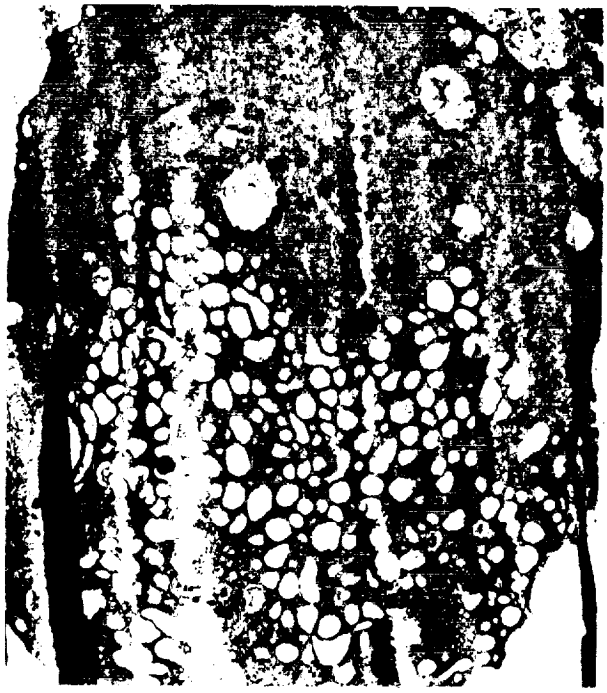

Figure 56. Highly vacuolated macrophage adjacent to textured PTFE at 4 weeks (material in direction of bottom of photograph)(5000X).

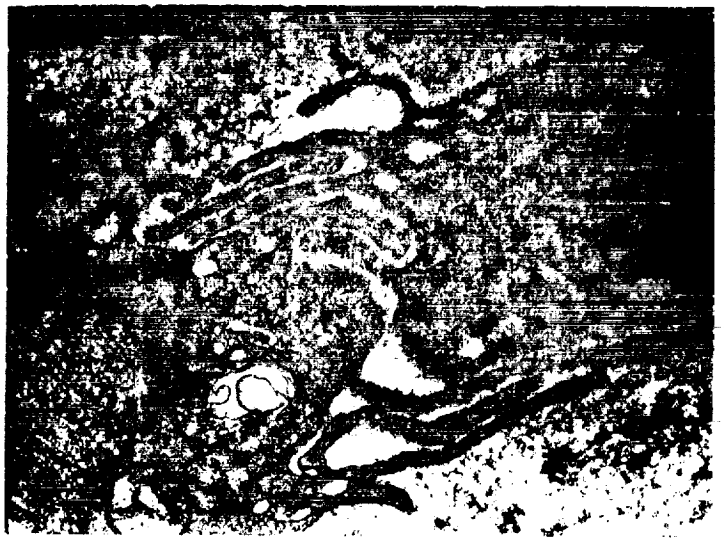

Figure 57. Interdigitation of filopodia between macrophages near a textured PTFE surface (4 weeks) (material in direction of bottom of photograph)(20,000X).

Figure 58. Macrophages (darkly staining cells) with increased filopodia in direction of textured PTFE (4 weeks) (material in direction of bottom of photograph) (6700X).

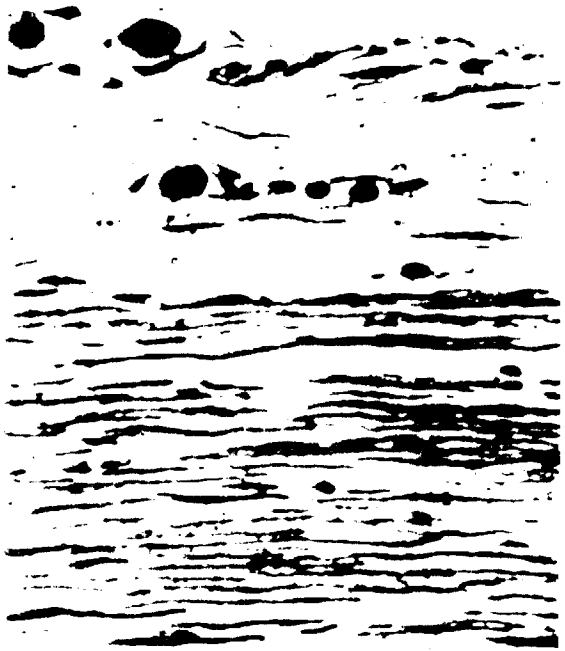

Figure 59. Fibrous capsule associated with as received PTFE at 8 weeks (material/tissue interface at bottom) (770X).

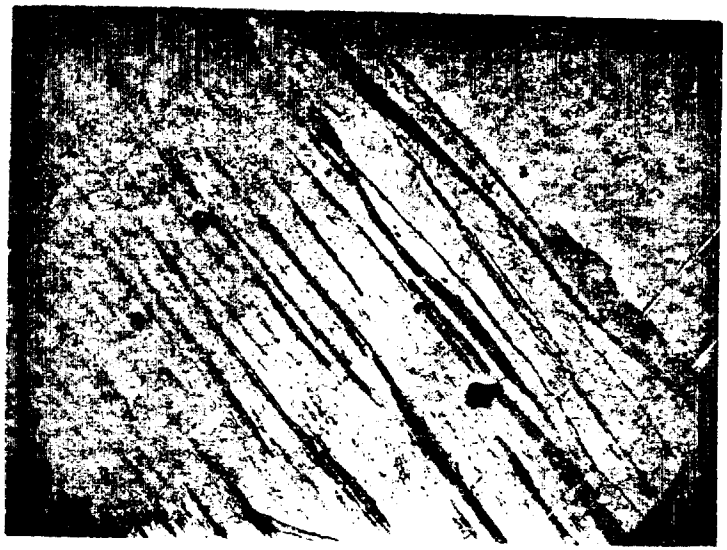

Figure 60. Fibrous capsule associated with as received PTFE at 8 weeks (material/tissue interface at bottom right) (1300X).

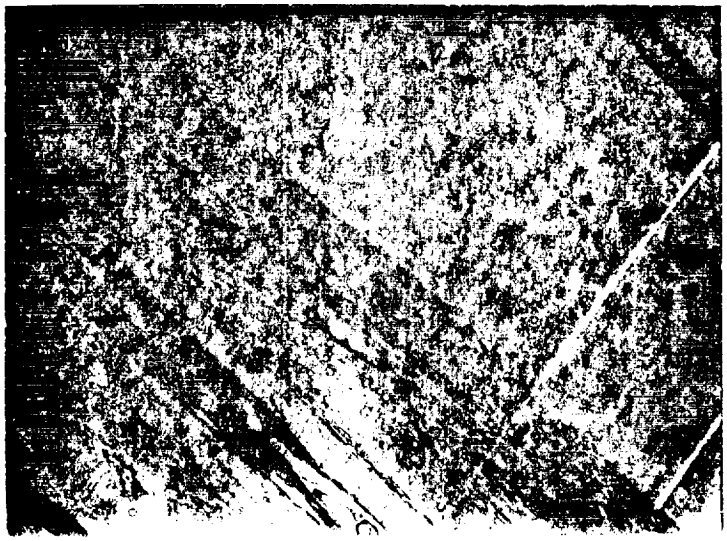

Figure 61. Interface of as received PTFE at 8 weeks (2700X).

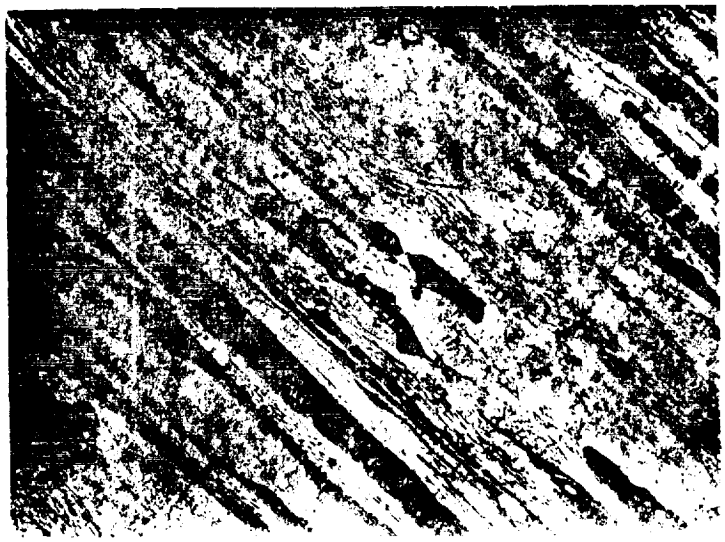

Figure 62. Fibrous capsule associated with as received PTFE at 8 weeks (material in direction of top right) (5000X).

Figure 63. Tissue response associated with textured PTFE at 8 weeks (770X).

Figure 64. Foreign body giant cell adjacent to textured PTFE at 8 weeks (material at bottom right corner) (2700X).

Figure 65. Fibrous capsule associated with as received PTFE at 8 weeks (tissue/material interface at bottom)(200X).

Figure 66. Decreased fibrous capsule associated with textured PTFE at 8 weeks in comparison to Figure 65. (200X).

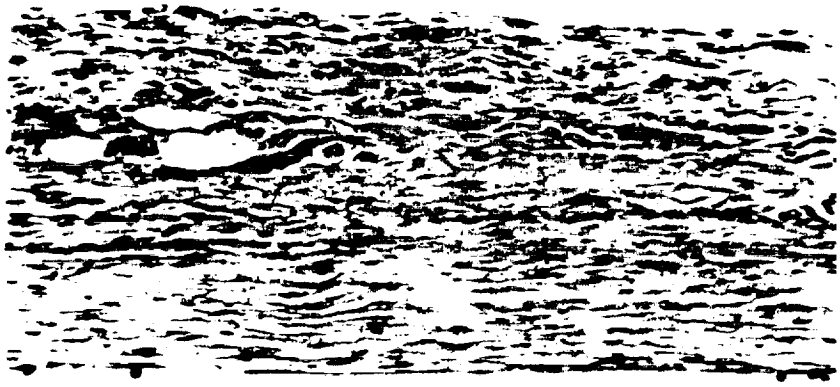

Figure 67. Fibrous capsule of 4 weeks, as received PTFE (tissue/material interface at bottom)(200X).

Figure 68. Fibrous capsule of 4 weeks, as received Delrin illustrating increased cell density over the comparable PTFE sample (Figure 67)(tissue/material interface at bottom)(770X).

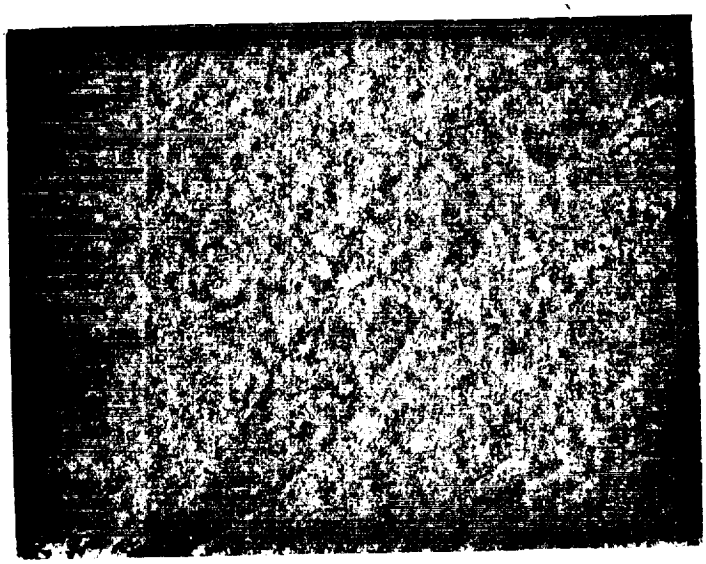

Figure 69. Myofibroblast within the fibrous capsule of as received Delrin at 1 week (5000X).

Figure 70. Interfacial region associated with as received Delrin at 4 weeks. Cells adjacent to interface (at bottom) appear non-viable (3300X).

Figure 71. Fibrous capsule associated with as received Delrin at 4 weeks (material in direction of bottom of photograph) (3300X).

Figure 72. Macrophage (m) phagocytizing cellular debris associated with nonviable interfacial cell (as received Delrin-8 weeks) (material at bottom) (3300X).

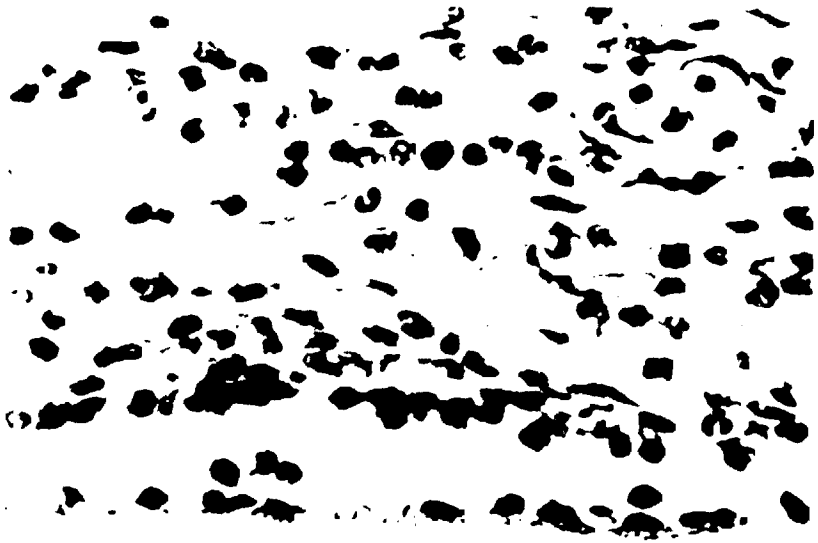

Figure 73. Tissue response associated with textured Delrin at 3 days (material at bottom)(770X).

Figure 74. Interfacial region of textured Delrin at 1 week (material at bottom)(2000X).

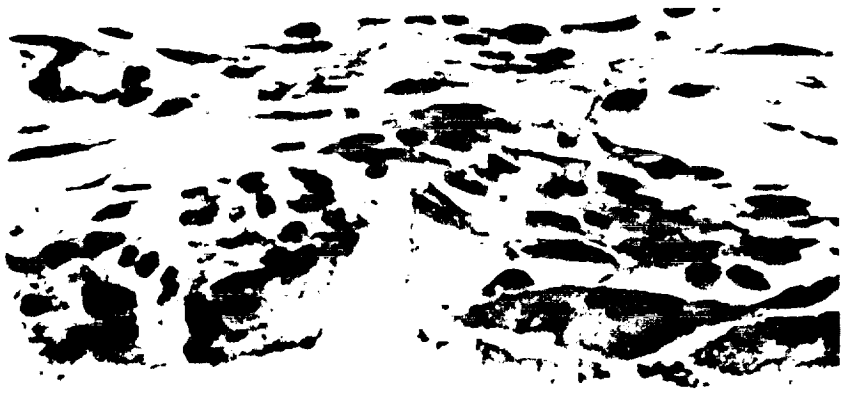

Figure 75. Foreign body giant cells adjacent to textured Delrin at 3 weeks (770X).

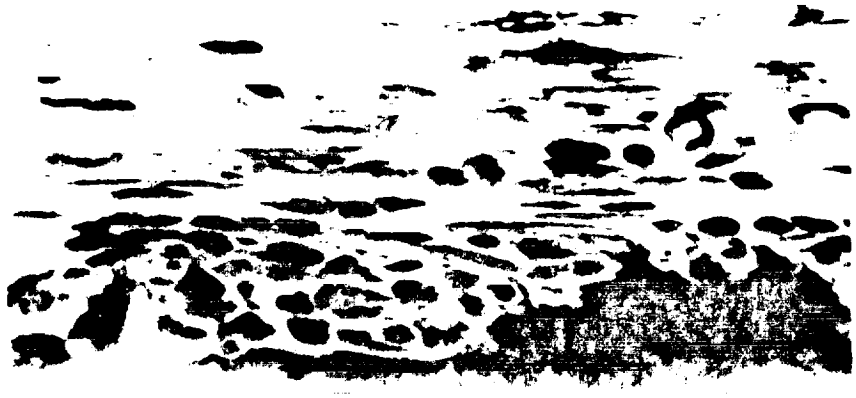

Figure 76. Tissue response to textured Delrin at 4 weeks (770X).

Figure 77. Interfacial region associated with textured Delrin at 4 weeks. FBGC's are adjacent to textured surface (at bottom) (2000X).

Figure 78. Interfacial cells and surrounding capsule associated with textured Delrin at 8 weeks (770X).

CHAPTER V. DISCUSSION

This invesgiation examined the soft tissue response to four variables: (1) texture, (2) chemical effects of the ion beam environment, (3) material composition, (4) material compliance. The following discussion will be organized according to these topics.

A. Texture

The ion beam etching process used to texture the materials did not produce significant changes in either surface elemental composition, as determined by Ion Scattering Spectroscopy, or surface energy, as determined by contact angle analysis. Thus a system was employed which allowed the investigation of the tissue response to only one variable - surface texture.

The surface texture used in this investigation does alter some of the characteristics associated with the foreign body response. The primary effects of the surface texture are to change the morphology of the interfacial cells and the kinetics of the fibrous capsule formation.

1. The Interfacial Cells

The textured interface promotes an increased adhesion of cells. By use of TEM these cells were identified to be of the mononuclear phagocyte system. Initially, the textured surfaces were covered by monocytes and macrophages. At times of one week and greater, several ultrastructural changes were observed in these cells. The macrophages developed numerous filopodia which were frequently

interdigitated with neighboring cells. FBGC's became the predominate cell at the interface. Cells that did not fuse to form FBGC's showed increased vacuolization and an increased cytoplasmic to nuclear ratio. Concurrent with these morphologic and ultrastructural changes, the interfacial cells adjacent to textured surfaces displayed an increased metabolic activity and increased acid phosphatase activity.

A transducing mechanism which might account for these phenomenon can be approached by two avenues. First, the adsorbed exudate could in some way promote the observed events. Second, the physical nature of the texture itself may in some way directly alter cell function.

The implantation of any material into the soft tissue is followed by the adsorption of proteins from the wound exudate. In blood contacting systems, this initial film has been implicated as mediating subsequent blood interactions at the interface (66,114,127,229). The proportions of the various plasma proteins (93) and their equilibrium exchange rates have been suggested to be a critical factor in the response of blood to a material. The adsorbed exudate proteins on subcutaneous implants may also transduce subsequent cellular and humoral responses (11,125,169).

Recent in vitro work has demonstrated the requirements of specific serum components for attachment and spreading of cells (46,159,265, 266,267). One of the most important of these factors is serum fibronectin (cold insoluble globulin). It is possible that the physiochemical nature of the texture induces increased plasma fibronectin adsorption which in turn increases cell attachment. Plasma fibronectin has a high affinity for fibrin (142). Thus if the

texture induces increased fibrin accumulation, which then increases the amount of adsorbed plasma fibronectin, subsequent cell attachment may be increased.

The incidence of protein adsorption and adsorption induced conformational change is a function of the molecular structure of the surface as well as the nature of the protein involved (8,46). It is also conceivable that the physical nature of the texture used in this study could affect protein adsorption and the ensuing exchange rates of these proteins. The small radii of curvature that exists at the tips of the texture spikes will have an increased surface energy (79). This increased energy may have an affect on the type, rate of adsorption and conformational change of adsorbed proteins.

Even if the surface energy of a curved surface can be assumed to be constant, the vapor pressure above a curved surface will be different from that above a planar surface as predicted by the Gibbs-Thomson equation (79):

$$\ln\left(\frac{P_i}{P_i^\circ}\right) = \frac{\bar{V}_i \gamma}{RT}\left(\frac{1}{r_1} + \frac{1}{r_2}\right). \qquad (1)$$

This equation specifies that above a curved surface the partial pressure P_i of component i is different from P_i°, the value above a plane surface. $\bar{V}_i$ is the partial molal volume of component i in the condensed phase; r_1 and r_2 are the principle radii of curvature and are considered negative when the surface is concave toward the solution. Extending this further, $\frac{P_i}{P_i^\circ}$ is equavalent to the activity of species i. The negative radii of curvature located at the bottom of the texture (between spikes) creates an activity gradient in the direction of the

troughs. This could influence protein exchange at the interface, which could alter the local environment of interfacial cells and produce the observed cellular behavior.

At 4 weeks, mononuclear cells adjacent to and in the vicinity of the textured interface display increased filopodia and an oriented morphology with the nuclei displayed away from the contact surface. These observations are indicative of chemotactic stimulation (70). In additon, the increased cytoplasmic to nuclear ratio and increased filopodia formation on one side of the cell are also changes that can be induced by chemotactic stimulation. The sequence of the inflammatory cells responding to both textured and smooth surfaces was similar to that described in the literature (140,157,163,180,226, 227,264). Within the specified fields no difference in the numbers of cell types could be distinghished between textured and smooth surfaces at any time interval. A model to account for the observed morphology would, therefore be difficult to attribute to constant generation of chemotactic factors by the textured surface.

So far, the physiochemical nature of the texture has been suggested to alter protein concentrations, protein exchange, and possibly protein conformation. Although polystyyene particles in the same size range as the spike tips have been shown to produce an immunogenic response, no such response was observed in this study with any of the surfaces.

The textured surface may not produce any change in adsorbed proteins, and elicit the altered responses in the interfacial cells simply by the increased amounts of exudate trapped within the

interstices of the texture. The increased amount of exudate on the texture would present a larger volume to be disposed by the macrophages which would account for the debris seen within many of the vacuoles.

Enzyme production has been shown to be governed by environmental stimuli (40,41) which would be consistent with the observed increase in acid phosphatase production in the cells adjacent to the textured interface. Since phagocytosis is an energy dependent process (146,202,203), the increased metabolic needs would also account for the increased SDH staining.

An alternate approach is to consider the morphological nature of the texture which may interact directly with cells, and produce the observed phenomenon. The texture spikes may be seen by the cells as particles, so that initial adherence of the mononuclear cells to the texture may be an act to phagocytize the projections; adhesion is a necessary requirement in the process of phagocytosis (142,202,203). If the spike tip can be modeled as a spherical particle with another spherical particle (the cell) approaching it, an expression relating the force of repulsion (electrostatic) with the forces of attraction (van der Waals) may be written (244,245,246).

$$V_t = V_r + V_a \qquad (2)$$

V_t = total energy of interaction

V_r = electrostatis energy of repulsion

V_a - van der Waal forces of attraction

For two interfacing particles of radius a_1 and a_2 with surface potentials ψ_1 and ψ_2 separated by distance H in a medium of bulk dielectric constant ε, V_t is given by:

$$V_r = \frac{\varepsilon}{4} \frac{a_1 a_2}{a_1 + a_2} \{(\psi_1 + \psi_2)^2 \ln (1 + \exp(-KH)) + (\psi_1 + \psi_2)^2 \ln(1 - \exp(1-KH))\} \quad (3)$$

Where 1/K is the Debye - Huckel parameter representing the effective width of the diffuse electrical double layer (245).

$$\frac{1}{K} = \left(\frac{8\pi ne^2 Z}{\varepsilon kT} \right) \quad (4)$$

n = half the total numbers of ions per cubic centimeter in the bulk solution

e = electronic charge

k = Boltzmann's constant

Z = valence

T = absolute temperature

The force of attraction may be expressed as follows:

$$V_a = - \frac{Aa_1 a_2}{6(a_1 + a_2)H}$$

Where A is the Haemaker constant (246). Equation 3 will give information about V_r only when the two surfaces are within approximately $\frac{2}{K}$ of each other. For a more exact understanding of interactions between a cell and a material surface separated by less than $\frac{2}{K}$, the problem may then be examined in terms of intermolecular interactions (245). However, before details of an intermolecular interaction can be described, a detailed knowledge of the chemical nature of the interacting species is required. This knowledge is

lacking for the cell periphery (245) and this series of equations neglects the possibility of an intermediate protein film on the material surface. There is also a problem of using bulk phase dielectric constants. It is well known that the structural properties of water and proteinacous materials near charged surfaces are different from that in the bulk phase (93,245). Other problems faced with this approach are: assumption of uniform charge density on the cell surface (not true) (245) and the uniform radius of curvature (varies with the size of the pseudopod).

The texture may induce changes in the interfacial cells via the very high pressures produced at the spike tips. Pressure and tension have been shown to alter cell migration, allignment, and metabolic activity (16). Alterations in cell shape may change the cell's functional capacity. Stretching the cell membrane may alter steric configuration of its components and subsequent diffusion through the membrane, which affects the types of substances entering the leaving the cell. A monrandom distribution of certain compounds within the cell, caused by these external factors, may signal selective triggering of reactions that culminate in morphological and functional changes in the cell (16,248).

Irrespective of whether physical or physiochemical mechanisms are responsible for the phenomenon at the interface, specific biological phenomena were observed. The interfacial cells adjacent to the textured interfaces display several features found in epitheloid cells. Interdigitation of filopodia between neighboring cells is prominent (2,154,205a). Although light microscopy reveals

many of the cells on the texture to be fused (4 weeks PTFE), the frequent interdigitation of filopodia observed with TEM may account for some of the apparently merged cytoplasms (154). The clear vacuoles within these cells may be lipid droplets, another characteristic of the epithelioid cell (59,154). Lipid droplets may also be indicative of an aging macrophage (10). Epithelioid cells are typically described as secretory (2,154,195), having a prominent Golgi apparatus (59,154). No Golgi apparatus, however, was observed in any of the interfacial cells. Regardless of whether these cells may be described as epithelioid cells or macrophages, they eventually fuse to form FBGC's.

Many mechanisms for FBGC formation have been proposed, but none have been substantiated (2,133,195). Surface roughness associated with implant movement has been implicated as an inciting agent (95). If surface roughness can be equated with small radii of curvature and small radii of curvature with implant edges, then there may exist a commonality between FBGC's associated with the textured surfaces and edges of implant discs. The occasional FBGC's seen on "smooth" PTFE surfaces may be due to the microscopic surface pits illustrated in Figure 4. In any event, the physical state of an implant material is strongly suggested as a participating variable in FBGC formation (33a).

Of the cells within the mononuclear phagocyte system, FBGC's have maximal numbers of mitochondria and lysosomes (205a). This would account for at least some of the increased staining of SDH and acid phosphatase at textured interfaces. The lysosomes within FBGC's

decrease with age which may relate to the decreased acid phosphatase activity observed at 8 weeks. Previous investigations employing roughened PTFE rods have revealed similar histochemical observations (186,187). Alkaline phosphatase shows a similar activity for both textured and smooth surfaces indicating that the acute response involving PMN activity is unaltered by the surface morphology used in this investigation.

2. The Fibrous Capsule

A major difference noted between smooth and textured surfaces was the kinetics of capsule development. At 8 weeks, the capsule adjacent to textured surfaces was reduced in thickness when compared to smooth surfaces. No significant difference in the density of collagen between smooth and textured samples could be distinguished.

One possible mechanism for reduction of capsule thickness is via a reduction in fibroblast proliferation. Macrophages have been shown to release substances which both increase and decrease the ability of cells to proliferate in vivo (2,121,122,214). However, no differences in cell type, cell density, and consequently fibroblast numbers were observed between smooth and textured surfaces.

If fibroblast numbers are the same for each type surface, the reduced capsule thickness associated with textured surfaces may be a result of decreased collagen production. Substances released from macrophages in culture have been described to inhibit collagen production by fibroblasts (104). The increased presence of active macrophages at the textured interface may produce a substance that communicates to the fibroblasts and diminishes their collagen output.

Reduced capsule thickness associated with foreign bodies has been exhibited during kinin depletion (237). A mechanism has not been proposed, but it is possible that depletion of kinins reduces an influx of imflammatory cells via decreased vascular permeability and depleted kallikrein (a chemotactic factor). Decreased numbers of PMN's and mononuclear cells might result in decreased amounts of fibroplastic substances. Although kinin depletion is not likely to be the mechanism involved with the textured surfaces (numbers and cell types were similar), it does point out the intricate pathways and mediators involved in the control of the fibroblastic response. Elucidation of the signals responsible for turning the fibroblast "on and off" will be critical to understanding the foreign body response.

Myofibroblasts have been associated with wound contracture and capsule contracture in conjunction with breast prostheses (78, 178,179). In this investigation, cells were occasionally seen within the capsule having gross characteristics of the myofibroblast - elongated, RER, convolucted nuclei, and neighboring collagen running perpendicular to the cell axis. Unfortunately, the sample did not have the resolution necessary to observe the microfilaments along the plasma membrane, which is typically used to identify the myofibroblast (178,179). The reduced sample resolution may have resulted from fixation. It is important to embed samples within 1 to 3 days after fixation, which was not the case with some of the samples. The cell shown in Figure 69 is from a 1 week, as received, Delrin sample. Because no attempt was made to quantify myofibroblasts,

no correlation can be made between decreased capsule thickness and the appearance of myofibroblasts.

The mononuclear cells adjacent to the texture were shown to have an increased acid phosphatase activity. It is possible that other enzyme systems were also stimulated. Latex particles have been shown to stimulate collagenase and elastase secretion in mouse macrophages (249,250) The macrophages adjacent to the texture may be essentially degrading the capsule closest to the material interface, keeping the capsule from developing the thickness seen in smooth samples. The high degree of membrane ruffling in the interfacial cells may therefore be a phagocytic response to the collagen breakdown products. A preliminary experiment indicates that at 18 weeks there is no difference in capsule thickness between smooth and textured samples. The interfacial cells show a decline in their enzymatic activity at 8 weeks which may continue to decline with time. The diminished enzyme activity of these cells may correlate with the renewed growth of the fibrous capsule between 8 and 18 weeks.

The collagen that develops near the textured interface may also be of an altered structure, such that insufficient cross-links leads to a soluble form. An imbalance in the production or secretion of acid proteases in macrophages could lead to alterations in the extracellular matrix protein polysaccharide and hense effect the formation of fibrous collagen (167). Irregular formation of collagen in the fibrous capsules around implants has been reported (166).

The collagen development associated with smooth implants was similar to that described in previous investigations (57,173,260,261).

Although some have reported collagen production to be complete by 5 weeks (260), the capsules in this investigation show increases in thickness up to 18 weeks.

In this study, cells were occasionally observed within the fibrous capsule which possessed characteristics of both fibroblasts and macrophages (see Figure 71). These cells were elongated with an elognated nucleus and appeared as fibroblasts at low magnification. Ultrastructurally, the cells possessed numerous lysosomes, scant RER, and small numbers of filopodia. Monocytes have been described as pluripotential (132), and macrophages have been suggested by some to transform into fibroblasts during wound healing (49,117). The observations reported here suggest a transformation of macrophages to fibroblasts yet obviously do not directly confirm such a transformation. The issue of the source of the fibroblast in would healing and the fibrous capsule is far from resolved.

B. The Chemical Effect of the Ion Beam Envirnment

The results of this investigation indicate that there are no distinguishable alterations in the soft tissue response between "as received", "masked", and "ion polished", samples of either PTFE or Delrin. SEM of implant surfaces indicated no difference in cell adhesion. Previous investigations have indicated an increase in cellular adhesion with samples exposed to ionized argon in radio frequency discharge chambers (192). Although the cells respond to textured surfaces and adhere in large numbers, the slight roughening of ion polished surfaces does not trigger the same response.

C. PTFE vs. Delrin

Initially, smooth Delrin samples reveal increased cellular adhesion in comparison to smooth PTFE samples. One obvious difference between these materials is their surface energy. Increased cell adhesion has been related to increased surface energies (12). However, attempts to relate cell adhesion to surface wettability of the unmodified substrate suffer from lack of knowledge of the actual surface properties of the substrate in the presence of the adsorbed components in vivo environments. It is more likely that the adsorbed proteins are altered selectively and present different outermost aspects which reflect differences in adhesion (12). Perhaps cell adhesion factors (cold insoluble globulin) preferentially adsorb to the higher energy surface of Delrin. Another material parameter that distinguishes Delrin from PTFE is that Delrin's surface energy has a large polar component while PTFE is predominately dispersive. This difference could affect subsequent protein adsorption (93) and consequently cell adhesion.

The tissue reaction at the Delrin interface at times of 1 week and more, however, is overshadowed by the release of formaldehyde. In response to this release, interfacial cells develop picnotic nuclei, numerous vacuoles and electron dense bodies in the cytoplasm, and occasionally indistinguishable cell membranes. The formaldehyde probably alters cell function by cross-linking cell membrane components as well as internal and external proteins. The interfacial cells eventually become non-viable and appear as debris to incoming viable macrophages. Breakdown products of these interfacial cells may account for the influx of greater numbers of cells resulting in

increased cellular density of the capsule surrounding Delrin samples. Unfortunately, the release of formaldehyde from Delrin makes it impossible to attribute any altered response of textured samples to morphology alone.

FBGC's are observed on textured Delrin samples at all times. As time progressed, the cells became less viable as evidenced by TEM. It may be that as the cells were phagocytized they were replaced by new cells, thus maintaining cells at the interface (155,195).

At 8 weeks, the fibrous capsule associated with textured and as received Delrin is significantly less than the corresponding PTFE samples. It is possible that the formaldehyde released from Delrin suppresses fibroblast activity directly or indirectly via the macrophage. Macrophage function may be altered so that fibrogenesis factor(s) are not produced resulting in a decreased fibrous capsule. Preliminary experiments indicate that there is no difference in fibrous capsule thickness between textured PTFE and Delrin samples at 18 weeks. A comparison of as received samples, however, indicate Delrin to possess a thicker capsule. The reduced formaldehyde release after 8 weeks (Figure 17) may allow normal cell function. The increased macrophage numbers may now be able to produce stimulatory sybstances which increase fibroblast activity and collagen production. In addition, components released from the non-viable macrophages at the Delrin interface may increase fibroblast activity (4a,87). Additional experiments will be necessary to better quality these observations.

A preliminary 18 week experiment indicates that Delrin exhibits much more vascularity in the fibrous capsule than PTFE. The cell

density of Delrin is similar to PTFE at 18 weeks, so that this difference in vascularity cannot be correlated with increased cell density. However, up to 8 weeks, Delrin exhibited a significantly greater cell density in comparison to PTFE, and the increased vascularity may represent a delayed response to angiogenesis factors released by mononuclear cells (35). Preliminary data demonstrates that the fibrous capsule of Delrin samples, both smooth and textured, exhibits a sharp increase in thickness between 8 and 18 weeks. It is not certain whether this is associated with the diminished formaldehyde released at this time (Figure 17). Fibrogenesis factors released by the increased numbers of mononuclear cells (per unit area) may account for the capsule increase. The increased vascular content of Delrin samples may also be a reflection of the metabolic needs of the fibroblast during their increased population of collagen between 8 and 18 weeks.

The release of formaldehyde from Delrin presents difficulty in the interpretation of the tissue response. If the polymer used in this study can be assumed to be properly end-capped, then the formaldehyde released may simply be a leaching of the monomer from the polymer. This would explain the first order kinetics of the release rate. The problem of formaldehyde release may be overcome by simply soaking the polymer as indicated by the decreased amounts released at later times (Figure 17). This process could be accelerated by heating the solution (56).

D. Material Compliance

A comparison of 250 μ and 125 μ as received Teflon reveals no difference in response with regards to cell response, capsule thick-

ness, and vascularity. Thus the difference in compliance between these thicknesses is not detectable by the soft tissue. The 50 μ textured sample has an increased capsule thickness in comparison to the 250 μ textured sample. This would indicate that the phenomena of a decreased fibrous capsule associated with a textured surface also requires the presence of a stiff or low compliance material. The difference in compliance between a 50 μ thick PTFE sample and a sample 250 μ thick, appears to be dectable by the soft tissue. FBGC's however, are formed on the textured surface irrespective of the material compliance used in this study.

Figure 79. Fibrous capsule associated with as received PTFE at 18 weeks. (material/tissue interface at bottom)(770X).

Figure 80. Fibrous capsule associated with as received Delrin at 18 weeks (material/tissue interface at bottom) (770X).

CHAPTER VI. CONCLUSION

The cells involved in the reparative process respond unequivocably to humoral mediators produced by proteolytic enzyme systems within the plasma and by the cells themselves. The implementation of fabrics, porous materials, and particulates as implants has indicated that the cellular (and possibly humoral) component of the inflammatory process also responds to variations in surface morphology. Unfortunately, these material systems have not lent themselves to the investigation of morphology alone due to additional factors such as mechanical effects, permeability, and difficulty in characterizing the morphology.

The texturing method employed in this investigation, ion beam texturing, provided a material with an altered and definable surface morphology, yet produced no change in surface chemistry. Thus, a system was developed for observing the soft tissue response to one material variable - surface morphology. The texture developed by this process induced modifications in the mononuclear phagocytes adjacent to the surface: increased cell adhesion, increased metabolism, increased acid phosphatase activity, increased vacuolization, increased filopodia formation, and increased FBGC formation. In additon, the kinetics of the fibrous capsule formation are altered by the presence of an ion textured surface. Physiochemical mechanisms can be hypothesized for the interfacial phenomena, however, the altered capsule development has a dependence on material compliance. A textured surface with an increased compliance develops a fibrous

capsule similarly to a smooth counterpart.

In the study of biomaterials, the biologic environment is responsive to all parameters of the material - physical, chemical, and physiochemical. Cells can detect small variations in surface chemistry as well as small changes in physical size. The results of this investigation demonstrate that the soft tissue response is altered by surface morphology and in particular the presence of the micro "hairlike" projections produced by ion beam texturing.

REFERENCES

1. Abercrombie, M. "Behavior of Cells Toward One Another". In Advances in Biology of Skin, vol. 5, ed. by W. Montagna and R.E. Billingham. MacMillan Co., New York, 1964, pp. 95-111.

2. Adams, D.O. "The Granulomatous Inflammatory Response - A Review". Am. J. Pathol. 84:164-91, 1976.

3. Akutsu, T. and A. Kantrowitz. "Problems of Materials in Mechanical Heart Systems". J. Biomed. Mat. Res. 1:33-54, 1967.

4. Alexander, P. and E.S. Horning. "Observations on the Oppenheimer Method of Inducing Tumors by Subcutaneous Implantation of Plastic Films". In Carcinogenesis, ed. by G.E.W. Wolstenholme and M. O'Connor. J. and A. Churchill, Ltd. London, 1959, pp. 12-25.

4a. Allison, A.C., J.S. Harrington, M. Birbeck. "An Examination of the Cytotisic Effect of Silica on Macrophages". J. Exp. Med. 124: 141-53, 1966.

5. Ambrose, E.J. "Cell Contact". In Recent Progress in Surface Science, vol. 1, ed. by J.F. Danielli, K.G.A. Pankhurst, A.C. Riddiford. Academic Press, New York, 1964, p. 338.

6. Anand, S.C., K.R. St. John, D.D. Moyle, D.F. Williams. "Stress Distribution in Porous Surfaced Medullary Implants". Ann.Biomed. Eng. 5: 410-20, 1977.

7. Andrade, J.O. "Interfacial Phenomena and Biomaterials". Med. Instrument. 7: 110-20, 1973.

8. Andrade, J.D., H.B. Lee, M.S. Jhon, S.W. Kim, J.B. Hibbs. "Water as a Biomaterial". Trans. Am.Soc. Art. Int. Org. 19: 1, 1973.

9. Arnon, R., H. Levinhau, M. Sela. "Immunospecific and Nonspecific Fixation of Complement by Poly-L-Lysine". Israel J. Med. Sci. 1: 404, 1965.

10. Axline, S.G. "Functional Biochemistry of the Macrophage". Sem. Hematol. 1: 142-60, 1970.

11. Bagnall, R.D. "An Approach to the Soft Tissue/Synthetic Material Interface". J. Biomed. Mat. Res. 11: 939-44, 1977.

12. Baier, R.E. "Surface Properties Influencing Biological Adhesion". In Adhesion in Biological Systems, ed. by R.S. Manly. Academic Press, New York, 1970, pp. 15.

13. Banks, B.A., A.J. Weigand, C.A. Babbush, C.L. VanKampen. "Potential Biomedical Applications of Ion Beam Technology". NASA TMX-73512, 1976.

14. Banks, R.E. Fluorocarbons and Their Derivatives. Daniel Davey and Co., Inc. New York, 1964, pp. 37-8.

15. Barvic, M. K. Kliment, M. Zavadil. "Biologic Properties and Possible Uses of Polymer-Like Sponges". J. Biomed. Mat. Res. 1: 313-23, 1967.

16. Basset, A.L. "Concurrent Concepts of Bone Formation". J. Bone and Joint Surg. 44-A: 217-44, 1962.

17. Bates, R.R. and M. Klein. "Importance of a Smooth Surface in Carcinogenesis by Plastic Film". J. Natl. Cancer Inst. 37: 145-51, 1966.

18. Becker, E.L. "The Reactions of Complement to Other Systems". Proc. Roy. Soc. London, Ser B. 173: 383-92, 1969.

19. Beller, D.I., A.G. Farr, E.R. Unanue. "Regulation of Lymphocyte Proliferation and Differentiation by Macrophages". Fed. Proc. 37: 91-6, 1978.

20. Bianco, C., A. Eden, F.A. Cohn. "The Induction of Macrophage Spreading: Role of Coagulation Factors and the Complement System". J. Expt. Med. 144: 1531-44, 1976.

21. Black, M.M. "Dynamics of Multinucleate Giant Cell Formation in vitro and in vivo". Br. J. Dematol 91 705-8, 1974.

22. Bloom, W. and D.W. Fawcett. A Textbook of Histology, 10th ed. W.B. Saunders Co., Philadelphia, 1975.

23. Bornstein, P., D. Duksin, G. Balian. "Organization of Extracellular Proteins on the Connective Tissue Cell Surface: Relevance to Cell Matrix Interactions in vitro and in vivo". Ann. N.Y. Acad. Sci. 312: 93-105, 1978.

24. Brady, G.S. and H.R. Clauser. Materials Handbook, 11th ed. McGraw-Hill Book Co., New York, 1977, pp. 911-12.

25. Brand, K.G., K.H. Johnson, L.C. Buoen. "Foreign Body Tumorigenesis". CRC Crit. Rev. Toxicol. 14: 353-94, 1976.

26. Braunwald, N.S. and B.S. Bull. "Factors Controlling the Development of Tissue Layers on Fabrics". In Prosthetic Heart Values, L.A. Brewer ed.-in-chief. Charles C. Thomas, Springfield, Ill, 1969, pp. 228-42.

27. Brown, N. "Polymerization of Formaldehyde". In Polyaldehydes, ed. by O.Vogl, Marcel Dekker, Inc., New York, 1967, pp. 8-10

28. Burg, K.H., and G. Sextro. "Physical Constants of Poly (oxymethylene)". In Polymer Handbook, 2nd ed., ed. by J. Brandrup and E.H. Immergut. John Wiley and Sons, New York, 1975, pp. V 63-70.

29. Burstone, M.S. "Histochemical Observations on Enzymatic Processes in Bones and Teeth".Ann. N. Y. Acad Sci. 85 431-44, 1960.

30. Calderon, J., R.T. Williams, E.R. Unanue, "An Inhibitor of Cell Proliferation Released by Cultures of Macrophages". Proc. Natl. Acad. Sci. (U.S.A.) 71: 4273-77, 1974.

31. Calnan, J. "The Use of Inert Plastic Material in Reconstructive Surgery I. A Biological test for Tissue Acceptance II. Tissue Reaction to Commonly Used Materials". Br. J. Plastic Surg. 16: 1-22, 1963.

32. Cameron, H.V., R.M. Pilliar, I. MacNab. "Porous Vitallium in Implant Surgery". J. Biomed. Mat. Res. 8: 282-9, 1974.

33. Carter, R.L. and F.J.C. Roe. "Induction of Sarcomas in Rats by Solid and Fragmented Polyethylene: Experimental Observations and Clinical Implications". Br. J. Cancer 23: 401-7, 1969.

33a. Charnley, J. Acrylic Cement in Orthopaedic Surgery, Williams and Wilkins Co., Baltimore, 1970.

34. Chu, C.H.U. "A Study of the Subcutaneous Connective Tissue of the Mouse, with Special Reference to Nuclear Type, Nuclear Division, and Mitotic Rhythm". Anatomical Record, 138: 11-25, 1960.

35. Clark, R.A., R.D. Stone, D.Y.K. Leung, I. Silver, D.C. Hohn, T.K. Hunt. "Role of Macrophages in Would Healing". Surg. Forum, 27: 16-18, 1976.

36. Clark, R.A., J.C. Boyd, J.F. Moran. "New Principles Governing the Tissue Reactivity of Prosthetic Materials: J. Surg. Res. 16: 510-22, 1974.

37. Cohen, I.K., R.F. Diegelmann, W.S. Wise. "Biomaterials and Collagen Synthesis". J. Biomed. Mater. Res. 10: 965-70, 1976.

38. Cohen, J. "Assay of Foreign-Body Reaction". J. Bone and Joint Surg. 41-A: 152-66, 1959.

39. Cohen, J. "Tissue Reactions to Metals - The Influence of Surface Finish". J. Bone and Joint Surg. 43-A: 687-99, 1961.

40. Cohn, F.A. and B. Benson. "The Differentiation of Mononuclear Phagocytes-Morphology, Cytochemistry, and Biochemistry". J. Exp. Med. 121: 153-69, 1965.

41. Cohn, F. A. "Macrophage Physiology". Fed. Proc. 34: 1725-9, 1975.

42. Coleman, D.L., R.N. King, J.D. Andrade. "The Foreign Body Reaction: A Chronic Inflammatory Response". J. Biomed. Mat. Res. 8: 199-211, 1974.

43. Colman, R.W. "Formation of Human Plasma Kinin". New England J. Med. 291: 509-15, 1974.

44. Copenhaver, W.M., Kelley, D.E., Wood, R.L. Bailey's Textbook of Histology, 17th ed. The Williams and Wilkins Co., Baltimore, 1978.

45. Crouse, G.S., R.D. Campo, M.S. Kodsi. "Incorporation Tolerance of Dacron Felt in the Bones of Rabbits". Plast. Reconstr. Surg. 54: 471-7, 1974.

46. Culp, L.A. "Biochemical Determinants of Cell Adhesion". In Cell Surface Glycoproteins: Structure, Biosynthesis, and Biological Function, ed. by R.L. Julians and R. Rothstein, Academic Press, New York, 1978, pp. 327-96.

47. Curran, R.L. and J.A.M. Ager. "Tissue Responses to Filter Membranes of Various Porosities". Nature 189: 1023-4, 1961.

48. Curran, R.L. and J.A.M. Ager. "Surface Dependence of the Peritoneal Response to Agar Gel". Nature 121: 494-5, 1962.

49. Curran, R.C. and A.E. Clark. "Phagocytosis and Fibrogenesis in Peritoneal Implants in the Rat". J. Path. Bacteriol. 88: 489-502. 1964.

50. Curran, R.C., D. Lowell, A.E. Clark. "Mucopolysaccharides in Peritoneal Granulomas in the Rat". J. Path. Bacteriol. 91: 429-39, 1966.

51. Davila, J.C., E.V. Lautsch, T.E. Palmer. "Some Physical Factors Affecting the Acceptance of Synthetic Materials as Tissue Implants". Am. N.Y. Acad. Sci. 146: 138-47, 1968.

52. Davis, S.D., D.F. Gibbons, R.L. Martin, S.R. Levitt, J. Smith, R.V. Harrington. "Biocompatibility of Ceramic Implants in Soft Tissue". J. Biomed. Mat. Res. 6: 425-49, 1972.

53. DiPasquale, G., L.V. Trip, B.G. Steinetz. "Effect of Locally Applied Anti-Inflammatory Substances on Rat Skin Wounds". Proc. Soc. Exp. Biol. Med. 124: 404-7, 1967.

54. Dressler, D.P., L. Barlyn, W.A. Skornick. "Viable Prosthetic Interface". J. Biomed. Mat. Res. Symp. 1: 169-78, 1971.

55. Dukes, C.E. and B.C.V. Metchley. "Polyvinyl Sponge Implants: Experimental and Clinical Observation". Br. J. Plast. Surg. 15: 225-35, 1962.

56. Dumbleton, J.H. "Delrin as a Material for Joint Prosthesis - A Review". In Corrosion and Degradation of Implant Materials, ed. by B.C. Syrett and A. Acharya. ASTM, Philadelphia, 1978, pp. 41-75.

57. Dunphy, J.E., and K.N. Udupa. "Chemical and Histochemical Sequences in the Normal Healing of Wounds". New England J. Med. 253: 847-51, 1955.

58. Escales, F., J. Galante, W. Rostoker, P. Coogan. "Biocompatibility of Materials for Total Joint Replacement". J. Biomed. Mat. Res. 10: 175-95, 1976.

59. Epstein, W.L. "Granuloma Formation in Man". Pathobiol. Annual 7: 1-30, 1977.

60. Federko, M.E. and J.G. Hirsch. "Structure of Monocytes and Macrophages". Seminars Hematol. 7: 109-24, 1970.

61. Fenn, W. O. "The Adhesiveness of Leukocytes to Solid Surfaces". J. Gen. Physiol. 5: 143-67, 1923.

62. Fenn, W.O. "Effect of Hydrogen in Concentration on the Phagocytosis and Adhesiveness of Leukocytes". J. Gen. Physiol. 5: 169-79, 1923.

63. Feralli, M.W. Personal Communications, Lord Corporation, Erie, PA. (1979).

64. Fowkes, F.M. "Attractive Forces at Interfaces". Ind. Eng. Chem. 56: 40-52, 1964.

65. Fox, H.W. and W.A. Zisman. "The Spreading of Liquids on Low Energy Surfaces. I. Polytetrafluorethylene". J. Colloid Sci. 5: 514-31, 1950.

66. Friedman, L.I., H. Leim, E.F. Grabowski, E.F. Leonard, C.W. McCord. "Inconsequentiality of Surface Properties for Initial Platelet Adhesion". Trans. Am. Soc. Art. Int. Org. 16: 63-73, 1970.

67. Galindo, B., E.R. Heise, Q.N. Myrvik. "Migration Inhibition Response of Mononuclear Cells Mediating Granulomatous Inflammation". Series Haematologica 3: 145-59, 1970.

69. Gallin, J.I., J.R. Durocher, A.P. Kaplan. "Interaction of Leukocyte Chemotactic Factors with the Cell Surface I. Chemotactic Factor-Induced Changes in Human Granulocyte Surface Charge". J. Clin. Invest. 55:967-74, 1975.

70. Gallin, J.I., E.K. Gallin, H.L. Malech, E.B. Cramer. "Structural and Ionic Events During Leukocyte Chemotaxis". In Leukocyte Chemotaxis, ed. by J.I. Gallin and P.G. Quie. Raven Press, New York, 1978, pp. 123-39.

71. Gibbons, D.F. "Effect of Surface Texture by Ion Beam Sputtering in Implant Biocompatibility and Soft Tissue Attachment". First Annual Report for NASA Grant NSG-3126, 1977.

72. Goldstein, I.M. and G. Weismann. "Nonphagocytic Stimulation of Human Polymorphonuclear Leukocytes: Role of the Plasma Membrane". Seminars Hematol. 16: 175-87, 1979.

73. Good, R.J., J.A. Kvikstad, W.O. Baily, "Anisotropic Forces in the Surface of a Stretch-Oriented Polymer". J. Colloid and Interface Sci. 35: 314-27, 1971.

74. Good, R.J. and L.A. Girifalco. "A Theory for the Estimation of Surface and Interfacial Energies III. Estimation of Surface Energies of Solids from Contact Angle Data". J. Phys. Chem. 64: 561-5, 1960.

75. Gordon, S. "Macrophage Neutral Proteinases and Chronic Inflammation". Ann. N.Y. Acad. Sci. 278: 176-89, 1976.

76. Gourlay, S.J., R.M. Rice, A.F. Hegyeli, C.W.R. Wade, J.G. Dillon, H. Jaffe, R.K. Kulkarni. "Biocompatibility Testing of Polymers: in vivo Implantation Studies". J. Biomed. Mat. Res. 12: 214-32, 1978.

77. Graham, Jr. R.C., R.H. Ebert, O.D. Ratnoff, J.M. Moses. "Pathogenesis of Inflammation II. In vivo observations of the Inflammatory Effects of Activated Hageman Factor and Bradykinin". J. Exptl. Med. 121: 807-17, 1965.

78. Guber, S. and R. Rudolph." The Myofibroblast". Surg., Gynec., Obstet. 146: 641-9, 1978.

79. Guy, A.C. Introduction to Materials Science. McGraw-Hill Book Co., New York, 1972, pp. 232-4.

80. Hall, C.W., D. Liotta, M.E. DeBakey. "Artificial Skin". Trans. Am. Soc. Art. Intern. Org. 12: 340, 1966.

81. Hall, C.W., D. Liotta, J.J. Ghidoni, M.E. DeBakey, D.P. Dressler. "Velour Fabrics Applied to Medicine". J. Biomed. Mat. Res. 1: 179-96, 1967.

82. Hall, C.W., M. Spira, F. Gerow, L. Adams, E. Martin, S.B. Hardy. "Evaluation of Artificial Skin Models: Presentation of Three Clinical Cases". Trans. Am. Soc. Art. Intern. Org. 16: 12, 1970.

83. Hall, C.W., "Developing a Permanently Attached Artificial Limb". Bull. Prosthet. Res. 10: 144-57, 1974.

84. Halstead, A., C.W. Jones, R.D. Rawlings. "A Study of the Reaction of Human Tissue to Proplast". J. Biomed. Mat. Res. 13: 121-34, 1979.

85. Ham, A.W. Histology, 7th ed. J. B. Lippincott Co., Philadelphia, 1975.

86. Harrison, J.H., D.S. Swanson, A.F. Lincoln. "A Comparison of the Tissue Reaction to Plastic Materials". A.M.A. Archives of Surg. 74: 139-44, 1957.

87. Heath, J.C. "Interactions of Particulate Metals with Living Tissues". In Biocompatibility of Implant Materials, ed. by D. Williams. Sector Publishing Ltd., London, 1976, pp. 49-54.

88. Hegyeli, R.J. "Limitations of Current Techniques for the Evaluation of the Biohazards and Biocompatibility of New Candidate Materials". J. Biomed. Mat. Res. Symp. 1: 1-14, 1971.

89. Helmus, M.N. "Plasma Interactions on Block Copolymers as Determined by Platelet Adhesion". M.S. Thesis, Case Western Reserve University, 1978.

90. Hench, L.L., R.W. Petty, G. Piotrowski. "An Investigation of Bonding Mechanisms at the Interface of a Prosthetic Material". Summary Report No. 9, U.S. Army Medical Research and Development Command, DAMD 17-76-C-6033, 1978.

91. Henson, P.M. and C.G. Cochrane. "The Effect of Complement Depletion on Experimental Tissue Injury". Ann. N.Y. Sci. 256: 426-40, 1975.

92. Hirschorn, J.S., A.A. McBeath, M.R. Dustoor. "Porous Titanium Surgical Implant Materials". J. Biomed. Mat. Res. Symp. 2: (Part 1): 49-67, 1971.

93. Hoffman, A.S. "Principles Governing Biomolecule Interactions at Foreign Surfaces". J. Biomed. Mat. Res. 5: 77-83, 1974.

94. Hohmann, A., J.A. Hilger, R. Carley. "Fate of Implants in Rats". Ann. Oto. 73: 791, 1964.

95. Homsy, C.A. and M.S. Anderson. "Functional Stabilization of Prostheses with a Porous Low Modulus Materials System". In Biocompatibility of Implant Materials, ed. by D. Williams, Sector Publishing Ltd., London, 1976, pp. 85-92.

96. Huber, H. and H.H. Fudenburg. "The Interaction of Monocytes and Macrophages with Immunoglobins and Complement". Sec. Haematologica 3: 160-75, 1970.

97. Hudson, W.R. "Nonpropulsive Applications of Ion Beams". AIAA International Electric Propulsion Conference, 1976.

98. Hudson, W.R., R.R. Robson, J.S. Sowery. "Ion Beam Technology and Applications". NASA TMX-3517, 1977.

99. Hueper, W.C. "Carcinogenic Studies on Water Soluble and Insoluble Macromolecules". A.M.A. Archives of Path. 67: 589-617, 1959.

100. Hulbert, S.F., S.J. Morrison, J.J. Klawitter. "Biocompatibility of Porous Ceramics with Soft Tissue: Application to Tracheal Prosthesis". J. Biomed. Mat. Res. Symp. 2 (Part 1): 269-79, 1971.

101. Huybrechts-Godin, G., P. Hauser, G. Vaes. "Macrophage-Fibroblast Interaction in Collagenase Production and Degradation". Biochem. J. 184: 643-50, 1979.

102. Ivanga, S. "Bovine Plasma Cold-Insoluble Globulin: Gross Structure and Function". Ann. N.Y. Acad. Sci. 312: 56-73, 1978.

103. Jackson, D.S., D.B. Flickinger, J.E. Dunphy. "Biochemical Studies of Connective Tissue Repair". Ann. N.Y. Acad. Sci. 86: 943-7, 1960.

104. Jimenez, S.A., W. McArthur, J. Rosenbloom. "Inhibition of Collagen Synthesis by Mononuclear Cell Supernates". J. Exp. Med. 150: 1421-31, 1979.

105. Johnson, K.H., H.K. G. Ghobrial, L.C. Buoen, I. Brand, K.G. Brand. "Foreign Body Tumougenesis in Mice: Ultrastructure of the Preneoplastic Tissue Reactions". J. Natl. Canc. Inst. 49: 1311-19, 1972

106. Johnson, Jr., R.E. and R.H. Dettre. "Wettability and Contact Angles". In Surface and Colloid Science, Vol. 2, ed. by E. Matijevic. Wiley-Interscience, New York, 1969, pp. 85-153.

107. Kaelble, D.H. "Dispersion-Polar Surface Tension Properties of Organic Solids". J. Adhesion 2: 66, 1970.

108. Kaminski, E.J., R.J. Oglesby, N.K. Wood, J. Sandrik. "The Behavior of Biological Materials at Different Sites of Implantation". J. Biomed. Mat. Res. 2: 81-8, 1968.

109. Kaminski, E.J., M.W. Shink, R.J. Oglesby. "Presence of Adipose Fat as a Criterion of Implant Compatibility". J. Biomed. Mat. Res. 11: 871-81, 1977.

110. Karp, R.D., K.H. Johnson, L.C. Buoen, H.K.G. Ghobrial, I. Brand, K.G. Brand. "Tumorigenesis by Millipore Filters in Mice: Histology and Ultrastructure of Tissue Reactions as Related to Pore Size". J. Natl. Canc. Inst. 51: 1275- 85, 1973.

111. Keller, H.V., M.W. Hess, H. Cottier. "Physiology of Chemotaxis and Random Motility". Sem. Hematol. 12: 47-57, 1975.

112. Kellermeyer, R.W. and R.C. Graham, Jr. "Kinins-Possible Physiologic and Pathologic Role in Man". New England J. Med. 279: 754-9, 802-7.

113. Kemp, A., P. Roberts-Thomason, S. Brown. "Inhibition of Human Neutrophil Migration by Aggregated Gammaglobulin". Clin. and Exp. Immunol. 36: 334-41, 1979.

114. Kim, S.W., S. Kisniewski, E.S. Lee, M.L. Winn. "Role of Protein and Fatty Acid Adsorption on Platelet Adhesion and Aggregation at the Boood - Polymer Interface". J. Biomed. Mat. Res. 8: 23-31, 1977.

115. Kochwa, S., M. Brownwell, R.E. Rosenfield, L.R. Wasserman. "Adsorption of Proteins by Polystyrene Particles I. Molecular Unfolding and Acquired Immunogenecity of IgG". J. Immunol. 99: 981-6, 1967.

116. Kordan, H.A. "Localized Interfacial Forces Resulting from Implanted Plastics as Possible Physical Factors Involved in Tumor Formation". J. Theoretical Biol. 17: 1-11, 1967.

117. Kouri, J., O. Ancheta. "Transformation of Macrophages into Fibroblasts". Exp. Cell Res. 71: 168-76, 1972.

118. Lack, C.H. "Some Biological and Biochemical Sequences of Inflammation in Connective Tissue". Biochem. Pharmacol. Suppl. (1968) pp. 197-203.

119. Laing, P.G., A.B. Ferguson, Jr., E.S. Hodge. "Tissue Reaction in Rabbit Muscle Exposed to Metallic Implants". J. Biomed. Mat. Res. 1: 135-49, 1967.

120. Lee, Jr., H.L. "Adhesion Between Living Tissue and Plastics I. Adhesion of Epoxy and Polyurethane Resin to Dentin and Enamel". J. Biomed. Mat. Res. 3: 349-67, 1969.

121. Leibovich, S. J. and R. Ross. "The Role of the Macrophage in Wound Repair-A Study with Hydrocortizone and Antimacrophage Serum". Am. J. Path. 78: 71-91, 1975.

122. Leibovich, S.J. and R. Ross. "A Macrophage-Dependent Factor that Stimulates the Proliferation of Fibroblasts in vitro. "Am. J. Path. 84: 501-13, 1976.

123. Leidholt, J.D. and H.A. Gorman. "Teflon Hip Prosthesis in Dogs". J. Bone and Joint Surg. 47-A: 1414-20, 1965.

124. Leinenger, R.I., V. Mirkovitch, A. Peters, W.A. Hawks. "Change in Plastics During Implantation". Trans. Am. Soc. Art. Int. Int. Org. 10: 320, 1964.

125. LeVeen, H.H. and J.R. Barberio. "Tissue Reaction to Plastics Used in Surgery with Special Reference to Teflon". Ann.Surg. 129: 74-84, 1949.

126. Lever, W.F. Histopathology of the Skin, 5th ed. J.B. Lippincott Co., Philadelphia, 1975.

127. Levine, S.N. "Thermodynamics of Adsorbed Protein Films". J. Biomed. Mat. Res. 3: 83-94, 1969.

128. Lewey, R.B. "Responses of Laryngeal Tissue to Granular Teflon in situ". Arch. Oto. 83: 79-83, 1966.

129. Lippman, M. "A Proposed Role for Mucopolysaccharides in the Initiation and Control of Cell Division". Trans. N.Y. Acad. Sci. Series II, 27: 342, 1965.

130. Lisanti, V.F. "Hydrolytic Enzymes in Peridontal Tissues". Ann. N.Y. Acad. Sci. 85: 461-6, 1965.

131. MacFarlane, R.G. "The Theory of Blood Coagulation". In Human Blood Coagulation Haemostases and Thrombosis, ed. by R. Biggs, Blackwell Scientific Publications, Oxford, 1976, pp. 1-31.

132. MacKenzie, J.R. M. Hackett, C. Topuzlur, D.J. Tibbs. "Origin of Arterial Prosthesis Lining from Circulating Blood Cells". Arch. Surg. 97: 879-85, 1968.

133. Mariano, M. and W.G. Spector. "The Formation and Properties of Macrophage Polykaryons (inflammatory giant cells)". J. Path. 113: 1-19, 1974.

134. Marzoni, F.A., S.E. Upchurch, C.J. Lambert. "An Experimental Study of Silicone as a Soft Tissue Substitute". Plast. and Reconstr. Surg. 24: 600-8, 1959.

135. Matlaga, B.F., L.P. Yasenchak, T.N. Salthouse. "Tissue Response to Implanted Polymers: The Significance of Sample Shape". J. Biomed. Mat. Res. 10: 391-97, 1976.

136. Matsuda, M., N. Yoshida, N. Aoki. "Distribution of Cold-Insoluble Globulin in Plasma and Tissues". Ann. N.Y. Acad. Sci. 312: 74-92, 1978.

137. Mercer, E.H. "The External Surface of the Cell and Intercellular Adhesion". In Recent Progress in Surface Science, Vol. 1, ed. by J.F. Danielli, K.G.A. Pankhurst, A.C. Riddiford, Academic Press, New York, 1964, pp. 360.

138. Miller, J. and E. Brooks, "Problems Related to the Maintenance of Chronic Percutaneous Electronic Leads". J. Biomed. Mat. Res. Symp. 2: 251-67, 1971.

139. Miller, M.E. "Pathology of Chemotaxis and Random Mobility". Sem. Hematol. 12: 59-82, 1975.

140. Monis, B., T. Weinberg, G.J. Spector. "The Carageenan Granuloma in the Rat - a Model for the Study of the Structure and Function of Macrophages" Br. J. Exp. Path. 49: 302-10, 1968.

141. Morrow, A.G. "The Use of Tantalum Guaze in the Closure of a Defect in the Chest Wall". Surgery 29: 288-92, 1951.

142. Mosesson, M.W. "Structure of Human Plasma Cold-Insoluble Globulin and the Mechanism of its Precipitation in the Cold with Heparin or Fibrin-Fibrinogen Complex". Ann. N.Y. Acad. Sci. 312: 11-30, 1978.

143. Murphy, W.M. "Tissue Reactions of Rats and Guinea Pigs to Co-Cr Implants with Different Surface Finishes". Br. J. Exp. Path. 52: 353-59, 1971.

144. NASA Lewis Research Center. "Ion Propulsion for Spacecraft". U.S. Govt. Print. Of. 1977-757-070/6307.

145. Normann, S.J. and M. Schardt. "A Macrophage Inflammation Test Using Subcutaneous Nitrocellulose Filters". J. Ret. Soc. 23: 153-60, 1978.

146. North, R.J. "Endocytosis". Sem. Hematol. 7: 161-71, 1970.

147. Nossel, H.L. "The Contact System". In Human Blood Coagulation Haemostasis and Thrombosis, ed. by R. Biggs. Blackwell Scientific Publications, Oxford, 1976, pp. 81-142.

148. Nyilas, E., W.A. Morton, R.D. Cumming, D.M. Lederman, T.H. Chiu. "Effectc of Polymer Surface Molecular Structure and Force-Field Characteristics on Blood Interfacial Phenomena". J. Biomed. Mat. Res. Symp. No. 8: 51-68, 1977.

149. Occumpaugh, D.E. and H.L. Lee, "Foreign Body Reactions to Plastic Implants". In Biomedical Polymers, ed. by A. Renbaum and M. Shan. Marcel Dekker, Inc., New York, 1971, pp. 101-19.

150. O'Flaherty, J.T. and P.A. Ward. "Leukocyte Aggregation Induced by Chemotactic Factors". Inflammation 3: 177-94, 1978.

151. O'Flaherty, J.T. and P.A. Ward. "Chemotactic Factors and the Nuetrophil". Sem. Hematol. 16: 163-74, 1979.

152. Oliver, J.F., C.Huh, S.G. Mason. "Resistance to Spreading of Liquids by Sharp Edges". J. Colloid and Interface Sci. 59: 568-81, 1977.

153. Oppenheimer, B.S., E.T. Oppenheimer, I. Danishefsky, A.P. Stout, F.R. Eirich. "Further Studies of Polymers as Carcinogenic Agents in Animals". Cancer Res. 15: 333-40, 1955.

154. Papadamitriou, J.M. and W.G. Spector. "The Origin, Properties, and Fate of Epitheloid Cells". J. Path. 105: 187-203, 1971.

155. Papadamitriou, J.M., D. Sforsina, L. Papaelias. "Kinetics of Multinucleate Giant Cell Formation and Their Modification by Various Agents in Foreign Body Reactions". Am. J. Path. 73: 349-61, 1973.

156. Parks, Jr., J.P. "Coagulation Studies on Selected Copolymers of γ-L Benzyl-Glutamate, L-Leucine, and L-Phenylalanine". Ph.D. Dissertation, Case Western Reserve University, 1977.

157. Paz, R.A. and W.G. Spector. "The Mononuclear-Cell Response to Injury". J. Path. and Bacteriol. 84: 85-103, 1962.

158. Peacock, E.E. and W. Van Winkle. Wound Repair, Saunders Co., Philadelphia, 1976, pp. 1-21.

159. Pearlstein, E. and L.I. Gold. "High-Molecular-Weight Glycoprotein as a Mediator of Cellular Adhesion". Ann. N.Y. Acad. Sci. 312: 278-92, 1978.

160. Pearse, A.G.E. Histochemistry, Theoretical and Applied, 2nd ed. Little Brown Co., Boston, 1960, pp. 872-881.

161. Perper, C.W., M. Sandra, V.J. Stecher, A.L. Oronsky. "Physiologic and Pharmacologic Alterations of Rat Leukocyte Chemotaxis in vitro". Ann. N.Y. Acad. Sci. 256: 190-209, 1975.

162. Petke, F.D. and B.R. Ray. "Temperature Dependence of Contact Angles". J. Colloid and Interface Sci. 31: 216-27, 1969.

163. Rae, T. "Action of Wear Particles from Total Joint Replacement Prostesis on Tissues". In Biocompatibility of Implant Materials, ed. by D. Williams. Sector Publishing Ltd., London, 1976, pp. 55-9.

164. Ratnoff, O.D. "Some Relationships Among Hemostasis, Fibrinolytic Phenomena, Immunity, and the Inflammatory Response". Adv. Immunol. 10: 145-227, 1969.

165. Ratnoff, O.D. and H. Saito. "Interactions Among Hageman Factor Plasma Prekallikrein, High Molecular Weight Kininogen, and Plasma Thromboplastin Antecedent". Proc. Natl. Acad. Sci. U.S.A. 76: 958-61, 1979.

166. Raykhlin, N.T. and A.K. Kogan. "The Development and Malignant Degeneration of the Connective Tissue Capsules around Plastic Implants". Prob. Oncol. 7: 11-14, 1961.

167. Richards, R.J. and F.S. Wusteman. "The Effects of Silica Dust and Alveolar Macrophages on Lung Fibroblasts Grown in vitro". Life Sci. 14: 355-64, 1974.

168. Rigdon, R.H. "Local Reaction to Polyurethane - A Comparative Study in the Mouse, Rat and Rabbit". J. Biomed. Mat. Res. 7: 70-93, 1973.

169. Rigdon, R.H. "Plastics and Inflammation: An in vivo Experimental Study". J. Biomed. Mat. Res. 8: 97-117, 1974.

170. Rosen, J.J. "Cellular Interactions at Hydrogel Interfaces". Ph.D. Dissertation, Case Western Reserve Univ., 1976.

171. Rosenthal, A.S., P.E. Lipsky, E.M. Shevach. "Macrophage-Lymphocyte Interaction and Antigen Recognition". Fed. Proc. 34: 1743-8, 1975.

172. Rosenthal, A.S., M.A. Bareinski, L.Q. Rosenwasser. "Function of Macrophages in Genetic Control of Immune Responsiveness". Fed. Proc. 37: 79-85, 1978.

173. Ross, R. and E.P. Benditt. "Wound Healing and Collagen Formation I. Sequential Changes in Components of Guinea Pig Skin Wounds Observed in the Electron Microscope". J. Biophys. and Biochem. Cytol. 11: 677-700, 1968.

174. Ross, R. "The Fibroblast and Wound Repair". Biol. Rev. 43: 51-96, 1968.

175. Ross, R., N.B. Everett, R. Tyler. "Would Healing and Collagen Formation-The Origin of the Would Fibroblast Studied in Parabiosis". J. Cell Biol. 44: 645-54, 1970.

176. Rubin, L.R., B.E. Bromberg, R.H. Walden. "Long Term Human Reaction to Synthetic Plastics". Surg., Gynecol., Obstet. 121: 603-8, 1971.

177. Ruddy, S., I. Gigli, K.F. Austen. "The Complement System of Man". New England J. Med. 287: 489-95, 545-9, 592-6, 642-6, 1972.

178. Rudolph, R., S. Guber, M. Suzuki, M. Woodward. "The Life Cycle of Myofibroblasts". Surg. Gynec., Obstet. 145: 389-94, 1977.

179. Rudolph, R., J. Abraham, T. Vecchione, S. Guber, M. Woodward. "Myofibroblasts and Free Silicone Around Breast Implants". Plast. and Reconstr. Surg. 62: 185-96, 1978.

180. Ryan, G.B. "The Origin and Sequence of the Cells Found in the Acute Inflammatory Response". Australian J. Exp. Med. and Biol. 45: 149-62, 1967.

181. Ryan, G.B. and W.G. Spector. "Macrophage Turnover in Inflamed Connective Tissue". Proc. Roy. Soc. London, Ser. B, 175: 269-92, 1970.

182. Salthouse, T.N. and D.A. Willigan. "An Enzyme Histochemical Approach to the Evaluation of Polymers for Tissue Compatibility". J. Biomed. Mat. Res. 6: 105-13, 1972.

183. Salthouse, T.N., B.F. Matlaga, R.K. O'Leary. "Microspectrophotometry of Macrophage Lysosomal Enzyme Activity: A Measure of Polymer Implant Tissue Toxicity". Toxicol and Appl. Pharmacol. 25: 201-11, 1973.

184. Salthouse, T.N. and B.F. Matlaga. "An Approach to the Numerical Quantification of Acute Tissue Response to Biomaterials". Biomat., Med. Dev., and Art. Org. 3: 47-56, 1975.

185. Salthouse, T.N. "Cellular Enzyme Activity at the Polymer-Tissue Interface: A Review". J. Biomed. Mat. Res. 10: 197-229, 1976.

186. Salthouse, T.N. "Effects of Implant Shape and Surface on Cellular Activity and Evaluation of Histocompatibility". First Europeon Conf. on Evaluation of Biomaterials. Strasburg, France, 1977.

187. Salthouse, T.N. "Effects of Implant Surface on Cellular Activity and Evaluation of Histocompatibility". In Advances in Biomaterials, ed. by G.D. Winter. John Wiley and Sons Ltd., Chichester, U.K. (to be published).

188. Salvatore, J.E., W.S. Gilmer, Jr., M. Kashgarian, W.R. Barber. "An Experimental Study of the Influence of Pore Size of Implanted Polyurethane Sponges Upon Subsequent Tissue Formation". Surg. Gynecol., and Obstet. 112: 463-8, 1961.

189. Scales, J.T. "Tissue Reaction to Synthetic Materials". Proc. Roy. Soc. Med. 46: 647-52, 1953.

190. Scales, J.T. "Internal Prostheses - The Problem in Relation to Materials". J. Bone and Joint Surg. 38-B: 754, 1956.

191. Senn, H.J. and W.F. Jungi. "Neutrophil Migration in Health and Disease". Sem. Hematol. 12: 27-45, 1975.

192. Smith, L., D. Hill, J. Hibbs, S.W. Kim, J. Andrade. "Glow Discharge Surface Treatment for Improved Cellular Adhesion". Polymer Preprints 16: 186-90, 1975.

193. Spector, W.G. "Studies on the Mechanism of Chronicity in Inflammation". from Inflammation, Excerpts Medical Foundation, New York. 1968, pp. 17-25.

194. Spector, W.G. "The Macrophage in Inflammation". Ser. Haematol. 3: 132-44, 1970.

195. Spector, W.G. "Epithelioid Cells, Giant Cells, and Sarcoidosis". Ann. N.Y. Acad. Sci. 278: 3-6, 1976.

196. Sperati, C.A. "Physical Constants of Poly (tetrafluoroethylene)". In Polymer Handbook, 2nd ed. by J. Brandrup and E.H. Immergut. John Wiley and Sons, New York, 1975, pp. V-29-36.

197. Spira, M. J. Fissette, C.W. Hall, S.B. Hardy, F.J. Gerow. "Evaluation of Synthetic Fabrics as Artifical Grafts to Experimental Burn Wounds". J. Biomed. Mat. Res. 3: 213-34, 1969.

198. Šprincl, L. J. Kopecek, D. Lim. "Effects of Porosity of Heterogeneous Poly (glycol monomethacrylate) gels on the Healing-in of Test Implants". J. Biomed. Mat. Res. 4: 447-58, 1971.

199. Stinson, N.E. "Tissue Reaction Induced in Guinea Pigs by Particulate PMMA, Polyethylene, and Nylon of the Same Size Range". Br. J. Exp. Path. 46: 135-46, 1964.

200. Stone, K.G. Determination of Organic Compounds. McGraw-Hill Book Co., New York, 1956, pp. 77-8.

201. Stossel, T.P. "Phagocytosis: Recognition and Ingestion". Sem. Hematol. 12: 83-116, 1975.

202. Stossel, T.P. and J.H. Hartwig. "Interaction of Action, Myosin, and New Binding Protein of Rabbit Pulmonary Macrophages". J. Cell Biol. 68: 602-19, 1976.

203. Stossel, T.P. "The Mechanism of Phagocytosis". J. Ret. Soc. 19: 237-45, 1976.

204. Sultan, A.M., C.J. Dunn, D.A. Willoughby. "The Role of Kallikrein in Leukocyte Migration Inhibition". Inflammation 3: 295-303, 1979.

205. Sultan, A.M., C.J. Dunn, D.A. Willoughby/ "Leukocyte Migration Inhibition Activity of Nonimmune Acute Inflammatory Pleural Exudate". Inflammation 3: 305-17, 1979.

205a. Sutton, J.S. and L. Weiss. "Transormation of Monocytes in Tissue Culture into Macrophages, Epithelioid Cells, and Multinucleated Giant Cells - An Electron Microscope Study". J. Cell Biol. 28: 303-31, 1966.

206. Szilagyi, D.E., J.R. Pfeifer, F.J. DeRusso. "Long Term Evaluation of Plastic Arterial Substitutes: An Experimental Study". Surgery 55: 165-83, 1964.

207. Taylor, A.C. "Adhesion of Cells to Surfaces". In Adhesion in Biological Systems, ed. by R.S. Manly, Academic Press, New York, 1970, pp. 51-70.

208. Thaler, M.S., R.D. Klausner, H.J. Cohen. Medical Immunology. J.B. Lippincott Co., Philadelphia, 1977, p. 16.

209. Tilney, N.L. and P.J. Boor. "Host Response to Implanted Dacron Grafts". Arch. Surg. 110: 1469-72, 1975.

210. Tucker, S.B., R.V. Pierre, R.E. Jordan. "Rapid Identification of Monocytes in a Mixed Mononuclear Cell Preparation". J. Immun. Methods 14: 267-9, 1977.

211. Turco, S.J. and P.W. Robbins. "Synthesis and Function of Carbohydrate Units of Cell Surface Glycoproteins". Ann. N.Y. Acad. Sci. 312: 392-8, 1978.

212. Uranue, E.R. "Function of Macrophages - Introduction". Fed. Proc. 34: 1723-4, 1975.

213. Unanue, E.R. and J. Calderon. "Evaluation of the Role of Macrophages in Immune Induction". Fed. Proc. 34: 1737-42, 1975.

214. Unanue, E.R., D.I. Beller, J. Calderon. "Regulation of Immunity and Inflammation of Mediators from Macrophages". Am. J. Path. 85: 465-78, 1976.

215. Unanue, E.R. "Macrophage Functions in Immunity-Introduction". Fed. Proc. 37: 77-8, 1978.

216. Usher, F.C. and S.A. Wallace. "Tissue Reaction to Plastics-A Comparison of Nylon, Orlon, Dacron, Teflon, Marlex". A.M.A. Arch. Surg. 76: 907-9, 1958.

217. Usher, F.C. and J.P. Gannon. "Marlex Mesh, a New Plastic Mesh for Replacing Tissue Defects I. Experimental Studies". A.M.A. Arch. Surg. 78: 131-7, 1959.

218. Van der Rhee, H.J., C.P.M. Van de Burgh-de Winter, W. Th. Daems. "The Differentiation of Monocytes into Macrophages, Epithelioid Cells, and Multinucleated Giant Cells in Subcutaneous Granulanas I. Fine Structure". Cell Tissue Res. 197: 355-78, 1979.

219. Van Furth, R. "Origin and Kinetics of Monocytes and Macrophages". Sem. Hematol. 7: 125-41, 1970.

220. Van Furth, R.,M.M.C. Diesselhoff-Den Dulk, H. Mattie. "Quantitative Study on the Production and Kinetics of Mononuclear Phagocytes During an Acute Inflammatory Reaction". J. Exp. Med. 138: 1314-30, 1973.

221. Van Furth, R. "Origin and Kinetics of Mononuclear Phagocytes". Ann. N.Y. Acad. Sci. 278: 161-75, 1976.

222. Van Kampen, C.L. "Effects of Implant Surface Chemistry upon Arterial Thrombosis and Endothelialization". Ph.D. Dissertation Case Western Reserve University, 1977.

223. Van Winkle, W. "The Fibroblast in Wound Healing". Surg.,Gynecol., and Obstet. 124: 369-86, 1967

224. Vasko, K.A. and R.O. Rawson. "A Chronic Nonreactive Percutaneous Lead System". Trans. Am. Soc. Art. Int. Org. 13: 143-5, 1967.

225. Vogl, O. "Polyaldehydes: Introduction and Brief History". In Polyaldehydes, ed. by O. Vogl. Marcel Dekker, Inc. New York, 1967, pp. 3-7.

226. Volkman, A. and J.L. Gowans. "The Production of Macrophages in the Rat". Br. J. Exp. Path. 46: 50-61, 1964.

227. Volkman, A. and J.L. Gowans. "The Origin of Macrophages from Bone Marrow in the Rat". Br. J. Exp. Path. 46: 62-70, 1964.

228. Volkman, A. "Disparity in Origin of Mononuclear Phagocyte Population". J. Ret. Soc. 19: 249-68,1976.

229. Vroman, L., A.L. Adams, M. Kings. "Interactions Among Human Blood Proteins at Interfaces". Fed. Proc. 30: 1494-1502, 1971